

**Comparative Investigation of Key Biosynthetic Transformations in Fungal
Indole Alkaloid Natural Product Pathways**

Hong T. Tran

**A dissertation submitted in partial fulfillment
of the requirements for the degree of
Doctor of Philosophy
(Chemical Biology)
in the University of Michigan
2015**

Doctoral Committee:

**Professor David H. Sherman, Chair
Professor David P. Ballou
Professor Anuj Kumar
Professor Janet L. Smith**

To my parents, the source of my inspiration.

Acknowledgements

Firstly, I would like to thank my advisor Dr. David H. Sherman for giving me the opportunity to work on a challenging and stimulating project for my dissertation. I am humbled by the faith you have had in my abilities as a scientist and intellectual, and I am thankful that you spotted my strengths early in my career and gave me the chance to demonstrate them. I would also like to thank my committee members Prof. David Ballou, Prof. Anuj Kumar, and Prof. Janet Smith for all their insight, help, and guidance through my dissertation progress.

I would like to thank Dr. Shengying Li, who mentored and guided me as I began my project. I would also like to thank Dr. Karoline Chiou, Dr. Eli Eisman, and Dr. Kyle Bolduc for their indispensable scientific and graduate school advice, and for being my supporters in the face of adversity. Dr. Andrew Lowell and Dr. Ashootosh Tripathi were also key mentors and teammates in my development during my tenure here.

Thank you Ms. Shamilya Williams and Ms. Pam Schultz. You both strengthen the walls at our backs and build bridges for us where they would normally be absent, and the support does not go unnoticed.

I would also like to thank Dr. Robert M. Williams for being a second advisor to me, particularly as a synthetic opinion and complement to our biosynthetic studies. Much of the work described in this dissertation was made possible thanks to the strong collaborative effort between the Sherman and Williams laboratories. Dr. James D. Sunderhaus and Dr. Jennifer M. Finefield were key collaborators I worked with and provided much of the synthetic approach described in this dissertation.

I would like to thank all my friends and family. Thank you for always believing in me and my ability to succeed even when my own faith wavered. Thank you for being there to celebrate, for being there to share in times when I was down, and for all the fond memories. Additionally, I

would like to thank all my friends in Brazil. The experience of doing research abroad has been an essential part of my development as a scientist and as a person, and I am grateful for the warmth and comfort with which I was received. Never once did I feel like an alien in your country, and I can only hope to be able to return the favor someday.

I would like to thank all the teachers and professors who have led me to where I am today, but I would especially like to thank my 9th grade English teacher. The spirit you showed me exemplifies what I hope to be as a mentor, a role model, and a human being.

Lastly, thanks to my two troublesome cats, Sora and Riku, for taking care of me.

Preface

This dissertation contains five chapters covering my investigations on three key biosynthetic steps involved in the formation of the bicyclo[2.2.2]diazaoctane compounds. Chapter 1 begins with an introduction to natural products and particular the fungal indole alkaloids, which were the focus of my dissertational work. Chapter 2 is an adaptation of a submitted manuscript titled “Substrate Controlled Flavin Monooxygenases Reveal Strategy for Fungal Indole Alkaloid Structural Diversification,” for which I am first author. This manuscript was prepared for submission to the *Journal of the American Chemical Society* for peer review during the completion of my dissertational work, and it focuses on the flavin monooxygenases NotI, NotI' and PhqK. Chapter 3 focuses on my extensive work covering the prenyltransferase MalE from the malbrancheamide biosynthetic pathway. In this chapter I describe our attempts at discovering Diels-Alder biosynthetic activity and how investigations will be continued in the laboratory following the completion of my Ph.D. Chapter 4 summarizes our investigation of the MalA halogenase from the malbrancheamide pathway. This work is currently being prepared for submission to a peer-reviewed journal. Finally, I discuss potential future directions in Chapter 5 based on the findings in my dissertational research.

Table of Contents

Dedication.....	ii
Acknowledgements.....	iii
Preface.....	v
List of Figures.....	viii
List of Tables.....	xvi
List of Schemes.....	xvii
Abstract.....	xviii
Chapter	
1 Introduction to fungal indole alkaloid natural products	1
1.1 Natural products are a rich source of bioactive molecules with interesting chemistry....	1
1.2 Fungal indole alkaloids comprise a class of natural products.....	2
1.3 The Notoamides	5
1.4 The Malbrancheamides	10
1.5 The intramolecular Diels-Alder hypothesis	13
1.6 Dissertation directions and goals.....	15
2 Formation of the spirooxindole moiety	17
2.1 Introduction	17
2.2 Results	21
2.2.1 Determination of NotI and NotI' as the (+)-Notoamide B synthase via semipinacol rearrangement.	21
2.2.2 Analysis of NotI Substrate Flexibility.	23
2.2.3 Determination of PhqK activity and substrate flexibility.	24
2.2.4 Determining the structure of Notoamide T9.....	24
2.3 Discussion	27
2.4 Materials and Methods.....	31
2.5 Appendix	37
3 Prenyltransferases	81
3.1 Introduction	81
3.2 Results	86
3.2.1 MalE demonstrates prenyltransferase activity	86
3.2.2 MalE substrate synthesis.....	87
3.2.3 Investigation of MalE activity with biomimetic synthetic compounds	88

3.2.4	Investigation of MalE activity with predicted native substrate 8	89
3.3	Discussion	91
3.4	Methods.....	94
3.5	Appendix A	96
3.6	Appendix B	104
4	Halogenation.....	108
4.1	Introduction	108
4.2	Results	111
4.2.1	Determination of MalA as a flavin-dependent halogenase and malbrancheamide synthase.....	111
4.2.2	MalA performs bromination reactions when using bromide as a source ion	112
4.3	Conclusion.....	114
4.4	Methods.....	117
4.5	Appendix	120
5	Future Work.....	125
	References.....	129

List of Figures

Figure 1-1. Sources of natural products. (Left) Chinese herbal remedies. (Center) The willow tree, the source of salicylic acid and aspirin. (Right) Penicillium fungus from which penicillin was isolated.	1
Figure 1-2. Examples of prenylated fungal indole alkaloids, their producing organisms, and their biological activities (if known).	3
Figure 1-3. Depiction of the bicyclo[2.2.2]diazaoctane core that defines this class of fungal indole alkaloids.	5
Figure 1-4. Comparison of biosynthetic gene clusters from <i>A. protuberus</i> , <i>A. amoenus</i> , <i>P. fellutanum</i> , and <i>M. aurantiaca</i> . Genes identified with comparable function are depicted in the same color across gene clusters.	11
Figure 1-5. The basic components of a Diels-Alder reaction.	13
Figure 2-1. Representative fungal prenylated indole alkaloids bearing the spirooxindole moiety.	17
Figure 2-2. (A) Native reaction for NotI and NotI' based on catalytic activity against (+) and (-)-16. (B) HPLC analysis depicting extracted ion chromatograms (EICs) of (a) authentic (+)-17; (b) NotI' + (-)-16; (c) NotI + (-)-16; (d) authentic (-)-16.	22
Figure 2-3. (A) Observed conversion from Notoamide T to Notoamide T9 by NotI. (B) HPLC analysis of NotI in vitro reaction with Notoamide T (15) to generate new compound Notoamide T9 (19): (a) 15 + NotI'; (b) 15 + NotI; (c) 15 in reaction solution without enzyme. The asterisk denotes a possible diastereomer of Notoamide T (15). (C) Planar	

structure of Notoamide T9 (19) showing COSY correlation with bold bonds and HMBC correlations with arrows.....	25
Figure 2-4. Proposed biosynthetic conversion of (±)-16 to (±)-17.....	30
Figure 2-5. (A) 4-12% Bis-Tris in MES buffer SDS page analysis of NotI and NotI'. The calculated molecular weight of NotI is 47.1 kDa and the calculated molecular weight of NotI' is 49.2 kDa. (B) 4-12% Bis-Tris in MOPS buffer SDS page analysis of PhqK. The calculated molecular weight of PhqK is 51.2 kDa.....	37
Figure 2-6. UV-Vis spectra of purified NotI protein solution (top) and the supernatant of denatured NotI protein solution (bottom). Denatured protein was generated by boiling for 15 minutes. The flavin cofactor peaks at 360 and 450 nm are present in both the native protein solution and the denatured supernatant.	38
Figure 2-7. Identification of FAD as the non-covalently bound NotI flavin cofactor. (a) FMN standard; (b) FAD standard; (c) NotI supernatant after denaturation of protein by boiling and centrifugation.	39
Figure 2-8. Kinetic curve of NotI against (-)-16.....	39
Figure 2-9. Substrates used to test NotI, NotI', and PhqK activities.	40
Figure 2-10. From EIC traces in Figure 2-2: (A) MS of (-)-16; (B) MS of (+)-17 formed from reaction with NotI; (C) MS of (+)-17 formed from reaction with NotI'	41
Figure 2-11. LC-MS Q-TOF analysis depicting EICs of (a) NotI' + (+)-16; (b) NotI + (+)-16; (c) <i>A. protuberus</i> isolated authentic (+)-16. Some (-)-17 is observed in the substrate trace (c). Integrating the traces to determine percent conversion yielded values of approximately 21% (-)-17 in trace (a), 15% (-)-17 in trace (b), and 14% (-)-17 in trace (c).....	42

Figure 2-12. Mass spectra of (A) (+)-16 standard; (B) (-)-17 produced by NotI; (C) (-)-17 produced by NotI' 43

Figure 2-13. LC-MS Q-TOF analysis depicting EICs of (a) NotI' + (±)-16; (b) NotI + (±)-16; (c) authentic (±)-16. The asterisk denotes a possible artifact from the reaction solution. 44

Figure 2-14. Mass spectra of (A) (±)-16 standard; (B) 17 produced by NotI; (C) 17 produced by NotI' 45

Figure 2-15. LC-MS Q-TOF analysis depicting EICs of (a) NotI' reaction with 7; (b) NotI reaction with 7; (c) authentic 7 standard. Product formed is denoted with P. 46

Figure 2-16. Mass spectra of (A) 7 standard; (B) Product formed from NotI + 7..... 47

Figure 2-17. LC-MS Q-TOF analysis depicting EICs of (a) NotI' reaction with 8; (b) NotI reaction with 8; (c) authentic 8 standard. Product formed is denoted with P. Asterisk denotes a possible diastereomer of 8..... 48

Figure 2-18. Mass spectra of (A) 8 standard with 3 ¹³C label; (B) Product formed from NotI + 8; (C) Product formed from NotI' + 8..... 49

Figure 2-19. LC-MS Q-TOF analysis depicting EICs of (a) NotI' reaction with 9; (b) NotI reaction with 9; (c) authentic 9 standard. Product(s) formed is denoted with P. 50

Figure 2-20. Mass spectra of (A) 9 standard; (B) Product formed from NotI + 9 observed at 594.3 seconds; (C) Product formed from NotI + 9 observed at 540.0 seconds; (D) Product formed from NotI + 9 observed at 526.6 seconds; (E) Product formed from NotI' + 9 observed at 595.7 seconds; (F) Product formed from NotI' + 9 observed at 538.5 seconds; (G) Product formed from NotI' + 9 observed at 526.0 seconds..... 52

Figure 2-21. LC-MS Q-TOF analysis depicting EICs of (a) NotI' reaction with 10; (b) NotI reaction with 10; (c) authentic 10 standard. Product(s) formed is denoted with P. Asterisk denotes possible diastereomer of 10.	53
Figure 2-22. Mass spectra of (A) 10 standard with 2 ¹³ C label; (B) Product formed from NotI + 10 observed at 621.5 seconds; (C) Product formed from NotI + 10 observed at 573.0 seconds; (D) Product formed from NotI' + 10 observed at 620.2 seconds; (E) Product formed from NotI' + 10 observed at 573.1 seconds.....	55
Figure 2-23. Mass spectra of (A) (±)-15 standard; (B) Product formed from NotI + (±)-15; (C) Product formed from NotI' + (±)-15.	56
Figure 2-24. LC-MS Q-TOF analysis depicting EICs of (a) NotI' reaction with (±)-18; (b) NotI reaction with (±)-18; (c) authentic (±)-18 standard. Product(s) formed is denoted with P. Asterisk denotes possible diastereomer of 18.....	57
Figure 2-25. Mass spectra of (A) (±)-18 standard; (B) Product formed from NotI + (±)-18; (C) Product formed from NotI' + (±)-18.	58
Figure 2-26. ¹ H NMR spectrum of Notoamide T9 (19) recorded at 700 MHz (in DMSO-d ₆)	59
Figure 2-27. ¹³ CNMR spectrum of Notoamide T9 (19) recorded at 700 MHz (in DMSO-d ₆)	60
Figure 2-28. HSQCAD spectrum of Notoamide T9 (19) recorded at 700 MHz (in DMSO-d ₆) ..	61
Figure 2-29. gCOSY spectrum of Notoamide T9 (19) recorded at 700 MHz (in DMSO-d ₆)	62
Figure 2-30. gHMBCAD spectrum of Notoamide T9 (19) recorded at 700 MHz (in DMSO-d ₆)	63
Figure 2-31. LC-MS Q-TOF analysis depicting EICs of (a) PhqK reaction with 8; (b) authentic 8 standard. Product(s) formed is denoted with P.	64
Figure 2-32. Mass spectra of (A) 8 standard with 3 ¹³ C label; (B) Product formed from PhqK + 8.	65

Figure 2-33. LC-MS Q-TOF analysis depicting EICs of (a) PhqK reaction with 9; (b) authentic 9 standard. Product(s) formed is denoted with P. 66

Figure 2-34. Mass spectra of (A) 9 standard; (B) Product formed from PhqK + 9. 67

Figure 2-35. LC-MS Q-TOF analysis depicting EICs of (a) PhqK reaction with 10; (b) authentic 10 standard. Product(s) formed is denoted with P. 68

Figure 2-36. Mass spectra of (A) 10 standard with 2 ¹³C label; (B) Product formed from PhqK + 10..... 69

Figure 2-37. LC-MS Q-TOF analysis depicting EICs of (a) PhqK reaction with 15; (b) authentic 15 standard. Product(s) formed is denoted with P. 70

Figure 2-38. Mass spectra of (A) 15 standard; (B) Product formed from PhqK + 15. 71

Figure 2-39. LC-MS Q-TOF analysis depicting EICs of (a) PhqK reaction with 20; (b) authentic 20 standard. Product(s) formed is denoted with P. 72

Figure 2-40. Mass spectra of (A) 20 standard; (B) Product formed from PhqK + 20. 73

Figure 2-41. LC-MS Q-TOF analysis depicting EICs of (a) PhqK reaction with 21; (b) authentic 21 standard. Product(s) formed is denoted with P. 74

Figure 2-42. Mass spectra of (A) 21 standard with 2 ¹³C label; (B) Product formed from PhqK + 21..... 75

Figure 2-43. LC-MS Q-TOF analysis depicting EICs of (a) PhqK reaction with 22; (b) authentic 22 standard. Product(s) formed is denoted with P. 76

Figure 2-44. Mass spectra of (A) 22 standard; (B) Product formed from PhqK + 22. 77

Figure 2-45. LC-MS Q-TOF analysis depicting EICs of (a) PhqK reaction with 23; (b) authentic 23 standard. Product(s) formed is denoted with P. 78

Figure 2-46. Mass spectra of (A) 23 standard; (B) Product formed from PhqK + 23. 79

Figure 3-1. Indole ring and two types of prenyl modifications.	81
Figure 3-2. The classical mevalonate (MVA) pathway to form IPP and DMAPP.....	82
Figure 3-3. Examples of known prenyltransferases and the positions they modify along the indole ring. Actual substrate structures are not shown for simplicity.....	83
Figure 3-4. Malbrancheamide gene cluster.....	84
Figure 3-5. (A) Observed in vitro reaction containing MalE, DMAPP, and Brevianamide F. (B) HPLC traces depicting (a) Brevianamide F in reaction with MalE and (b) Brevianamide F in reaction with no enzyme.	86
Figure 3-6. Predicted prenyltransferase reaction yielding premalbrancheamide (6).....	87
Figure 3-7. Deprotection of compound 7 will yield putative native substrate 8, which spontaneously oxidizes to form 9.	88
Figure 3-8. Reactions with 10 successfully generate product 11. HPLC traces depict (a) reaction containing 10 and MalE enzyme and (b) reaction containing 10 and no enzyme. A slight shift in trace (b) was observed for substrate 10 due to possible pump error.	88
Figure 3-9. Observed enzymatic reaction containing MalE and synthesized substrate.....	89
Figure 3-10. Reactions containing 8. HPLC traces of (a) authentic premalbrancheamide standard, (b) MalE with synthetic product 8, (c) synthetic product 8 (seen as 9) from deprotection of 7, and (d) 7 standard.....	91
Figure 3-11. Alternative order of biosynthesis where prenylation occurs before loading onto the NRPS.....	93
Figure 3-12. Alternative order of biosynthesis where a separate enzyme is responsible for the stabilization of the prenylated intermediate and Diels-Alder reaction.	93
Figure 3-13. Representative fungal prenylated indole alkaloids.	98

Figure 3-14. Mass spectrum of substrate 10 with [M+H] peak at 270.05 <i>m/z</i>	104
Figure 3-15. Mass spectrum of product 11 with [M+H] peak at 338.00 <i>m/z</i>	104
Figure 3-16. Mass spectrum of compound 9 with [M+H] peak at 265.80 <i>m/z</i>	105
Figure 3-17. Mass spectrum of compound 7 with [M+H] peak at 508.15 <i>m/z</i>	105
Figure 3-18. Mass spectrum of deprotected 7 appears as 9 with [M+H] peak at 266.00 <i>m/z</i>	105
Figure 3-19. Mass spectrum of compound 12 with [M+H] peak at 336.00 <i>m/z</i>	106
Figure 3-20. Mass spectrum of compound 13 with [M+H] peak at 334.10 <i>m/z</i>	106
Figure 3-21. Mass spectrum of standard premalbrancheamide 6 with [M+H] peak at 336.10 <i>m/z</i>	106
Figure 4-1. Characterized tryptophan halogenase reactions.	109
Figure 4-2. Results from incorporation studies using isotopically labeled premalbrancheamide.	109
Figure 4-3. Chlorination reactions on malbrancheamide B and isomalbrancheamide B produce malbrancheamide using MalA.	111
Figure 4-4. Bromination reactions on malbrancheamide B and isomalbrancheamide B produce malbrancheamide D and isomalbrancheamide D using MalA.	112
Figure 4-5. HPLC traces of reactions using MalA and malbrancheamide B. HPLC traces depict (a) negative control reaction with no enzyme, (b) reaction + MalA + NaCl, (c) reaction + MalA + NaBr.	113
Figure 4-6. Traces of reactions containing MalA and isomalbrancheamide B. HPLC traces depict (a) negative control reaction with no enzyme, (b) reaction + MalA + NaCl, (c) reaction + MalA + NaBr.	113
Figure 4-7. Currently discovered malbrancheamides with different halogen modifications.....	115

Figure 4-8. Mass spectrum of malbrancheamide B (2) with [M+H] observed at 370.15 m/z....	120
Figure 4-9. Mass spectrum of malbrancheamide product (4) from reaction with malbrancheamide B substrate. [M+H] observed at 404.10 m/z.....	120
Figure 4-10. Mass spectrum of malbrancheamide D product (5) from reaction with malbrancheamide B substrate. [M+H] observed at 448.10 m/z.....	121
Figure 4-11. Mass spectrum of isomalbrancheamide B (3) with [M+H] observed at 370.15 m/z.....	121
Figure 4-12. Mass spectrum of malbrancheamide product (4) from reaction with isomalbrancheamide B substrate. [M+H] observed at 404.05 m/z.....	121
Figure 4-13. Mass spectrum of isomalbrancheamide D product (6) from reaction with isomalbrancheamide B substrate. [M+H] observed at 448.05 m/z.....	122
Figure 4-14. MalA protein sequence with BLAST tryptophan halogenase domain identification and Lys78 highlighted.....	123

List of Tables

Table 1-1. Comparison of amino acid sequences of Not and NotI' and description of the putative function of each gene.....	7
Table 2-1. Comparison of amino acid sequences of Not and NotI'	20
Table 2-2. Structures of substrates tested and summary of products formed in reactions with NotI, NotI', and PhqK	23
Table 2-3. Structures of monooxopiperazine substrates tested and summary of products formed in reactions with PhqK.....	24
Table 2-4. NMR spectroscopic data for Notoamide T9 (19) in DMSO-d6 at 700 MHz.....	27
Table 2-5. Primers for NotI, NotI', and PhqK intron removal and amplification.....	36
Table 3-1. Predicted functions of gene products from the malbrancheamide gene cluster.	84

List of Schemes

Scheme 1-1. Notoamide biosynthetic pathway. Biochemically confirmed and characterized gene products are colored in red.....	8
Scheme 1-2. Proposed malbrancheamide biosynthetic pathway. Gene products that have been biochemically characterized are colored in red.	12
Scheme 2-1. Putative biosynthetic pathway of the Stephacidin and Notoamides. Gene products that have been biochemically characterized are labeled in red.	18
Scheme 3-2. Precursor incorporation experiments of monooxpiperazine and dioxopiperazine substrates.....	99
Scheme 3-3. Biomimetic synthesis of pre-malbrancheamide.....	101
Scheme 3-4. Biomimetic synthesis of spiromalbramide.....	103
Scheme 4-1. Adjusted malbrancheamide biosynthetic pathway based on MalA investigation results.....	114

Abstract

Comparative Investigation of Key Biosynthetic Transformations in Fungal Indole Alkaloid Natural Product Pathways

**by
Hong T. Tran**

Chair: David H. Sherman

My dissertational research has focused on the elucidation of three key biosynthetic steps involved in the formation of fungal indole alkaloid natural products. Beginning with the comparative analysis of four assembled putative gene clusters, we performed a detailed annotation of the predicted gene functions and proposed a biosynthetic pathway for each compound: (+)-notoamide, (-)-notoamide, malbrancheamide, and paraherquamide. Although these molecules have demonstrated interest in biological activity and intriguing chemical synthesis, our understanding of their biosynthesis has been limited. Therefore, we sought a stronger biochemical understanding of the biosynthetic enzymes involved in the formation of these molecules. Additionally, an intriguing intramolecular Diels-Alder mechanism is expected to occur in the biosyntheses of these bicyclo[2.2.2]diazaoctanes. Although the Diels-Alder reaction has been predicted to be involved in the formation of many natural products, the biochemical mechanism has remained fairly elusive and thus has been a topic of intense debate within the field.

Firstly, NotI, NotI', and PhqK were identified as flavin monooxygenases from the notoamide and paraherquamide gene clusters. These enzymes catalyze an epoxidation followed by semipinacol rearrangement to generate the spirooxindole moiety found in this class of compounds. Additionally, their utility as tools in synthetic biology was demonstrated by the wide range of flexibility of substrates accepted by these enzymes to broaden the pool of chemical diversity, yielding a new metabolite named notoamide T9. However, further efforts to optimize the catalytic activities of these enzymes is likely necessary in order to develop an effective approach to extend structural diversification of the bicyclo[2.2.2]diazaoctanes.

Second, we pursued a thorough biochemical investigation of the MalE prenyltransferase as the primary candidate for the intramolecular Diels-Alder reaction in the malbrancheamide biosynthetic pathway. Early experiments demonstrated the ability of MalE to reverse prenylate early intermediate dipeptides. However, reactions containing the putative native substrate led to the conclusion that MalE is a capable reverse prenyltransferase, but it does not seemingly perform the intramolecular Diels-Alder reaction. Interestingly, the lack of cyclization to form the Diels-Alder product supports the prediction that a biocatalyst is needed to facilitate the reaction within the biosynthetic system.

Finally, we investigated the halogenase MalA from the malbrancheamide pathway as an alternate candidate for the Diels-Alder reaction. The enzyme demonstrated catalytic activity and performed a halogenation event as predicted. However, contrary to expectations, the enzyme is only able to perform the second halogenation to form the final metabolite malbrancheamide, rather than the initial halogenation on premalbrancheamide. Interestingly, we were also able to generate new metabolites with mixed halogen substituents named malbrancheamide D and isomalbrancheamide D.

In summary, we elucidated three key steps in bicyclo[2.2.2]diazaoctane biosynthesis. These studies contribute directly to the understanding of complex fungal biosynthetic enzymes and the transformations they catalyze. Furthermore, these enzymes have demonstrated utility in diversification of chemical structures in this family of compounds, and thus have implications in their use as biocatalysts.

Chapter 1

Introduction to fungal indole alkaloid natural products

1.1 Natural products are a rich source of bioactive molecules with interesting chemistry

Long ago, before we began to call these compounds “natural products,” herbalists had been collecting and identifying plants that could be used to treat ailments and disease. Herbal medicine can be collected from the various parts of the plant: seeds, roots, berries, etc., and are often used to treat disease or increase the vitality of the patient.¹ Even in my own life, I was raised by parents who purchased and used eastern remedies to treat illness. Today, although we no longer rely exclusively on herbal medicines to treat pain or disease, we still use the active ingredients contained within those sources that have been identified and produced for



Figure 1-1. Sources of natural products. (Left) Chinese herbal remedies. (Center) The willow tree, the source of salicylic acid and aspirin. (Right) Penicillium fungus from which penicillin was isolated.

consumption. Aspirin, for example, was developed from salicylic acid collected from the willow tree, which was known to provide relief from pain since its historical use by the Babylonians.² Penicillin, another well-known natural product, was initially identified in the 1920s and gave way to the beginning of the antibiotic age. Since then, a class of antibiotics derived from

penicillin has been developed to treat pneumococcal, streptococcal, meningococcal, and gonococcal infections.³ This process of developing medicine from an identified lead compound isolated from a natural source drives much of our pharmaceutical industry today.⁴ Based on these criteria, natural products (NPs) have accounted for approximately 47% of the new drug discoveries in the past 25 years.⁵

Eukaryotes, particularly plants and fungi, have long been a source of unique and effective natural products, although their potential as a resource for NP discovery is frequently understated.⁶ High environmental stress, along with an impressive ability to absorb nutrients from the soil or decomposing material, drives the incorporation of foreign chemical components into product formation.⁷ While these complex interactions between the environment and the producing organism may produce useful and unique NPs, they also contribute to the difficulty of investigating or replicating the production of these organisms within a laboratory setting. Another example of an important therapeutic derived from plants is taxol, an important anticancer agent discovered in the 1970s. Taxol is isolated from the bark of yew and unmodified when sold to the consumer.⁸ The story of taxol presents an interesting case, where the producing organism *Taxus brevifolia* is an endangered species but the most reliable source of the low toxicity, broad-spectrum anticancer agent.⁹ It is from this impending crisis that the motivation arose to find alternative approaches to obtaining precious materials like taxol. The need for alternative approaches to developing useful medications, along with the desire to generate new and interesting bioactive molecules, drives our motivation to understand the biosynthesis of these unique NPs within their producing organisms.

1.2 Fungal indole alkaloids comprise a class of natural products

The class of fungal indole alkaloids includes primarily the prenylated indole alkaloids and ergot alkaloids.^{10,11} The prenylated indole alkaloids, as is suggested by their name, are characterized by two main components: an indole ring (usually tryptophan) that is modified by prenyltransferase enzymes to install isoprene units on the molecule.¹² Ergot alkaloids, on the other hand, are formed from a tryptophan moiety that has been prenylated before undergoing a series of oxidation reactions to form their characteristic tetracyclic ergoline ring.¹³ The compounds are typically produced by *Penicillium* or *Aspergillus* strains and can be either terrestrial or marine in origin.¹⁰ Occasionally, the compounds will also be found in organisms in different domains of life. Lyngbyatoxin and Hapalindole H, for example, are produced by cyanobacteria,^{14,15} and the flustramines are isolated from a bryozoan.¹⁶

One of the largest groups within the fungal indole alkaloids is the group of prenylated derivatives constructed from L-proline and L-tryptophan.¹² The group includes the insecticidal brevianamides and sclerotiamides, anthelmintic paraherquamides, calmodulin-inhibitory

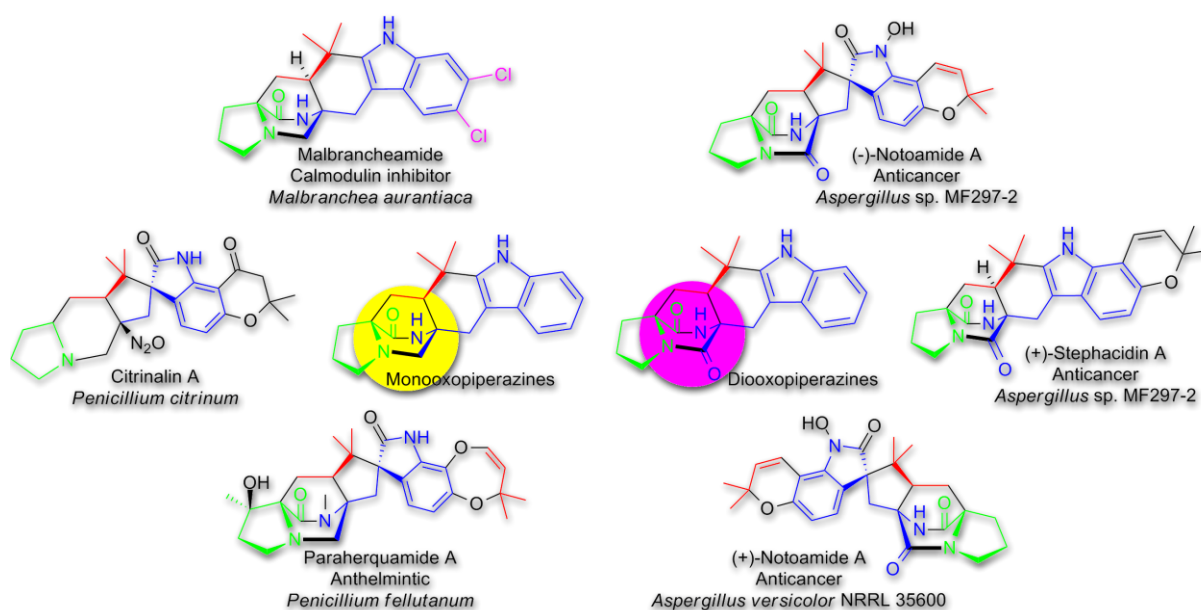


Figure 1-2. Examples of prenylated fungal indole alkaloids, their producing organisms, and their biological activities (if known).

malbrancheamides, mycotoxin fumitremorgin, anticancer notoamides, stephacidins, and citrinadins, among others.¹⁷⁻²¹ This class of compounds depicts a wide variability in biological activities, along with a diversity in chemical structures of the final compounds. Brevianamide F, the dipeptide fusion of proline and tryptophan, is the most common precursor to the formation of the majority of these molecules and is thus presumed to be an intermediate in the formation of aforementioned natural products.²²

One class of prenylated fungal alkaloids are the bicyclo[2.2.2]diazaoctanes, a family of compounds typified by their unique core (Figure 1-3).²³ The members of the bicyclo[2.2.2]diazaoctane alkaloid family demonstrate various desirable biological activities from anti-parasitic to anti-cancer, despite sharing the same core structure.^{24,25} We have been interested in the biosynthesis of these molecules not only for their pharmacological activities but also for their unique and complex chemistry. Extensive efforts have been put forth by the Williams group to synthesize these molecules in their entirety.²⁶ In particular, the formation of the bicyclo[2.2.2]diazaoctane ring system is expected to occur via an intramolecular Diels-Alder (IMDA) reaction as initially proposed in 1970 by Sammes and Birch.²⁷ While the reaction was initially performed using an intramolecular S_N2' cyclization,²⁸ later applications of a biomimetic Diels-Alder reaction have shown that the approach is a reasonable method for obtaining the bicyclo ring system, reinforcing the hypothesis that a biosynthetic Diels-Alder enzyme could exist in nature.²⁹

Along with the formation of the bicyclo[2.2.2]diazaoctane core, the various compounds within the family each bring with them a unique and rare set of biosynthetic origins and often potent bioactivities. An intriguing story of enantioselective biosynthesis can be found in the notoamides, where a terrestrial fungus produces one set of enantiomers while a marine fungus produces the opposite set.³⁰ The fumitremorgins are a tremorgenic group of mycotoxins that have also recently demonstrated possible utility as an anticancer agent.^{18,31} The malbrancheamides add halogen substituents to further diversify the chemistry found in these molecules.¹⁷ Other examples include the stephacidins,³² paraherquamides,³³ sclerotiamides,²⁰ and brevianamides.²⁷ Additionally, the bicyclo[2.2.2]diazaoctanes can be divided into two major categories: the



Figure 1-3. Depiction of the bicyclo[2.2.2]diazaoctane core that defines this class of fungal indole alkaloids.

monooxopiperazines and the dioxopiperazines (Figure 1-3). These compounds have demonstrated biological interest as potential anticancer agents and anthelmintic treatments, among others, and unexpectedly manage to do so despite sharing the same bicyclo core. That the same core molecule is produced by so many different organisms from so many different origins in nature is in and of itself a complex and fascinating story in the evolution of these biosynthetic gene clusters. Perhaps diversification was brought about by tailoring steps introduced or removed from the central gene cluster throughout many generations of fungi carried from one continent to another.

1.3 The Notoamides

The notoamides were discovered in 2007 from a marine derived fungus, *Aspergillus protuberus* (formerly known as *Aspergillus* MF297-2), which was isolated from the mussel *Mytilus edulis* collected off the Noto Peninsula of Japan by the Tsukamoto group.³⁴ These compounds added to the already existing library of bicyclo[2.2.2]diazaoctane fungal alkaloids, then including the stephacidins and paraherquamides. The notoamides were discovered during an extensive search for compounds that exhibited interesting pharmacological activities,^{35–38} and particularly during a screen for cytotoxic activity and possible use as anticancer agents. Since their original discovery in 2007, the notoamides have since seen an extensive expansion in the number of related metabolites,^{39–41} stretching today from molecules A through V (see Chapter 2).

In addition to the isolation of new notoamide compounds, extensive synthetic approaches have been performed by the Williams laboratory. Among them, key chemical transformations were addressed using biomimetic syntheses. The first investigation addressed the formation of the spirooxindole ring system via a pinacol rearrangement, resulting in the synthesis of notoamides C and D.⁴² The synthesis of notoamide J similarly addressed the formation of an intermediate via a pinacol rearrangement.⁴³ Notoamide S has been recently synthesized as a means to obtain an important, pivotal intermediate as the final common precursor between *A. amoenus* and *A. protuberus* before enantio-divergence.⁴⁴ Racemic stephacidin A was also synthesized, and in the process added to the desire to understand how the *Aspergillus* strains controlled the enantiomeric divergence presented by the notoamide group of compounds.⁴⁵

The biomimetic syntheses were important to the understanding of the biosynthetic pathways that drive the formation of notoamide, but they also provided an approach to obtaining compounds for isotopically enriched precursor incorporation studies. Extensive collaborative efforts have since been put forth by the Sherman, Williams, and Tsukamoto laboratories to test

Table 1-1. Comparison of amino acid sequences of Not and NotI' and description of the putative function of each gene.

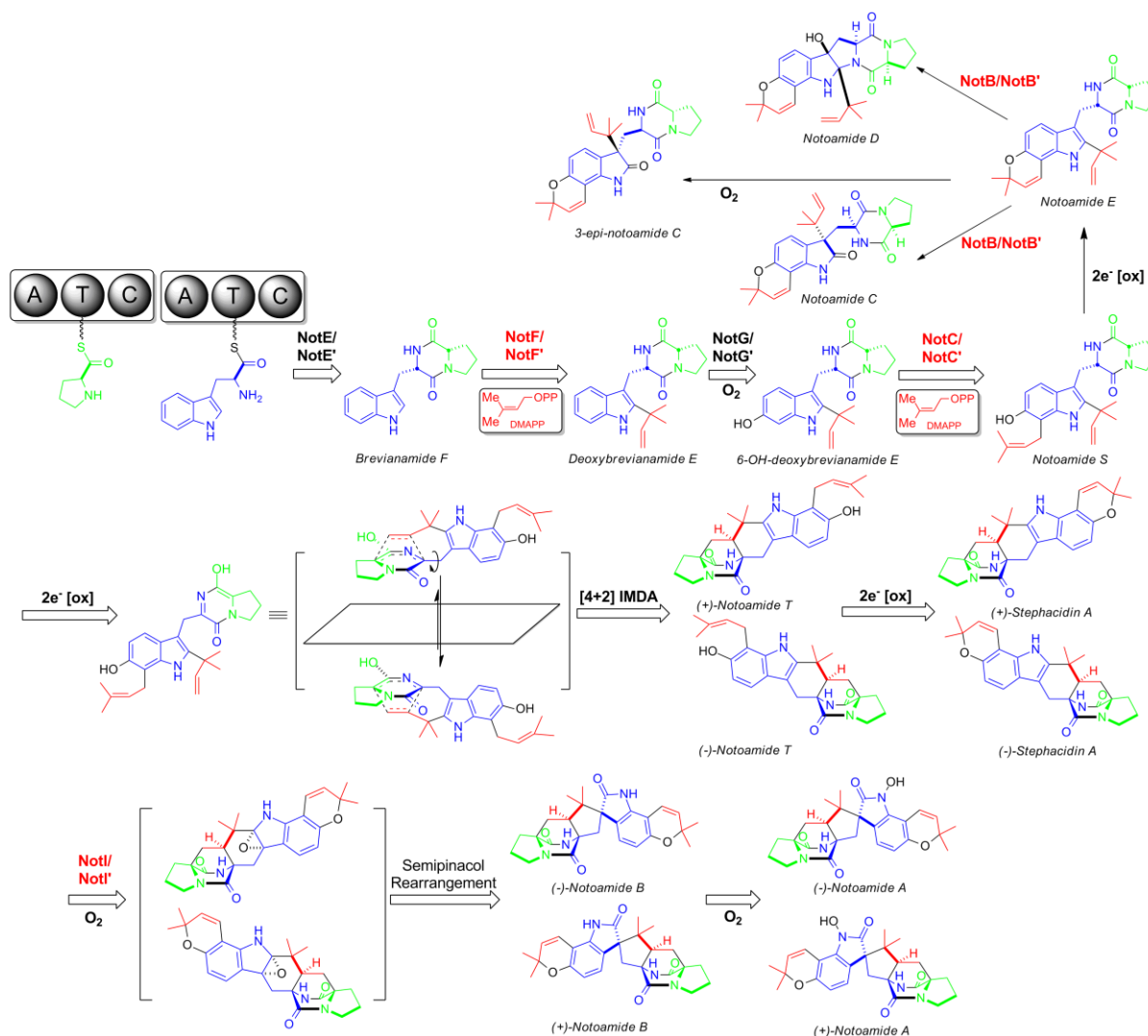
Not proteins <i>A. protuberus</i> (AA)	Not' proteins <i>A. amoenus</i> (AA)	Putative Function	(% AA identity)
NotA (339)	NotA' (334)	Negative regulator	70%
NotB (456)	NotB' (455)	FAD monooxygenase	88%
NotC (427)	NotC' (426)	Prenyltransferase	87%
NotD (621)	NotD' (612)	Oxidoreductase	80%
NotE (2241)	NotE' (2225)	NRPS [A-T-C-A-T-C]	79%
NotF (453)	NotF' (435)	Prenyltransferase	79%
NotG (544)	NotG' (544)	P450 monooxygenase	87%
NotH (502)	NotH' (499)	P450 monooxygenase	84%
NotI (434)	NotI' (433)	FAD monooxygenase	85%
NotJ (371)	NotJ' (362)	Unknown	80%

the incorporation of these molecules into the producing organisms. Upon feeding isotopically labeled stephacidin A precursor to the *A. amoenus* and *A. protuberus* producing organisms, the compound was found to be incorporated into notoamide B and sclerotiamide, indicating that both metabolites can be formed downstream of intermediate stephacidin A.⁴⁵ Notoamide T was also synthesized with isotopic labeling, and incorporation studies showed that the compound could be incorporated into stephacidin A and notoamide B, while synthetic approaches also showed possible formation of 6-*epi*-stephacidin A.⁴⁶

As we arrived closer to an understanding of the biosynthetic steps involved in the generation of the notoamide compounds, we still lacked biochemical evidence to support the steps we had proposed. Thus, the collaboration began a thorough and detailed bioinformatic analysis of the gene clusters involved in notoamide biosynthesis. The genomes of *A. amoenus* and *A. protuberus* were sequenced and annotated for candidate genes involved in the formation of secondary metabolites, marking the first biosynthetic gene cluster for the class of bicyclo[2.2.2]diazaoctane fungal alkaloids (Table 1-1).⁴⁷ Two putative prenyltransferases, NotC and NotF, were identified from the biosynthetic gene cluster and expressed for biochemical

characterization. In this study, NotF was determined to be a reverse prenyltransferase responsible for the formation of deoxybrevianamide E. NotC, on the other hand, was determined to be a normal prenyltransferase and the notoamide S synthase.

These data collected by biomimetic syntheses, isotope labeling incorporation studies, and bioinformatic and biochemical investigations together formed the foundation of our understanding of notoamide biosynthesis. Through further comparative analysis with other sequenced genomes from the bicyclo[2.2.2]diazaoctane family of producing organisms, we were



Scheme 1-1. Notoamide biosynthetic pathway. Biochemically confirmed and characterized gene products are colored in red.

able to generate a putative biosynthetic pathway resulting in the formation of notoamide A (Scheme 1-1).⁴⁸ Briefly, the formation begins with the nonribosomal peptide synthetase (NRPS) NotE, which fuses proline to tryptophan and offloads the common indole alkaloid precursor, brevianamide F, via a condensation domain. Brevianamide F is then prenylated by NotF to yield deoxybrevianamide E, which is then hydroxylated by NotG (unconfirmed) to yield 6-OH-deoxybrevianamide E. Notoamide S is synthesized by NotC and represents a branching point for notoamide biosynthesis. If the molecule does not undergo IMDA construction to form the bicyclo[2.2.2]diazaoctane ring, it will instead undergo a pyran ring closure to give notoamide E. Notoamide E will then undergo an epoxidation and pinacol rearrangement facilitated by NotB to form notoamides C and D. If, at the branch point, notoamide S instead undergoes the IMDA reaction, notoamide T will be formed instead. It is at this biosynthetic step that the enantio-divergence is observed. Notoamide T then undergoes a pyran ring closure to form stephacidin A, which then proceeds through a pinacol rearrangement reaction via NotI to yield notoamide B. Notoamide B is finally hydroxylated to yield notoamide A.

The biosynthetic pathway of notoamide presents a number of particularly rare and intriguing biosynthetic reactions. The first is the unusually constructed NRPS, which does not follow the typical C-A-T domain organization of these megasynthases.⁴⁹ The second are the semipinacol rearrangement reactions that generate the spirooxindole moiety of these molecules. This is a reaction infrequently observed in natural products and even less understood from a biochemical perspective.⁵⁰ Finally, the answer to whether an IMDA enzyme exists in nature remains elusive to the biosynthetic community. Although biomimetic syntheses have demonstrated the logic of constructing the bicyclo[2.2.2]diazaoctane core via IMDA reaction, there has been little to no evidence of an enzyme that can catalyze an IMDA reaction.

1.4 The Malbrancheamides

Malbrancheamide was originally discovered from *Malbranchea aurantiaca*, a fungus isolated from bat guano by the Mata laboratory.¹⁷ The compound was soon discovered to inhibit calmodulin (CaM) in a concentration-dependent manner, indicating its potential therapeutic use in a variety of ion channel regulatory functions including anti-tumoral, smooth muscle relaxants, and anti-psychotic effects.⁵¹ CaM is a widely used Ca²⁺-binding protein involved in the regulation of many Ca²⁺-dependent cellular activities, including but not limited to neurodegenerative disease, cancer, and inflammatory disease.⁵² Premalbrancheamide was shown to act as a functional inhibitor of phosphodiesterase 1 (PDE1), while the halogenated forms function as classical inhibitors that bind the CaM-Ca²⁺ complex, with the dichlorinated species showing the strongest affinity.⁵³ Currently, the malbrancheamides are the only members of the bicyclo[2.2.2]diazaoctanes to exhibit these clinical effects.

In comparison to its fellow bicyclo[2.2.2]diazaoctane compounds, malbrancheamide is currently the only identified molecule to contain halogen atoms in its structure. Halogenated molecules have demonstrated use in medicinal chemistry. Presence of halogens has been shown to be critical for the biological activity of many compounds, including vancomycin and chloramphenicol, and are a rapidly expanding category with over 3800 identified organohalogen compounds discovered by 2003.^{54,55} Nevertheless, halogenase mechanisms and their flexibility in substrate acceptance are still underexplored.⁵⁶⁻⁵⁸ Recent investigations have provided evidence supporting theories about the regioselective halogenation mechanisms, and attempts to reengineer the binding pocket to accept nonnative substrates for chemical transformation have been shown to be successful.⁵⁹⁻⁶¹

Similar to the notoamides, malbrancheamide has also been investigated through biomimetic syntheses and isotopically enriched precursor incorporation studies. Premalbrancheamide was synthesized and delivered to *M. aurantiaca* to demonstrate the formation of malbrancheamide B.⁶² Interestingly, no formation of isotopically labeled malbrancheamide was observed from this study. Synthetic schemes have also been applied to the formation of malbrancheamide and malbrancheamide B,²⁵ which demonstrated the variety of isomers that could be formed by the IMDA reaction by synthetic means. Efforts to overcome this challenge and produce an enantioselective product were developed to yield a domino reaction sequence with good diastereofacial control,⁶³ and eventually approaches were developed to yield

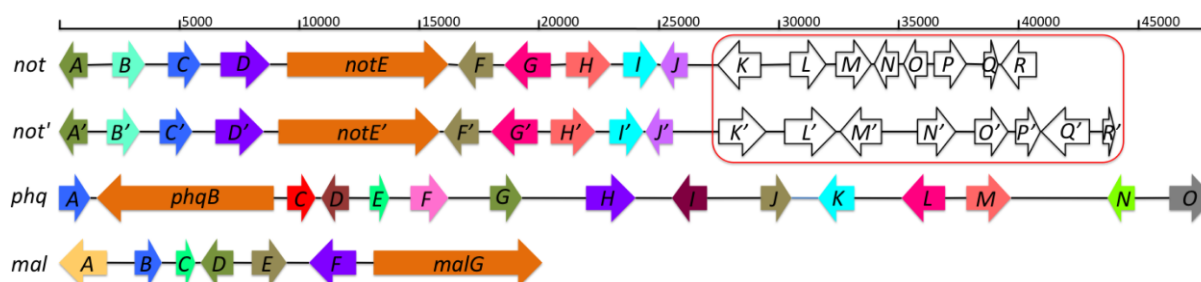
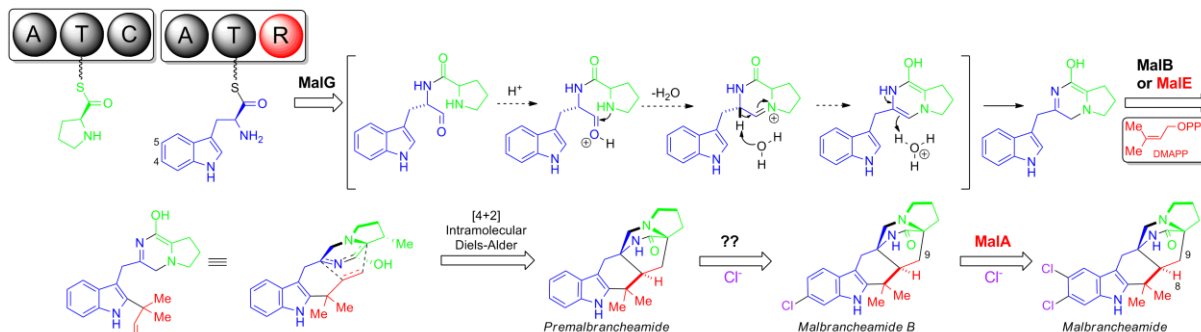


Figure 1-4. Comparison of biosynthetic gene clusters from *A. protuberus* (*not*), *A. amoenus* (*not'*), *P. fellutanum* (*phq*), and *M. aurantiaca* (*mal*). Genes identified with comparable function are depicted in the same color across

malbrancheamide B and its enantiomer, ent-malbrancheamide B.^{64,65}

The biochemical approach to elucidating the biosynthetic mechanisms involved in the formation of malbrancheamide was initiated in the Sherman laboratory in collaboration with the Williams group. Because we already had the added benefit of previously identifying the notoamide gene cluster, this time we could begin with a comparative analysis of putative biosynthetic gene clusters across the malbrancheamide, paraherquamide, and notoamide species (Figure 1-4).⁴⁸ The analysis facilitated the determination of homologous gene products based on amino acid sequence analysis. Homologous gene products were then assumed to perform the same or similar function within their respective biosynthetic systems. Based on these data, we



Scheme 1-2. Proposed malbrancheamide biosynthetic pathway. Gene products that have been biochemically characterized are colored in red.

were able to construct a putative biosynthetic scheme for the formation of malbrancheamide (Scheme 1-2). Briefly, proline and tryptophan are fused by the MalG NRPS, which offloads the product by a reductase domain to yield the aldehyde of the dipeptide. The reactive aldehyde group then facilitates the spontaneous cyclization to yield the azadiene, which is then reverse prenylated by MalB or MalE prenyltransferases to introduce the dienophile that can undergo IMDA construction to form premalbrancheamide. Premalbrancheamide is then chlorinated once to form malbrancheamide B and a second time to form malbrancheamide.

The malbrancheamide biosynthetic system also presents its own unique chemistry in a predicted total of three key steps. Firstly, the NRPS ends in a rare terminal reductase domain that is predicted to facilitate formation of the monooxopiperazine versus the dioxopiperazine core that would otherwise yield the common intermediate brevianamide F seen in the notoamide biosynthetic pathway (Scheme 1-1). Secondly, the biosynthesis of malbrancheamide is also proposed to undergo an IMDA reaction to form the bicyclo core. Lastly, premalbrancheamide would be halogenated to form malbrancheamide. The identification of only one halogenase initially suggested that it may be responsible for a sequential or simultaneous dichlorination, and thus presented an interesting question of how the substrate is accommodated within the active site of the protein for the halogenation reaction.

1.5 The intramolecular Diels-Alder hypothesis

The Diels-Alder reaction was developed in 1920 by Prof. Otto Diels and his student Kurt Alder.⁶⁶ It is an extremely versatile, commonly used reaction today in synthetic chemistry and earned Diels and Alder a Nobel Prize in 1950. The pericyclic [4+2] cycloaddition reaction has been studied thoroughly to understand the formation of endo- versus exo- products, and in the 1950s began to be applied to the total synthesis of natural products.⁶⁷ The numerous synthetic investigations performed suggested that nature was also capable of devising a strategy for performing the Diels-Alder reaction, and that the approach was likely involved in these natural product pathways. Additionally, the necessity of a Diels-Alder biocatalyst was supported by the presence of preceding intermediates, the necessity of a catalyzing action to generate the product, and the chirality of the resulting molecules.⁶⁸

Natural products formed by a presumed Diels-Alder mechanism occur frequently in nature, with well over 150 examples to date.⁶⁸ However, few biomolecules have been demonstrated to be involved with the reaction biosynthetically, and many have been met with justifiably skeptical debate. Of the more successful investigations include the use of antibodies.⁶⁹ Other investigations involved the use of RNA as ribozymes, which perform a reaction similar to the Lewis acid catalysis of the Diels-Alder reaction.^{70,71} Natural protein catalysts, on the other hand, have remained a more elusive subject of interest. Two proteins have been purified to homogeneity and shown to generate the Diels-Alder product from the substrate.⁷² However, the mechanism by which this occurs is still an intense topic of debate. The first of the two examples

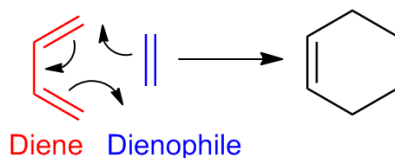


Figure 1-5. The basic components of a Diels-Alder reaction.

is LovB, a type I iterative PKS, that is involved in the synthesis of lovastatin, a cholesterol-lowering agent.⁷³ In reactions containing LovB and LovC incubated with the predicted hexaketide intermediate, the pericyclic reaction product was observed. However, the large molecular weight of LovB (335 kDa) is an inherent hurdle barring progress in further biochemical studies of the protein. The second of the two examples is the macrophomate synthase (MPS) enzyme.⁷⁴ Originally, the findings supported the identity of MPS as a potential Diels-Alderase.^{75,76} However, through quantum and molecular mechanics simulations,⁷⁷ combined with the solution to the crystal structure and further enzymology studies on the enzyme,^{78,79} evidence was found contradicting the Diels-Alder mechanism, instead supporting the formation of macrophomate by a Michael-aldol mechanism. More recently, during the investigation of spinosyn A biosynthesis, SpnF was determined to be a cyclase that catalyzes the [4+2] cycloaddition reaction.⁸⁰ While cyclization can occur nonenzymatically, the addition of SpnF was shown to increase the yield of product quantitatively. Furthermore, computational studies have supported the theory that SpnF serves as a scaffold or chaperone-like protein for the IMDA reaction, and that the enzyme additionally stabilizes the transition structure and thus reduces the activation energy of the reaction.⁸¹

Indeed, the existence of an enzymatic Diels-Alderase has long been sought after and is one of the main driving forces behind our investigation of the fungal indole alkaloid biosynthetic pathways. As described in sections 1.3 and 1.4, we expect that the formation of the bicyclo[2.2.2]diazaoctane core arises by an IMDA reaction. Due to the general lack of understanding of the biochemistry that drives this reaction, we believed that identifying the Diels-Alderase from any of these biosynthetic pathways would be a highly impactful contribution to the field. Similar to what has been previously proposed, we believed that our

Diels-Alderase would perform a dual-function, i.e., it would catalyze its biosynthetic reaction and simultaneously act as a scaffold for the IMDA reaction to occur. It was with this hypothesis in mind that we began our biochemical investigation of the biosynthetic pathways of the malbrancheamides, notoamides, and paraherquamides.

1.6 Dissertation directions and goals

For my own dissertation work described herein, I focused primarily on the elucidation of key chemical transformation steps from the malbrancheamide and notoamide biosynthetic pathways. I began by investigating our primary targets that we believed would be responsible for the IMDA reaction and investigated the putative identity of each gene product in the two gene clusters to identify the putative Diels-Alderase. The prenyltransferase in the malbrancheamide biosynthetic pathways was the primary target of interest. A second candidate would be the enzyme involved in the following step: the halogenase. The third primary candidate would be the NRPS megasynthase, in case the prenylation event occurs as an earlier event and our order for biosynthesis is incorrect. In the notoamide biosynthetic pathway, we believed that one of the oxidoreductases would be involved in the oxidation event preceding the IMDA reaction. NotB and NotI have been ruled out as candidates for this reaction by my colleague, Shengying Li, and myself, respectively.

I never identified the enzyme responsible for catalyzing the IMDA event. However, under the assumption that all biosynthetic genes are included within the gene clusters that we have mined, one of the gene products must be responsible for the Diels-Alder reaction. By process of elimination, the Diels-Alderase will be found eventually. However, the general lack of evidence and biochemical information available for Diels-Alderases makes the identification of the Diels-Alderase a very challenging investigation, as discussed in section 1.5. I am confident

that the Diels-Alderase will eventually be found, and that our understanding of the bicyclo[2.2.2]diazaoctane biosynthetic pathways will eventually lead us to the correct candidate. For my dissertation, I have contributed towards this goal by enhancing our understanding of the various rare and interesting biosynthetic transformations involved in the formation of these intriguing molecules. Rather than identifying the still elusive Diels-Alderase, my dissertation work therefore instead focuses on the identification and characterization of three key steps in fungal indole alkaloid biosynthesis, making a significant contribution overall to our understanding of these biosynthetic pathways.

Chapter 2

Formation of the spirooxindole moiety

2.1 Introduction

A semipinacol rearrangement is predicted to generate the spirooxindole moiety found in the Notoamides, Paraherquamides, and Spiromalbramide (Figure 2-1).^{82,83} Pinacol rearrangements have been proposed to occur in the biosynthetic pathways of various natural products, including

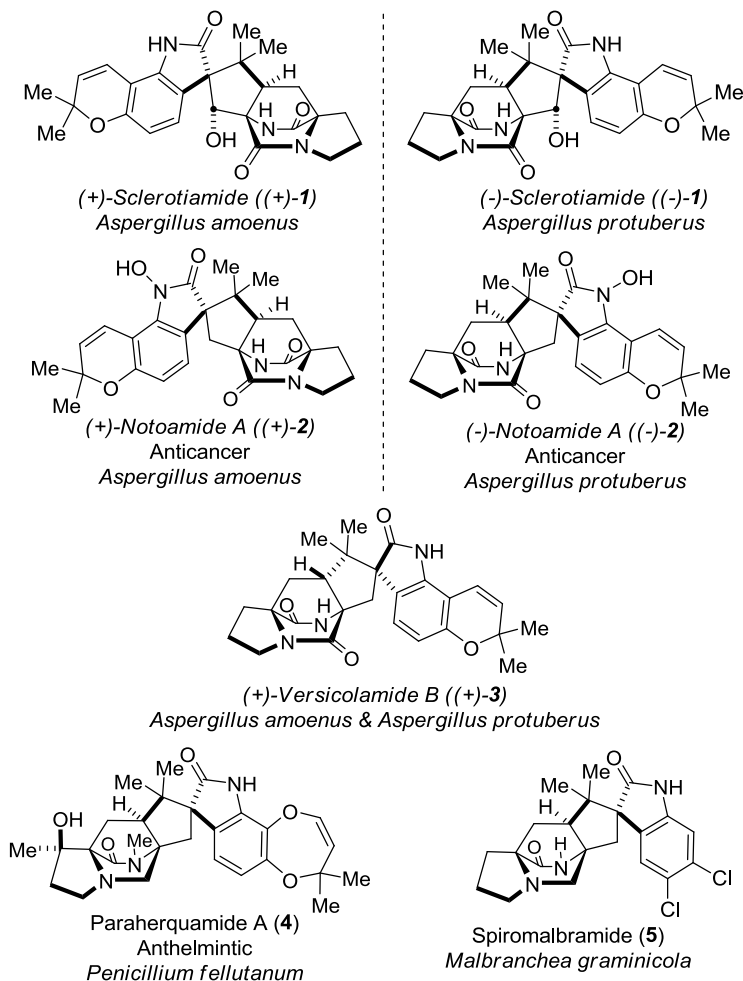
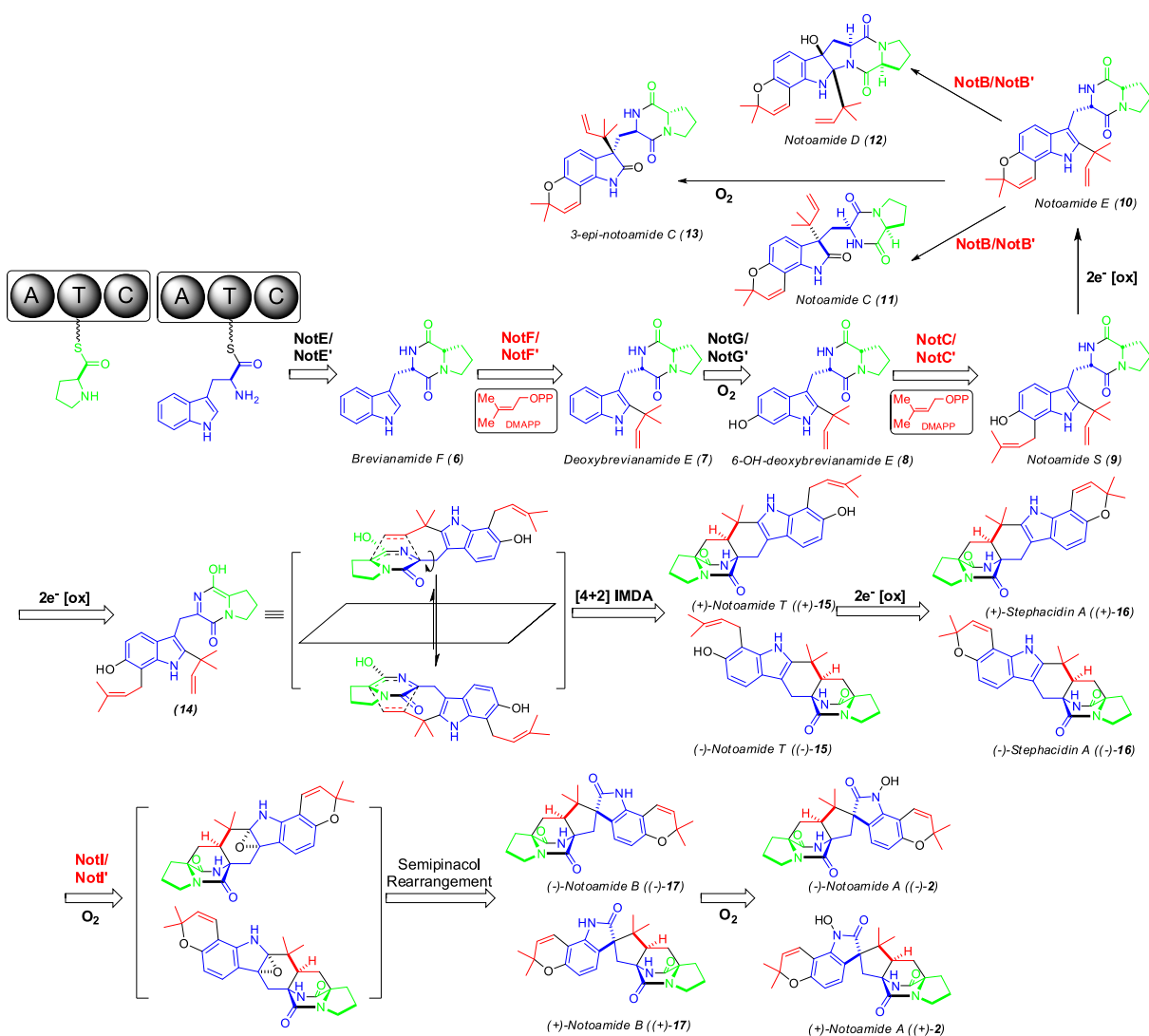


Figure 2-1. Representative fungal prenylated indole alkaloids bearing the spirooxindole moiety.

the Aurachins, 2-Tropolone, Brevianamides, and Spiromalbramide, among others.^{84–86}

Filamentous fungi, in particular, have been found to produce a number of spirocyclic compounds, including Geodin, Griseofulvin, Austinol, and Fumitremorgin.^{50,87–90} However, there has been little biochemical evidence to support the direct role of specific enzymes in the rearrangement reaction, leaving an incomplete understanding of the formation of these moieties in secondary metabolism.⁹¹

The Notoamides are a relatively new class of metabolites in the indole alkaloid



family.^{40,92} A fascinating finding regarding these fungal natural products is that (-)-Stephacidin A, (+)-Notoamide B, and (+)-Notoamide A are produced by the terrestrial strain *Aspergillus amoenus* (formerly *Aspergillus versicolor* NRRL 35600), while the enantiomeric products (+)-Stephacidin A, (-)-Notoamide B, and (-)-Notoamide A are produced by the marine *Aspergillus protuberus* (formerly *Aspergillus* sp. MF297-2).⁹³ The formation of enantiomeric natural products identified from one or more species is a highly unusual phenomenon that has been observed in less than 1% of the biosphere metabolome to date.⁹⁴ The existence of distinct metabolic systems that create exact antipodes suggests that the strains have evolved one or more biosynthetic gene products (e.g. NotD, NotH, and NotI) that catalyze an identical enzymatic reaction to produce and further modify enantiomeric compounds.²² To this end, extensive biomimetic synthetic schemes have been devised to generate Stephacidin A and Notoamide B.⁹⁵ These studies have supported the hypothesis that one or more biosynthetic enzymes determine the chirality of the molecule, however, the molecular mechanisms that control this divergence have remained a mystery. Thus, we reasoned that analysis of the flavin oxidases likely involved in formation of the spirooxindole functionality would provide further insights into the basis of enantiomeric induction in these systems, and whether these enzymes catalyze enantioselective reactions.

Table 2-1. Comparison of amino acid sequences of Not and NotI'

Not proteins (AA)	Not' proteins (AA)	Function	(% AA identity)
NotA (339)	NotA' (334)	Negative regulator	70%
NotB (456)	NotB' (455)	FAD monooxygenase	88%
NotC (427)	NotC' (426)	Prenyltransferase	87%
NotD (621)	NotD' (612)	Oxidoreductase	80%
NotE (2241)	NotE' (2225)	NRPS [A-T-C-A-T-C]	79%
NotF (453)	NotF' (435)	Prenyltransferase	79%
NotG (544)	NotG' (544)	P450 monooxygenase	87%
NotH (502)	NotH' (499)	P450 monooxygenase	84%
NotI (434)	NotI' (433)	FAD monooxygenase	85%
NotJ (371)	NotJ' (362)	Unknown	80%

The genomes of *A. protuberus* and *A. amoenus* have previously been sequenced in our laboratories.⁹⁶ The gene clusters were identified through *in silico* database mining, followed by open reading frame (*orf*) and BLAST analysis to complete a deeper annotation of the metabolic systems. These data, combined with previous isotopically enriched precursor incorporation studies supported our proposed biosynthetic pathway for the Notamides.²² Comparison of the two gene clusters shows an overall 71% DNA sequence identity (between *notA-J*), indicating a closely related ancestry between the two gene clusters and a high similarity between sequences of putative gene products (Table 2-1).⁹⁷ However, bioinformatic analysis provided a limited understanding of the biosynthetic pathway and little mechanistic information about the sequence divergence observed between the two enantiomeric natural products. Consequently, we were motivated to investigate the biochemical transformations involved in the formation of the Notoamides, and determine the basis for the structural branch-point that generates the antipodal indole alkaloid molecules.

Recently, significant progress has been made to elucidate the biosynthetic genes involved in the creation of the Notoamides (Scheme 2-1). NotF and NotC have previously been characterized as reverse and normal prenyltransferases, respectively, while NotB has been characterized as an FAD-dependent oxidase.^{82,96} Herein, we report the biochemical function of

NotI from *A. protuberus* as a flavin-dependent monooxygenase (FMO) that catalyzes a semipinacol rearrangement to generate the spirooxindole moiety found in many of the bicyclo[2.2.2] diazaoctane fungal indole alkaloids. We also report the biochemical activity of NotI' and PhqK as the first heterologously expressed and biochemically characterized gene products from *A. amoenus* and *P. fellutanum*, respectfully. Finally, we have demonstrated the ability to diversify the pool of Notoamide compounds by characterizing Notoamide T9 as a new metabolite generated through the remarkable substrate flexibility of homologues NotI, NotI', and PhqK.

2.2 Results

2.2.1 Determination of NotI and NotI' as the (\pm)-Notoamide B synthase via semipinacol rearrangement.

The functions of NotI and NotI', predicted FAD-dependent monooxygenases, were investigated. Compounds (+)-**16**, (-)-**16**, and (\pm)-**16** were separately incubated with NotI or NotI' at 28°C for approximately 16 hours (Figure 2-2A). Samples were extracted three times with CHCl₃ and subjected to analysis using LC-MS compared directly with synthetic standards (Figure 2-2B). The product **17** (448.2252 *m/z*) was observed by LC-MS Q-TOF for all reactions.

The reactions of NotI with Stephacidin A to generate Notoamide B were fit to Michaelis-Menten kinetics (Figure 2-8). The K_m and V_{max} values for NotI using (-)-**16** as substrate were determined to be $39 \pm 11 \mu\text{M}$ and $49 \pm 3 \mu\text{M}/\text{min}$, respectively. The k_{cat} was determined to be 20 min^{-1} , and the apparent specificity constant (k_{cat}/K_m) of the enzymatic reaction was shown to be $0.50 \mu\text{M}^{-1} \text{ min}^{-1}$.

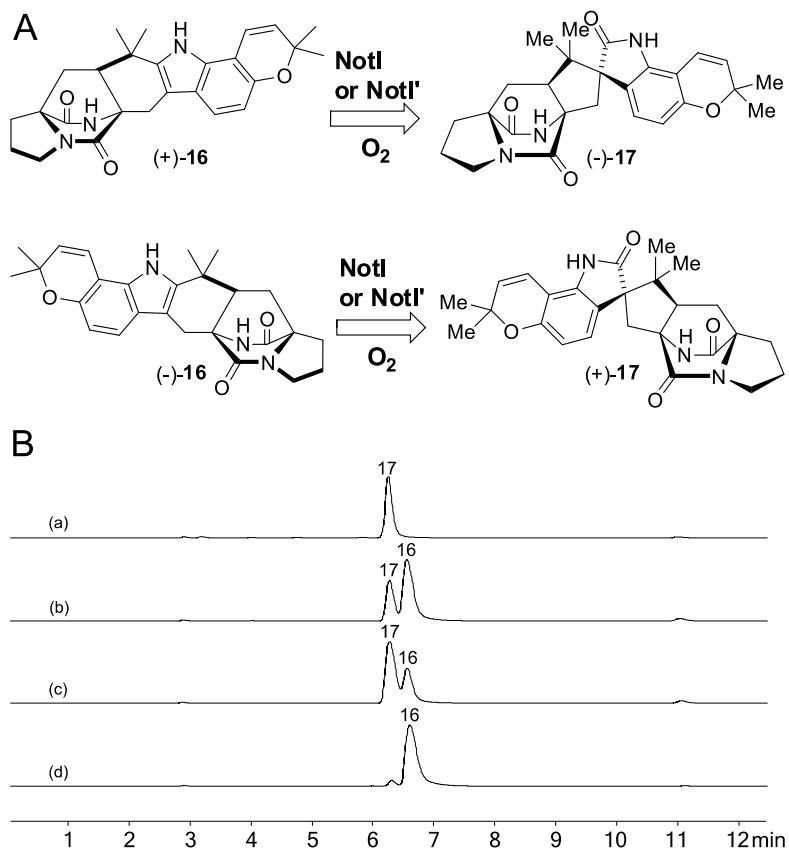


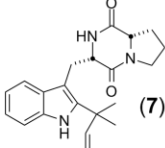
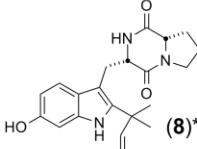
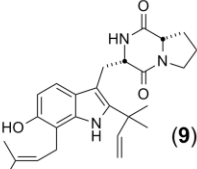
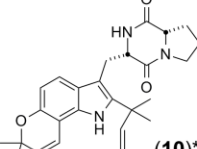
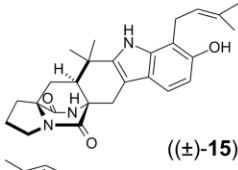
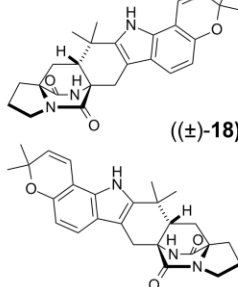
Figure 2-2. (A) Native reaction for NotI and NotI' based on catalytic activity against (+) and (-)-**16**. (B) HPLC analysis depicting extracted ion chromatograms (EICs) of (a) authentic (+)-**17**; (b) NotI' + (-)-**16**; (c) NotI + (-)-**16**; (d) authentic (-)-**16**.

2.2.2 Analysis of NotI Substrate Flexibility.

Next, we sought to determine the exact timing of epoxidation and pinacol rearrangement in Notoamide biosynthesis. Reactions were similarly conducted using NotI and NotI' with compounds **6**,⁹⁸ **7**,⁹⁸ **8**,⁹⁹ **9**,⁴⁴ **10**,⁴⁰ (\pm)-**15**,⁴⁶ (\pm)-**16**,¹⁰⁰ (\pm)-6-epi-stephacidin A (**18**),⁹³ and analyzed by LC-MS Q-TOF. To our surprise, both enzymes demonstrated a remarkable range of substrate tolerance, leading to new products with masses of [M+16]. With compounds **9** and **10**, the reactions were able to generate more than one visible product (Table 2-2).

The monooxopiperazines from the Malbrancheamide and Paraherquamide pathways were also tested *in vitro* with NotI and NotI' (Figure 2-9), but these reactions failed to convert substrates into products. Additionally, reactions with compound **6** did not generate observable products, suggesting that [C-2] prenylation of the indole could be important for substrate

Table 2-2. Structures of substrates tested and summary of products formed in reactions with NotI, NotI', and PhqK

Structure	Substrate masses observed	NotI product masses observed	NotI' product masses observed	PhqK product masses observed
 (7)	352.2084 (7)	368.1985	No product observed	No product observed
 (8)*	371.2016 (8)*	387.1955	387.1948	387.1962
 (9)	436.2660 (9)	452.2603	452.2594	452.2549
 (10)*	436.2479 (10)*	452.2392	452.2495	452.2461
 ((\pm)-15)	434.2461 ((\pm)-15)	450.2414	450.2404	450.2397
 ((\pm)-18)	432.2344 ((\pm)-18)	448.2305	448.2277	No product observed

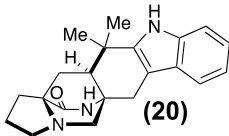
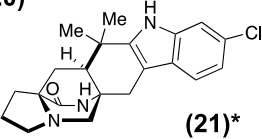
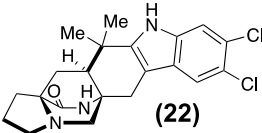
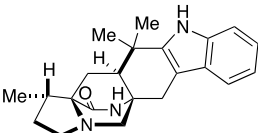
* Denotes compounds containing ¹³C label.

recognition.

2.2.3 Determination of PhqK activity and substrate flexibility.

We also examined the substrate flexibility of PhqK, the NotI homologue in the Paraherquamide biosynthetic gene cluster from *P. fellutanum*.⁹⁷ The enzyme was tested in reactions with monooxo- and dioxopiperazine substrates and analyzed by LC-MS Q-TOF (Table 2-2, Table 2-3). As expected, PhqK was able to convert its presumed native substrate Preparaherquamide

Table 2-3. Structures of monooxopiperazine substrates tested and summary of products formed in reactions with PhqK.

	Substrate masses observed	PhqK product masses observed
 (20)	336.23 (20)	352.30
 (21)*	372.16* (21)*	388.22*
 (22)	404.21 (22)	420.20
 (23)	350.22 (23)	366.22

* Denotes compounds containing ¹³C label.

(23)¹⁰¹ as well as the monooxopiperazine substrates **20**,²⁵ **21**,²⁵ and **22**⁵³ from the Malbrancheamide pathway. Additionally, PhqK was able to catalyze the formation of new products with [M+16] masses with **8**, **9**, **15**, and **16**. By contrast, no oxidative reactions were observed with **18**.

2.2.4 Determining the structure of Notoamide T9.

Assuming NotI and NotI' would perform a similar reaction on Notoamide T, we predicted that a

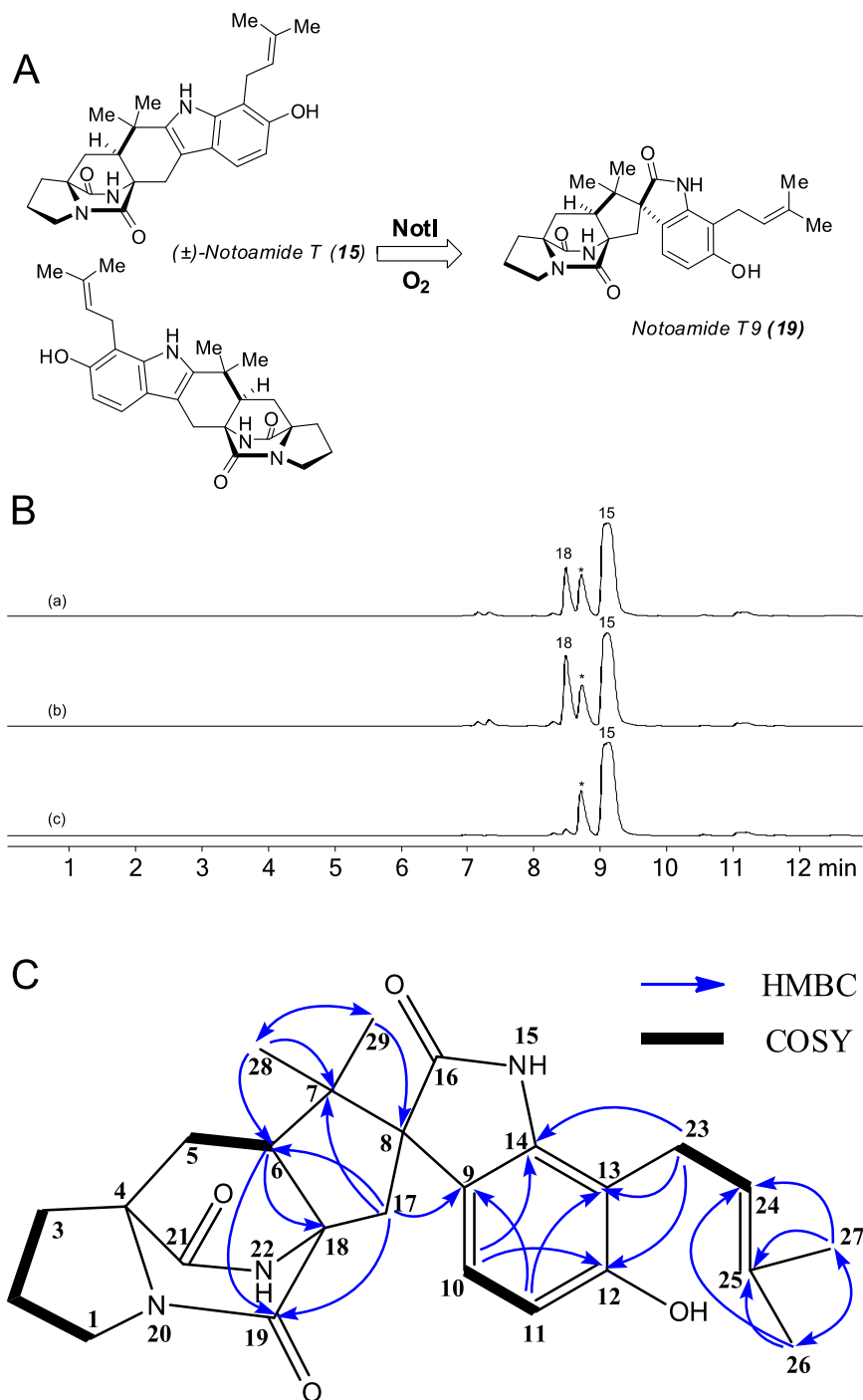


Figure 2-3. (A) Observed conversion from Notoamide T to Notoamide T9 by NotI. (B) HPLC analysis of NotI in vitro reaction with Notoamide T (**15**) to generate new compound Notoamide T9 (**19**): (a) **15** + NotI; (b) **15** + NotI; (c) **15** in reaction solution without enzyme. The asterisk denotes a possible diastereomer of Notoamide T (**15**). (C) Planar structure of Notoamide T9 (**19**) showing COSY correlation with bold bonds and HMBC correlations with arrows.

new metabolite may have been formed and investigated the structure by NMR spectroscopy. The product was generated in large scale reactions containing NotI and (\pm)-Notoamide T. The desired product was then isolated and purified via HPLC to yield approximately 2 mg of purified compound. NMR analysis was performed to determine the structure of Notoamide T9 (Figure 2-3).

Notoamide T9 (**19**) was obtained as white amorphous solid and possesses a molecular formula of $C_{26}H_{31}N_3O_4$ as suggested by HRESIMS based on $[M+H]^+$ ion peak at m/z 450.2414 (Figure 2-23), representing 13 degrees of unsaturation. Moreover, the UV spectrum in methanol with λ_{max} at 242, 309, and 335 (sh) nm was indicative of aromatic functionality. The 1H (Figure 2-26) and ^{13}C NMR (Figure 2-27) data, recorded in DMSO- d_6 , indicated the presence of amides or lactams with at least three carbonyl carbons with chemical shifts at δ 169.5, 173.1, and 183.1 (Table 2-2). In addition, HSQCAD spectra (Figure 2-28) revealed the presence of four methyl groups, six methylenes and three methine carbons (Table 2-4). Further, analysis showed eight ^{13}C NMR signals between δ 107.5 and 155.3 (Table 2-4) indicating the presence of four double bonds, which in addition to the above mentioned groups, cumulatively accounts for only seven degrees of unsaturation. Hence, there must be at least six rings in the structure, and therefore extensive 2D NMR experiments (HMBC and COSY) were employed (Figure 2-29, Figure 2-30), leading to the establishment of the connectivity of deduced functional groups to elucidate the planar molecular structure **19** (Figure 2-3).

Table 2-4. NMR spectroscopic data for Notoamide T9 (19) in DMSO-d6 at 700 MHz.

	δ_C	δ_H , multi (<i>J</i> in Hz)	COSY	HMBC
1	43.1	3.38, m	2	2, 3, 4
2	29.1	1.91, dd (1.93, 1.92)	1, 3	1, 3, 4
		1.78 (m)	1	
3	24.2	1.99 (m)	1, 3	1, 2, 4
		1.73 (m)		
4	67.9			
5	28.6	2.51 (m)	6	4, 6
		1.23 (m)		
6	55.3	3.24, t (3.2)	5	18, 19, 28
7	44.7			
8	61.2			
9	120.3			
10	123.4	6.82, d (6.8)	11	9, 12
11	107.5	6.41, d (6.8)	10	9, 13
12	155.3			
13	109.8			
14	141.1			
15	NH	9.07		
16	183.1			
17	33.2	2.77, d (2.7)		6, 7, 9, 19
		2.13, d (2.7)		7, 9, 19
18	65.2			
19	169.5			
20	N			
21	173.2			
22	NH	8.51		
23	23.2	3.18, m	24	12, 13, 14
24	122.5	5.13, t (5.1)	23	
25	130.3			
26	25.3	1.61, s		25, 27
27	17.6	1.69, s		25, 26
28	22.9	0.68, s		6, 7, 29
29	19.3	0.69, s		8, 28

2.3 Discussion

Pinacol rearrangements have long been predicted as steps in the biosynthetic schemes of numerous natural products, but few examples have been characterized. Gene disruption studies performed on the GsfF P450 monooxygenase support its role in a comparable reaction in the Griseofulvin biosynthetic pathway.¹⁰² Dihydrogeodin oxidase is a rare blue copper protein that generates diradicals involved in formation of the spiro center in Geodin.¹⁰³ FqzB, a FMO from the Fumitremorgin gene cluster, catalyzes the spirocycle rearrangement in Spirotryprostatin synthesis.¹⁰⁴ Interestingly, this enzyme was found to be specific for compounds containing a *p*-methoxy group and presents an intriguing contrast to the FMOs in this study that exhibit a wide degree of substrate flexibility. In comparison, we believe that we have identified three particularly unusual cases of FMO enzymes (NotI, NotI', PhqK) that could be further engineered for use in chemoenzymatic synthetic approaches due to their inherent substrate flexibility.

We initially hypothesized that the NotI, NotI', and PhqK proteins would be specific for their respective enantiomers, as enzymes are typically expected to be substrate and face selective in their reactions with some exceptions. However, our experimental findings have revealed the high degree of flexibility that these FMOs exhibit, with no apparent enantioselective discrimination. In contradistinction, the facial selectivity of the FMO-catalyzed oxidation appears highly diastereoselective, delivering the oxygen atom from the least-hindered face of the 2,3-disubstituted indole substrate species, and is thus a “substrate-controlled” reaction. These findings support our proposed biosynthetic pathway, in which NotI and NotI' are not responsible for the enantio-divergence in compounds produced between the two *Aspergillus* species, and that the creation of antipodal Notoamides is instead due to an earlier step in the biosynthetic pathway.^{100,105,106} With our current knowledge of the biochemical transformations involved, we

suspect that NotD or NotH, the gene product currently suspected of being responsible for the intramolecular Diels-Alder reaction, is the likely candidate for the enantio-divergent step.

NotI and NotI' demonstrated an unusual amount of substrate tolerance, converting many intermediates from the pathway to various products. Based on these data, it is highly possible that NotI/NotI' also perform as the Brevianamide E synthase, the Notoamide J synthase, and Versicolamide B synthase in their respective pathways, although further investigation is required to confirm these assignments.^{39,93,107} The acceptance of many substrates suggests that there may be some functional redundancy in the biosynthetic pathways of the Notoamide-producing systems. The other Notoamide FMO gene product NotB shares 42% protein sequence identity and 59% similarity with NotI.⁸² However, the fact that they can catalyze the same reactions on substrate Notoamide E was unexpected. We propose that within this system, NotB acts as a specialized, more efficient enzyme dedicated to the conversion of Notoamide E, while NotI behaves as a more universal catalyst at a lower rate of efficiency.

We also investigated the role of PhqK in the Paraherquamide pathway, one that involves the formation of a monooxopiperazine as opposed to the dioxopiperazines observed in the Notoamides and Stephacidins. PhqK and NotI share 34% amino acid sequence identity, thus suggesting that they perform comparable roles in their respective biosynthetic pathways. We sought to determine whether PhqK would be selective towards monooxopiperazine compounds, as NotI exhibited a specificity for dioxopiperazine metabolites. Investigating the activity of PhqK *in vitro* revealed that both monooxo- and dioxopiperazines can serve as PhqK substrates (Figure S5, Table 2-2), again demonstrating the broad, yet differential specificity in these biosynthetic FMOs.

Additionally, we were able to generate a novel indole alkaloid metabolite, Notoamide T9, further expanding the chemical diversity of bicyclo[2.2.2]diazaoctanes using *in vitro* reactions. The existence of Notoamide T9 suggests that there may be more than one pathway to the formation of Notoamide B. However, isotopically enriched precursor incorporation studies with Stephacidin A suggest that the proposed order depicted in Scheme 1 is likely to be the preferred

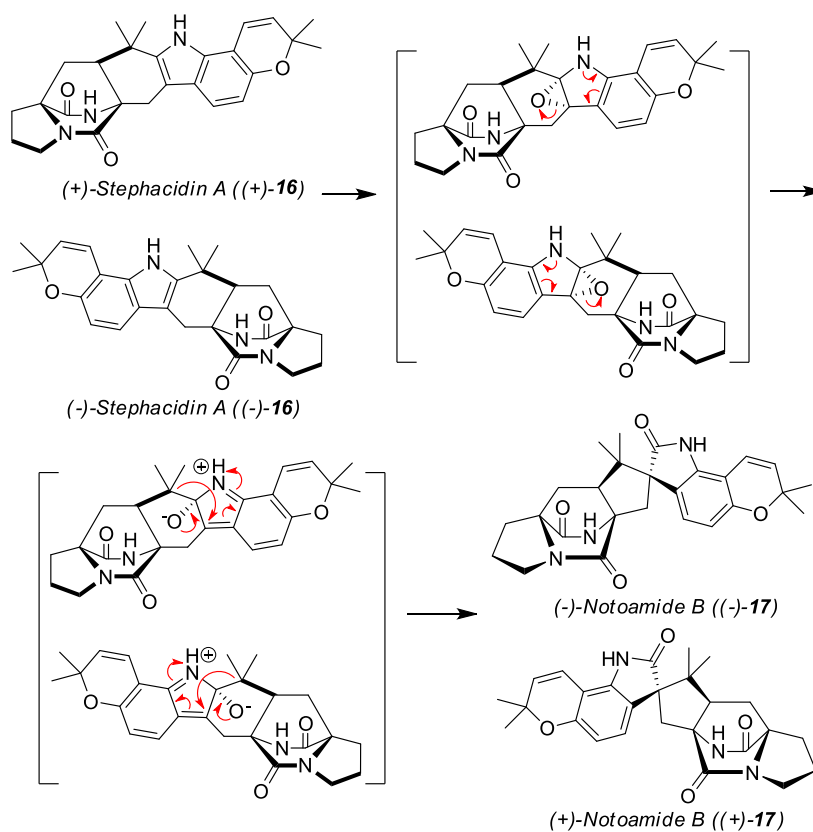


Figure 2-4. Proposed biosynthetic conversion of (±)-16 to (±)-17.

route.⁴⁵

In this investigation, three examples of flavin-dependent monooxygenases responsible for the formation of the spirooxindole center of various bicyclo[2.2.2]diazaoctane fungal alkaloids via semipinacol rearrangement were characterized. Although the exact mechanism of this reaction remains unknown, we believe the C2=C3 bond of the indole is epoxidized by the FMO on the less-hindered face, as has been observed in synthetic approaches.¹⁰⁰ The reactive epoxide

intermediate then collapses to form the 2-alkoxyindole iminium intermediate, followed immediately by a [1,5] sigmatropic shift to provide (+)-**17** (Figure 2-4). These findings suggest that an unusual substrate-controlled semipinacol rearrangement reaction is involved in Notoamide and Paraherquamide biosynthesis. Additionally, we have reported the first biochemical investigation of biosynthetic enzymes from the *A. amoenus* and *P. fellutanum* gene clusters. These data have important implications for the inherently flexible and previously underexplored FAD-dependent monooxygenases in fungal alkaloid biosynthesis, as well as for their origins in evolutionary biology. Further studies are being performed to enhance our understanding of the mechanisms that drive these unusual and intriguing reactions.

2.4 Materials and Methods

1. Fungal strains and Culture Conditions

Aspergillus amoenus, *Aspergillus protuberus*, and *Penicillium fellutanum* ATCC 20841 spores were generated on YPD agar plates over the course of 7 days. Spores were harvested into 5 mL sterile water per plate by gently scraping the surface of the culture with a sterile inoculating loop. Spores were stored at -80°C until ready to use. Genomic DNA was harvested using Wizard Genomic DNA Purification Kit from Promega.

2. cDNA preparation and cloning of *notI*, *notI'*, and *phqK*

Total RNA was extracted from a filter paper dried 17th day mycelia (roughly 500 mg fungal mat) culture of *Aspergillus protuberus* statically cultivated in liquid medium (50% seawater with 2.0% malt extract and 0.5% peptone) at 28°C, using Invitrogen PureLink RNA Mini Kit by following the plant tissue processing protocol. RNA was treated using DNase I. cDNA was generated using Invitrogen Superscript First Strand Synthesis. PCR was used to amplify NotI from the cDNA

template. Additionally, a codon optimized construct was purchased from GeneArt, Life Technologies and used in all enzymology studies. To generate *notI'*, introns were predicted by analysis using Softberry Fgenesh-M. Further analysis was performed by comparison with the *notI* sequence, which has 81% DNA sequence identity. The *notI'* and *phqK* genes were amplified from genomic DNA using overlapping PCR using primers in Table S1. Amplified genes were cloned into pET28b vectors using restriction enzyme digest and ligation. Plasmids were transformed into *E. coli* DH5 α for screening and plasmid maintenance.

3. Overexpression and Purification of Protein for Enzymology

The *Escherichia coli* BL21 (DE3) transformant containing PMCSG7-*notI* and Takara chaperone pGKJE8 was grown at 37°C overnight in LB media containing 50 μ g/mL of ampicillin and 25 μ g/mL of chloramphenicol. 25 mL of culture was used to inoculate 1 L of TB media containing the aforementioned concentrations of antibiotic and 4% glycerol, and cultures were supplemented with 0.5 mg/mL L-arabinose and 5 ng/mL tetracycline to induce chaperone expression. Cells were grown at 37°C for roughly 4 hours until A₆₀₀ reached 0.6-1.0, and isopropyl β -D-thiogalactoside (IPTG, 0.2 mM) along with riboflavin (50 μ M) was added to induce protein overexpression overnight at 18°C. The *Escherichia coli* BL21 pRARE transformant containing pET28b-*notI'* and Takara chaperone pTf16 was grown at 37°C overnight in LB media containing 50 μ g/mL of kanamycin, 25 μ g/mL of chloramphenicol, and 100 μ g/mL of spectinomycin. 25 mL of culture was used to inoculate 1 L of TB media containing the aforementioned concentrations of antibiotic and 4% glycerol, and cultures were supplemented with 0.5 mg/mL L-arabinose to induce chaperone expression. Cells were grown at 37°C for roughly 4 hours until A₆₀₀ reached 0.6-1.0, and isopropyl β -D-thiogalactoside (IPTG, 0.2 mM)

along with riboflavin (50 μ M) was added to induce protein overexpression overnight at 15°C. An *E. coli* BL21 pRARE transformant containing pET28b-*phqK* grown at 37°C overnight in LB media containing 50 μ g/mL of kanamycin was used to inoculate 6 L LB supplemented with kanamycin. The cells were grown at 37°C to $A_{600} \sim 0.8$ and subsequently cooled to 18°C and grown overnight (12-16 h) after the addition of isopropyl β -D-thiogalactoside (IPTG, 1 mM) and riboflavin (50 μ M).

All purification steps were conducted at 4°C. Briefly, 2 L of expression culture were spun down at 5,500 xg to yield approximately 20 mL of cell pellet volume. Harvested cell pellets were resuspended in 60 ml of lysis buffer (10 mM imidazole, 50 mM NaH_2PO_4 , 300 mM NaCl, 10% v/v glycerol, pH 8) and lysed by sonication. Insoluble material was removed by centrifugation at 38,000 xg for 30 min, and the supernatant was batch-bound for 1 hour to 4 mL of Ni^{2+} -NTA slurry (Novagen) that was equilibrated in lysis buffer. This batch-binding mixture was poured through a 50 ml fritted glass column where the retained resin was washed with 100 mL of lysis buffer, 50 mL of wash buffer (20 mM imidazole, 50 mM NaH_2PO_4 , 300 mM NaCl, 10% v/v glycerol, pH 8), and finally 10 ml of elution buffer (250 mM imidazole, 50 mM NaH_2PO_4 , 300 mM NaCl, 10% v/v glycerol, pH 8). Protein in the eluate was exchanged into storage buffer (50 mM NaH_2PO_4 , 1 mM EDTA, 0.2 mM DTT, 10% v/v glycerol, pH 7.3) using PD-10 columns. Samples were then flash frozen with liquid N₂ and stored at -80°C. PhqK was purified using similar methods with the exception of storage buffer, which was composed of 10 mM HEPES pH 7.6, 50 mM NaCl, 0.1 mM EDTA, 0.2 mM TCEP.

4. Enzyme assays and LC-MS Q-TOF analysis

The standard enzyme assay containing 0.5 mM substrate, 2.5 mM NADH, and 20 μ M enzyme in 100 μ L reaction buffer (50 mM NaH_2PO_4 , 1 mM EDTA, 0.2 mM DTT, 10% v/v glycerol, pH 7.3) was performed at 28°C overnight. Each reaction was extracted 3 times with 200 μ L chloroform, and the extract was dried down under N_2 gas. The product was resuspended in 100 μ L methanol for LC-MS Q-TOF analysis. HPLC conditions for NotI/NotI reactions: ZORBAX Eclipse Plus C18 reverse phase column, 3.5 μ m, 4.6 x 150 mm; monitoring wavelengths 240 nm and 280 nm; scanning 200 to 1200 m/z; solvent A: water + 0.1% formic acid, solvent B: 95% acetonitrile in water + 0.1% formic acid; flow rate: 0.8 mL/min; mobile phase: 20% B over 2 min, 20-100% B over 10 min, 100% B over 5 min, 100-20% B over 1 min, 20% B over 5 min. HPLC conditions for PhqK reactions: Agilent Extend C18 reverse phase column. 5 μ m, 4.6 x 150 mm; monitoring wavelengths 240 nm and 280 nm; scanning 200 to 2000 m/z; solvent A: water + 0.1% formic acid, solvent B: 95% acetonitrile in water + 0.1% formic acid; flow rate: 0.4 mL/min; mobile phase: 5% B over 1 min, 5-100% B over 20 min, 100% B over 5 min, 100-5% B over 1 min, 5% B over 5 min

5. NotI kinetic assays and LC-MS Q-TOF analysis

250- μ L reactions contained 2.5 μ M NotI, 5 mM NADH, and 0.1 mM FAD in reaction buffer (50 mM NaH_2PO_4 , 1 mM EDTA, 0.2 mM DTT, 10% v/v glycerol, pH 7.3). Concentrations of 10, 20, 40, 100, 150, 200, 300, and 500 μ M (-)-**16** were tested. The reactions were pre-warmed at room temperature for 5 minutes and initiated with addition of 5 mM NADH and mixed briefly. The reactions were stopped by transferring 50 μ L reaction mixture to equal volume methanol, vortexing vigorously, and placing on ice. The samples were then centrifuged at 17,000 xg at 4°C for 25 minutes to pellet protein, and the supernatant was transferred to analysis vials for LC-MS Q-TOF analysis. HPLC conditions: ZORBAX Eclipse Plus C18 reverse phase column, 3.5 μ m,

4.6 x 150 mm; monitoring wavelengths 240 nm and 280 nm; scanning 200 to 1200 m/z; solvent A: water + 0.1% formic acid, solvent B: 95% acetonitrile in water + 0.1% formic acid; flow rate: 0.8 mL/min; mobile phase: 50% B over 2 min, 50-55% B over 5 min, 55-50% B over 30 sec, 50% B over 2.5 min. All experiments were performed in duplicate. Quantitative analysis was performed by extracting ions corresponding to substrate and product masses and calculating the

Name	Sequence (5' -> 3')	Function
notI-F	GGAGTTCCATATGGCTATAGACGGATCT	<i>notI</i> amplification
notI-F	CAATGAAGCTTTCAACCAACCGGTATACC GGAATTCCATATG	<i>notI</i> amplification
FNdeI	GCTATAGACGCATCTGGTGCTG ATAAGAATGCGGCCGC	<i>notI</i> ' amplification
RNotI	TTAATCCACCGGTATACCACCGAAG	<i>notI</i> ' amplification

area under each peak. The data were fit to the Michaelis-Menten equation.

	CAAGAGCTACCGTTTGGG	
NotI'_Int1_F	AGACTTGATCAATGTGACCGGG	<i>notI'</i> intron removal
	CCCGGTCACATTGATCAAGTCTCCCAAACG	
NotI'_Int1_R	GTAGCTCTTG	<i>notI'</i> intron removal
	CGAGTGACAGAGAAGCTAAGGTACCAAAG	
NotI'_Int2_F	GGTTGCTGCAA	<i>notI'</i> intron removal
	TTGCAGCAACCCTTTGGTACCTTAGCTTCT	
NotI'_Int2_R	CTGTCACTCG	<i>notI'</i> intron removal
PhqK_Int1_F	ATGGGCTCTTTAGGTGAAGAAGTTCAAG	<i>phqK</i> intron removal
	GTTGCTTTGAAGACCAATACAGTCTCCGAT	
PhqK_Int1_R	GGACTTCAGTATATTGCTTTTC	<i>phqK</i> intron removal
	GAAAAGCAATATACTGAAGTCCATCGGAG	
PhqK_Int2_F	ACTGTATTGGTCTTCAAAGCAAC	<i>phqK</i> intron removal
	CAGACGTCTAGGAGATTTCTTGTATCCTGA	
PhqK_Int2_R	TGAATGCAGAACCACGAAAAG	<i>phqK</i> intron removal
	CTTTTCGTGGTTCTGCATTCATCAGGATAC	
PhqK_Int3_F	AAGAAATCTCCTAGACGTCTG	<i>phqK</i> intron removal
PhqK_Int3_R	CTAGGGTGACTTGTCTGCAATGG	<i>phqK</i> intron removal

Table 2-5. Primers for NotI, NotI', and PhqK intron removal and amplification

2.5 Appendix

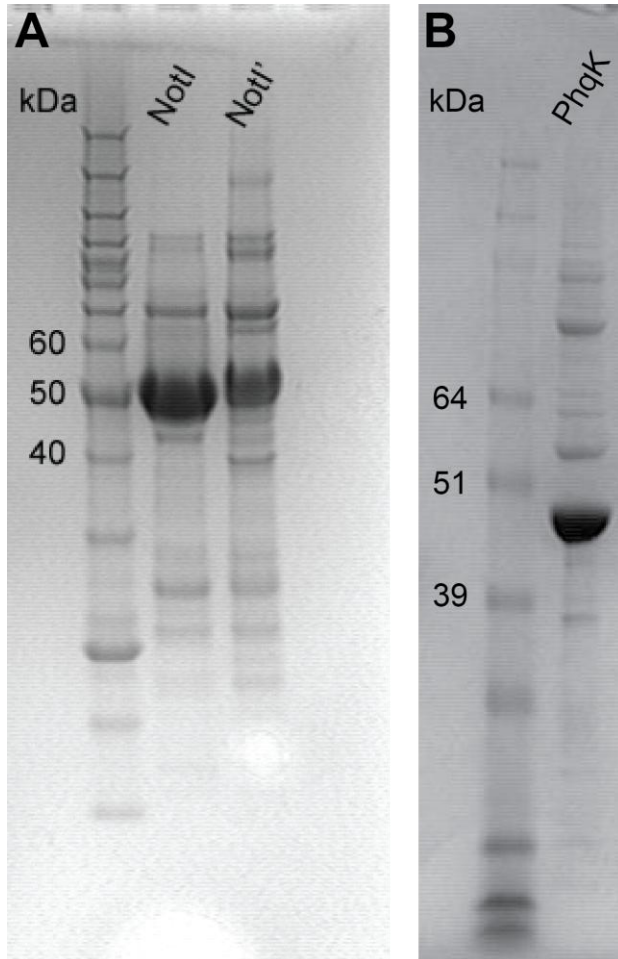


Figure 2-5. (A) 4-12% Bis-Tris in MES buffer SDS page analysis of NotI and NotI'. The calculated molecular weight of NotI is 47.1 kDa and the calculated molecular weight of NotI' is 49.2 kDa. (B) 4-12% Bis-Tris in MOPS buffer SDS page analysis of phqK. The calculated molecular weight of PhqK is 51.2 kDa.

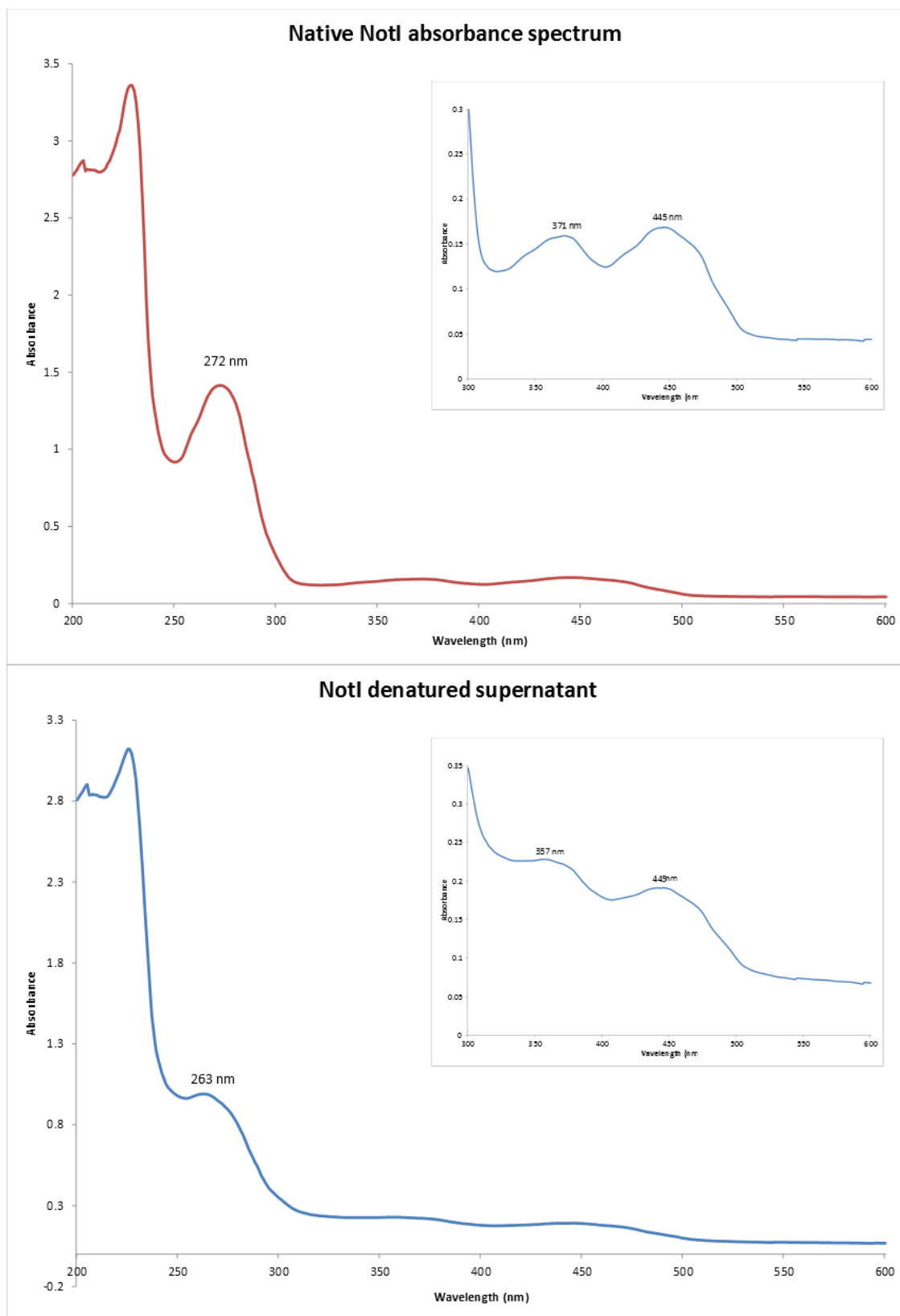


Figure 2-6. UV-Vis spectra of purified NotI protein solution (top) and the supernatant of denatured NotI protein solution (bottom). Denatured protein was generated by boiling for 15 minutes. The flavin cofactor peaks at 360 and 450 nm are present in both the native protein solution and the denatured supernatant.

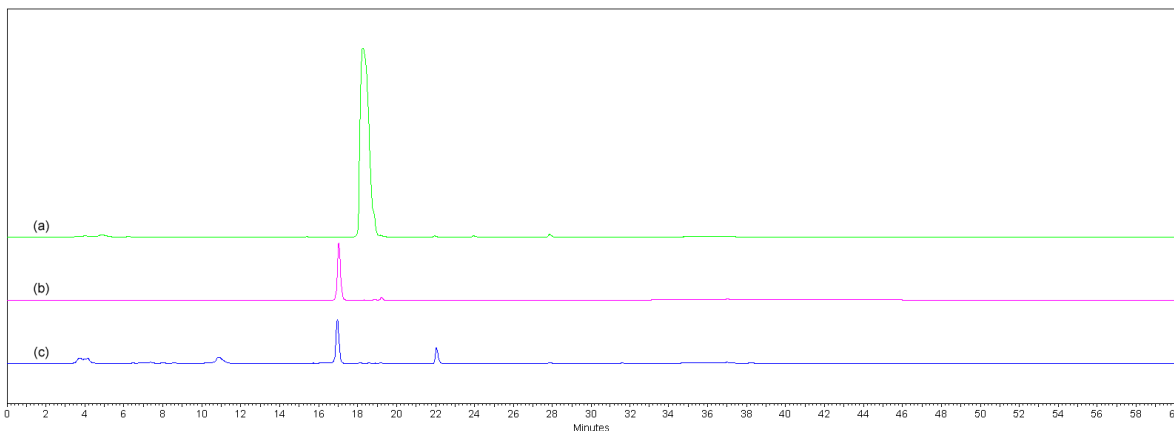


Figure 2-7. Identification of FAD as the non-covalently bound NotI flavin cofactor. (a) FMN standard; (b) FAD standard; (c) NotI supernatant after denaturation of protein by boiling and centrifugation.

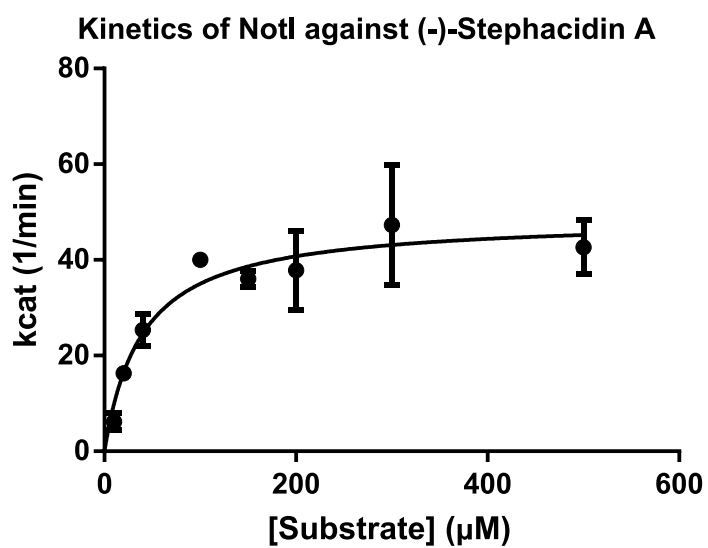


Figure 2-8. Kinetic curve of NotI against (-)-16.

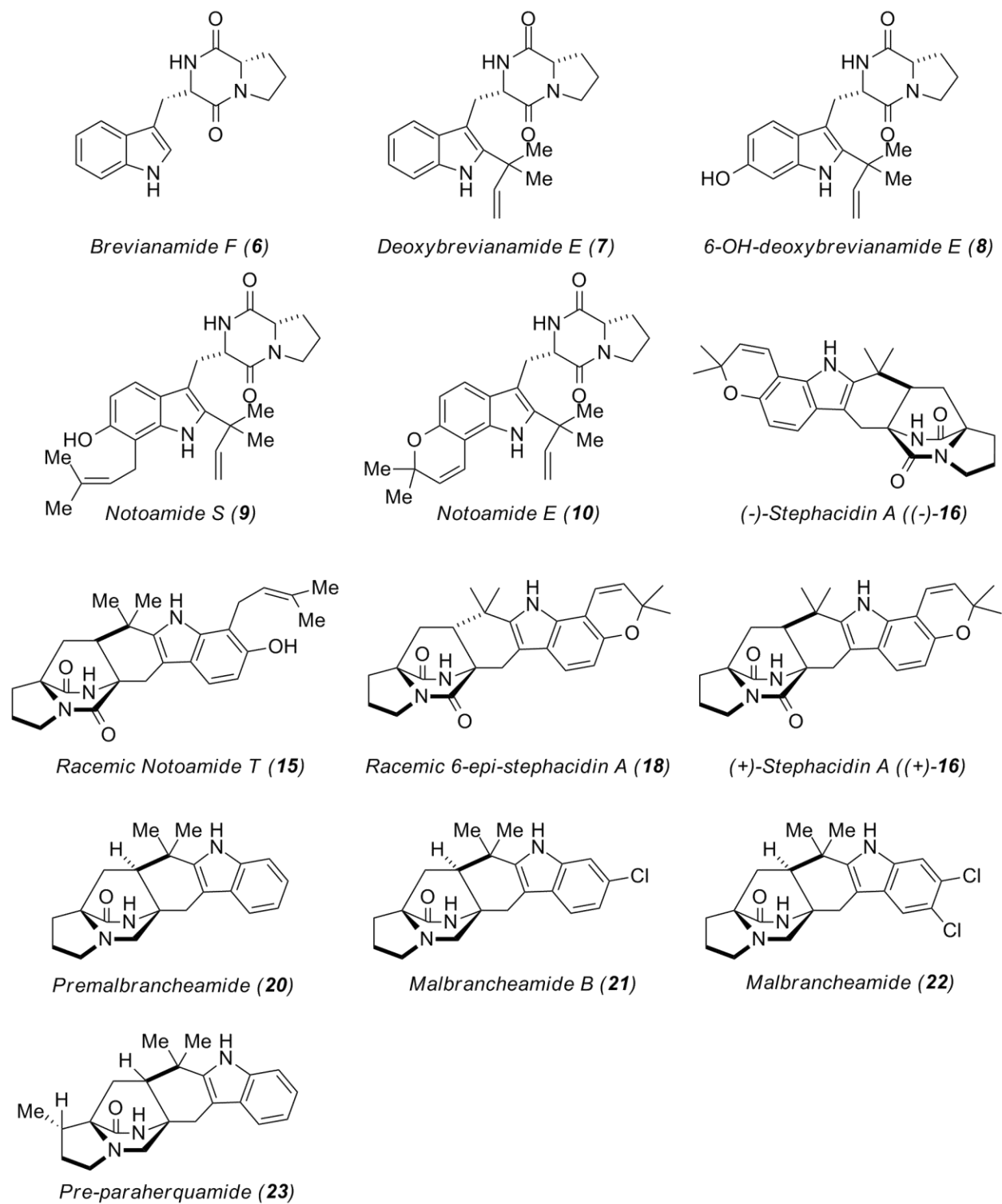


Figure 2-9. Substrates used to test NotI, NotI', and PhqK activities.

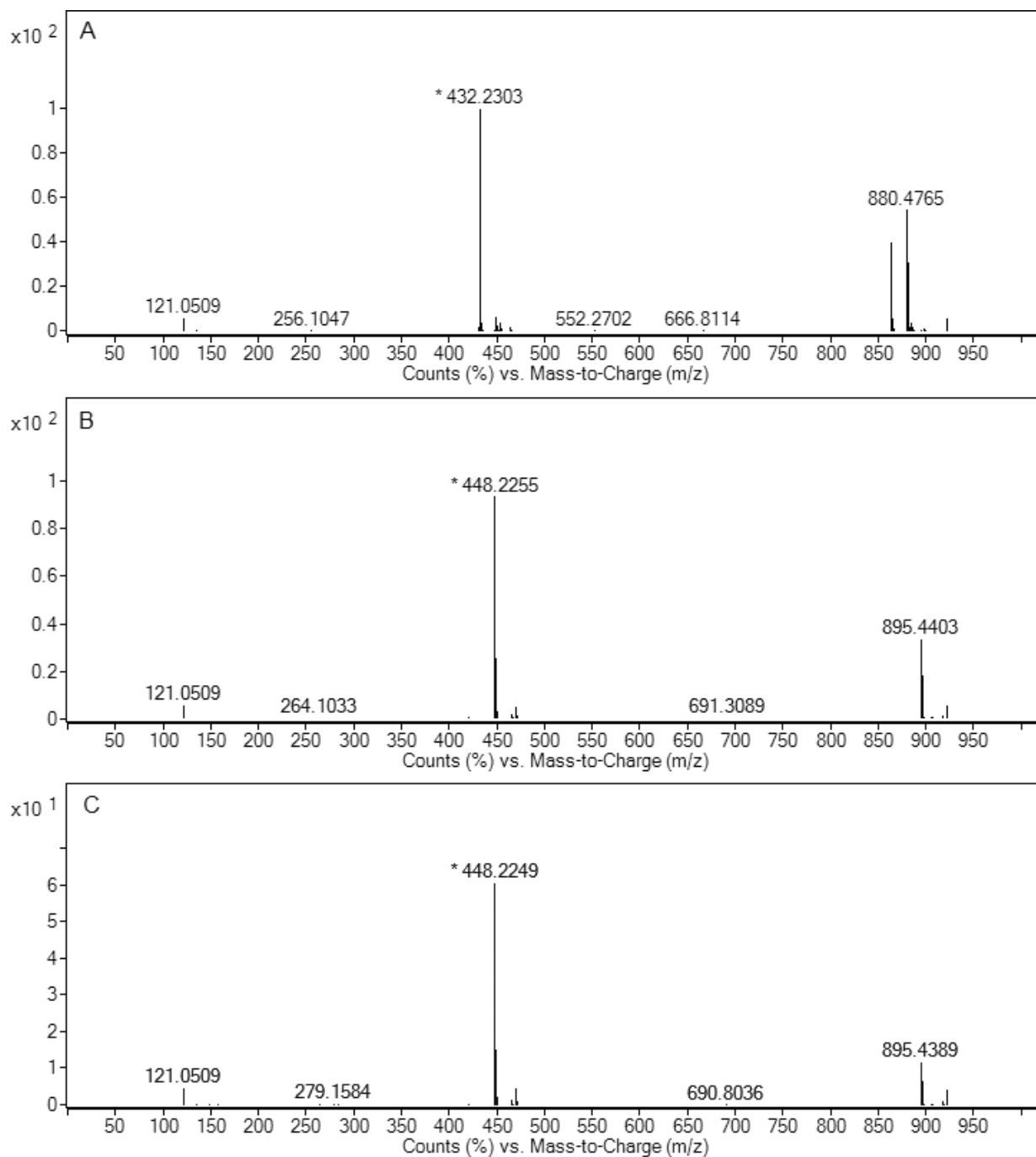


Figure 2-10. From EIC traces in Figure 2-2: (A) MS of (-)-16; (B) MS of (+)-17 formed from reaction with NotI; (C) MS of (+)-17 formed from reaction with NotI'.

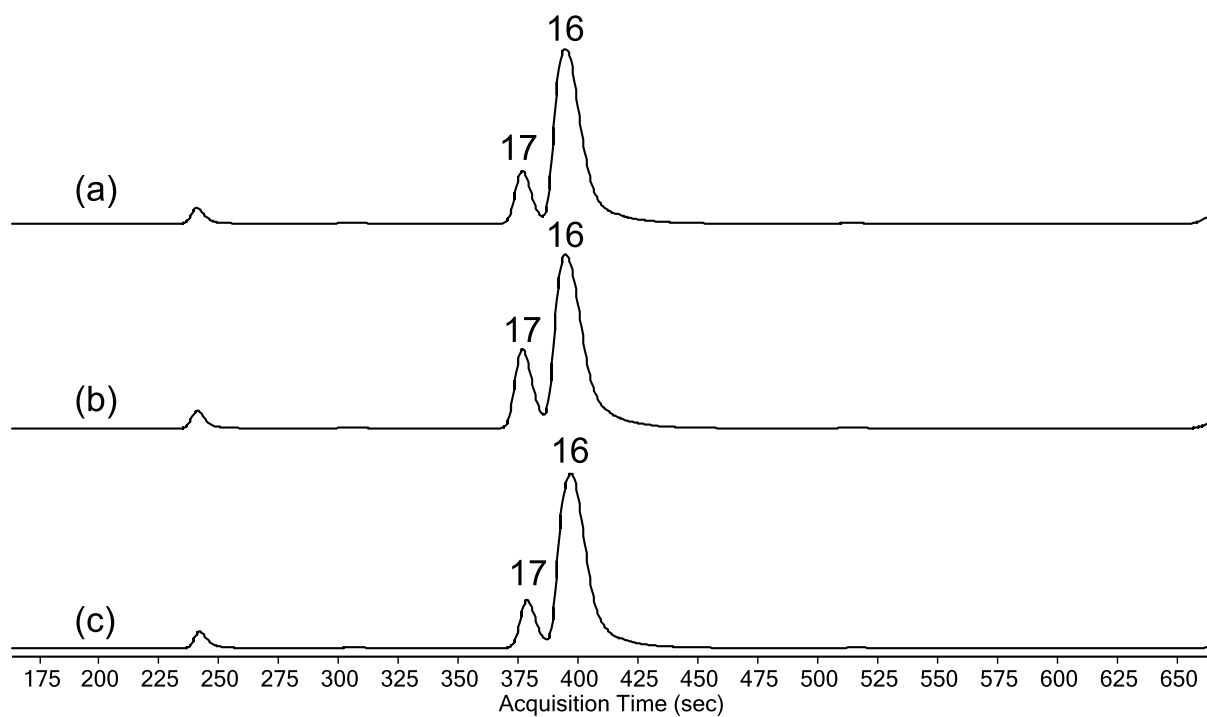


Figure 2-11. LC-MS Q-TOF analysis depicting EICs of (a) NotI + (+)-**16**; (b) NotI + (+)-**16**; (c) *A. protuberus* isolated authentic (+)-**16**. Some (-)-**17** is observed in the substrate trace (c). Integrating the traces to determine percent conversion yielded values of approximately 21% (-)-**17** in trace (a), 15% (-)-**17** in trace (b), and 14% (-)-**17** in trace (c).

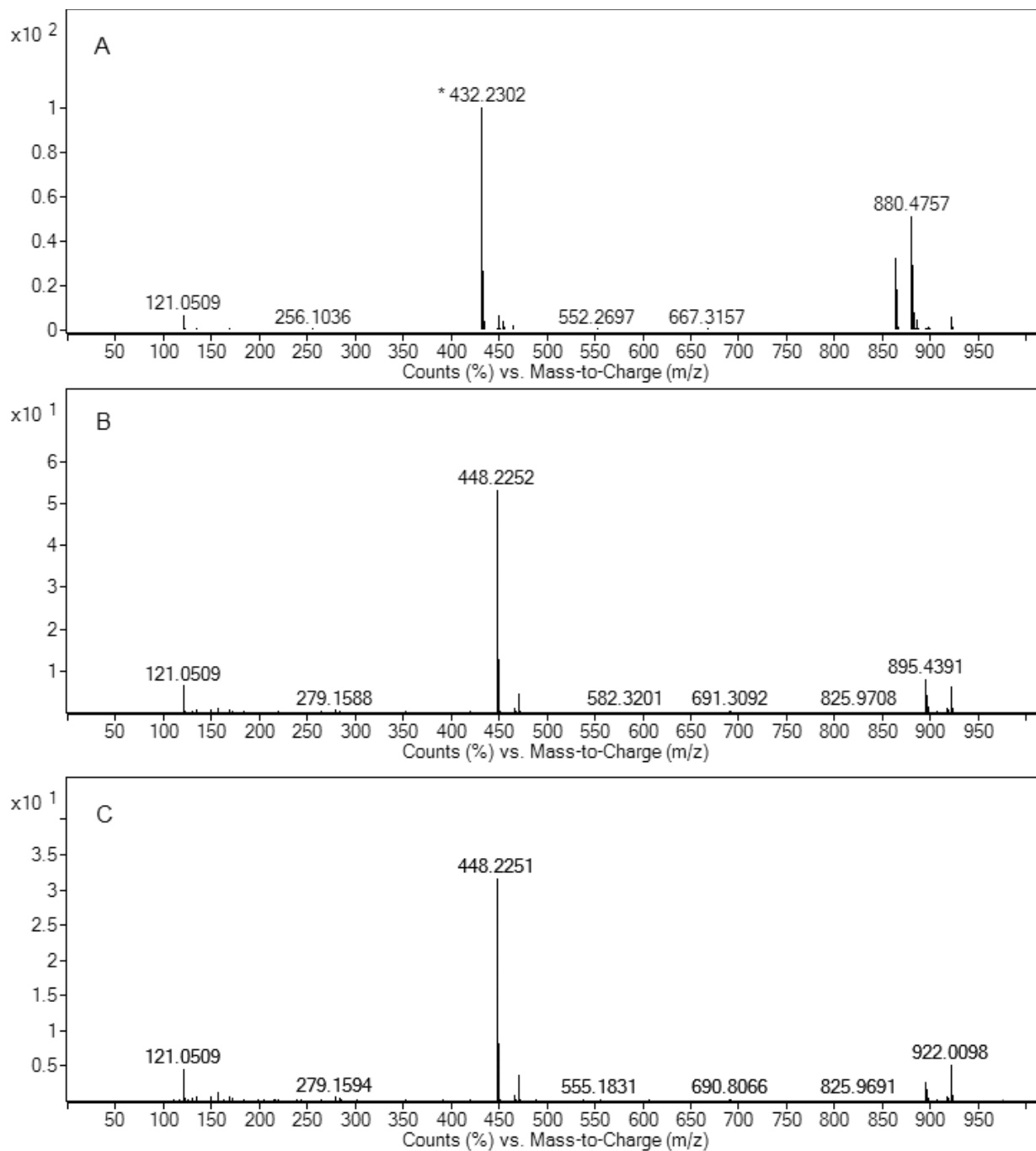


Figure 2-12. Mass spectra of (A) (+)-16 standard; (B) (-)-17 produced by NotI; (C) (-)-17 produced by NotI'.

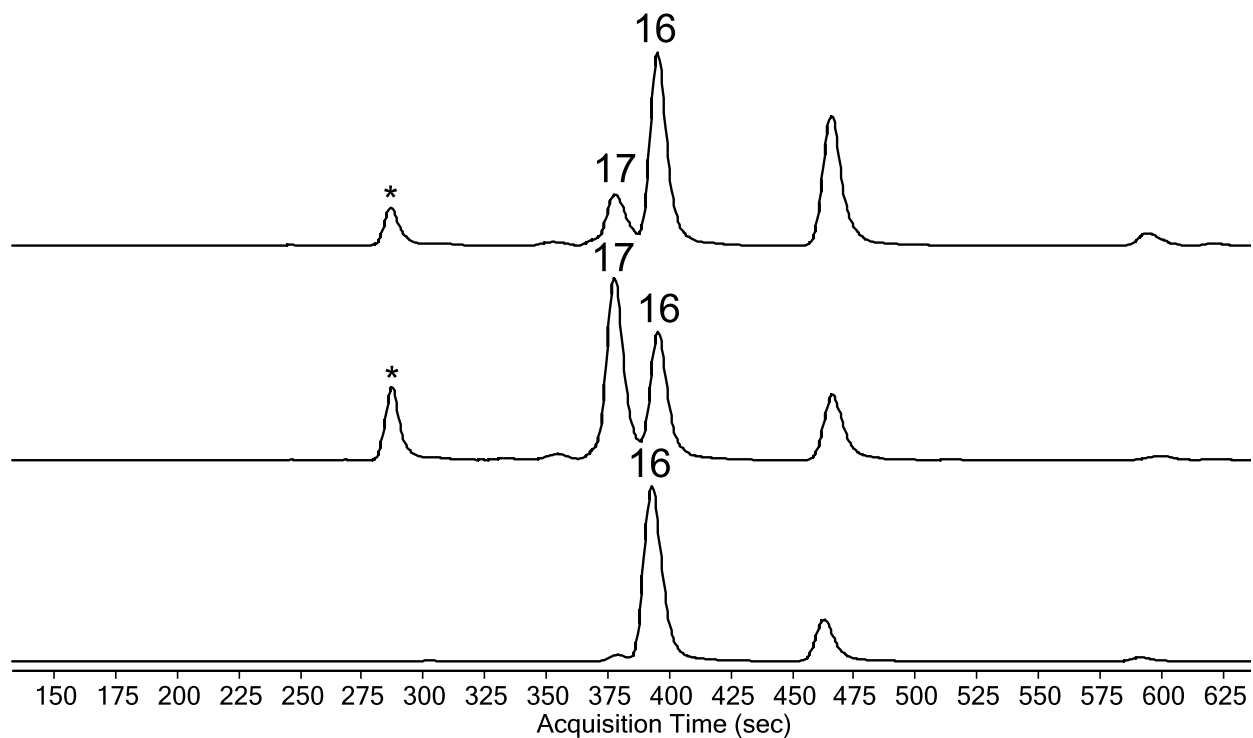


Figure 2-13. LC-MS Q-TOF analysis depicting EICs of (a) NotI' + (±)-16; (b) NotI + (±)-16; (c) authentic (±)-16. The asterisk denotes a possible artifact from the reaction solution.

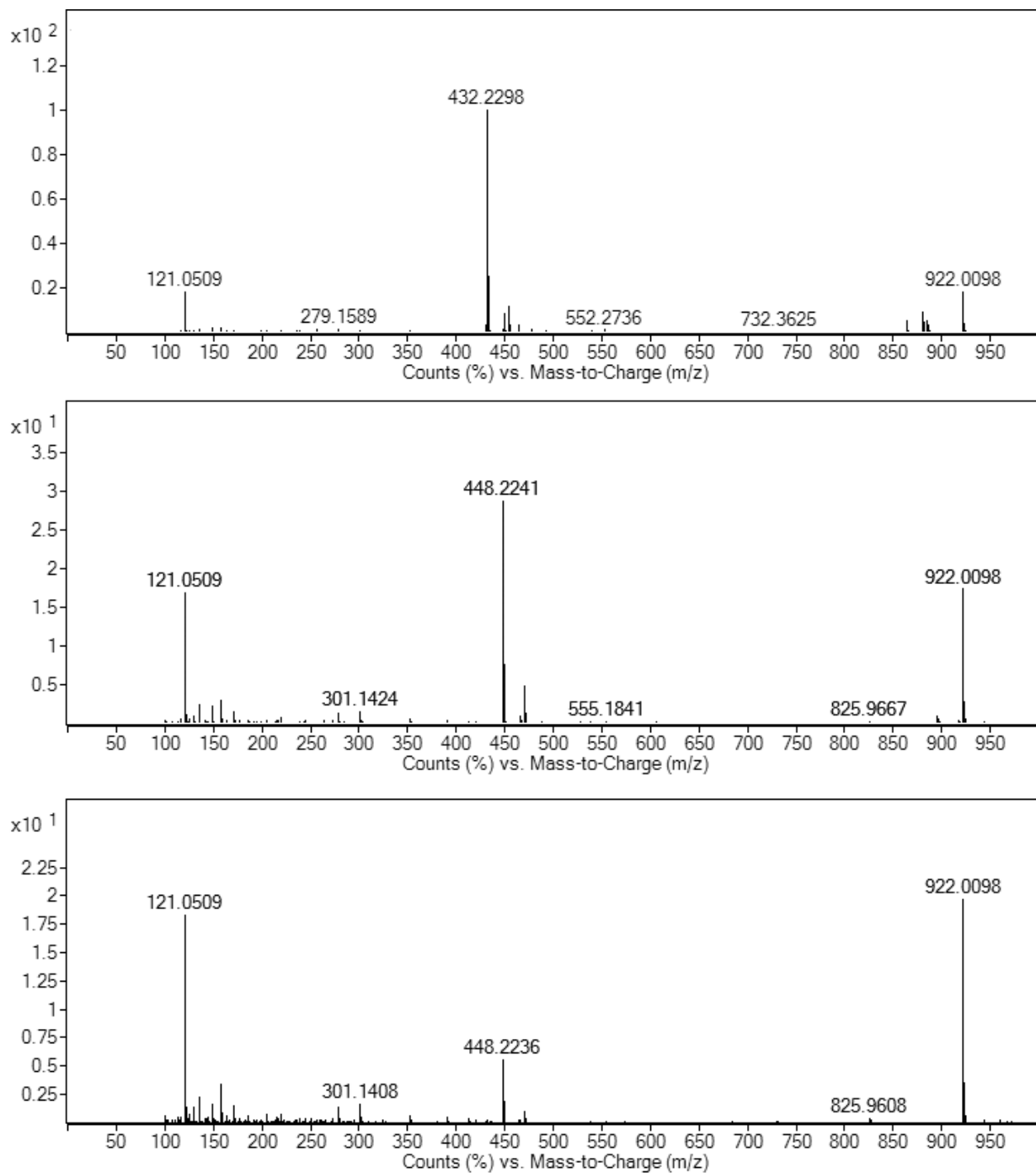


Figure 2-14. Mass spectra of (A) (\pm)-**16** standard; (B) **17** produced by NotI; (C) **17** produced by NotI'.

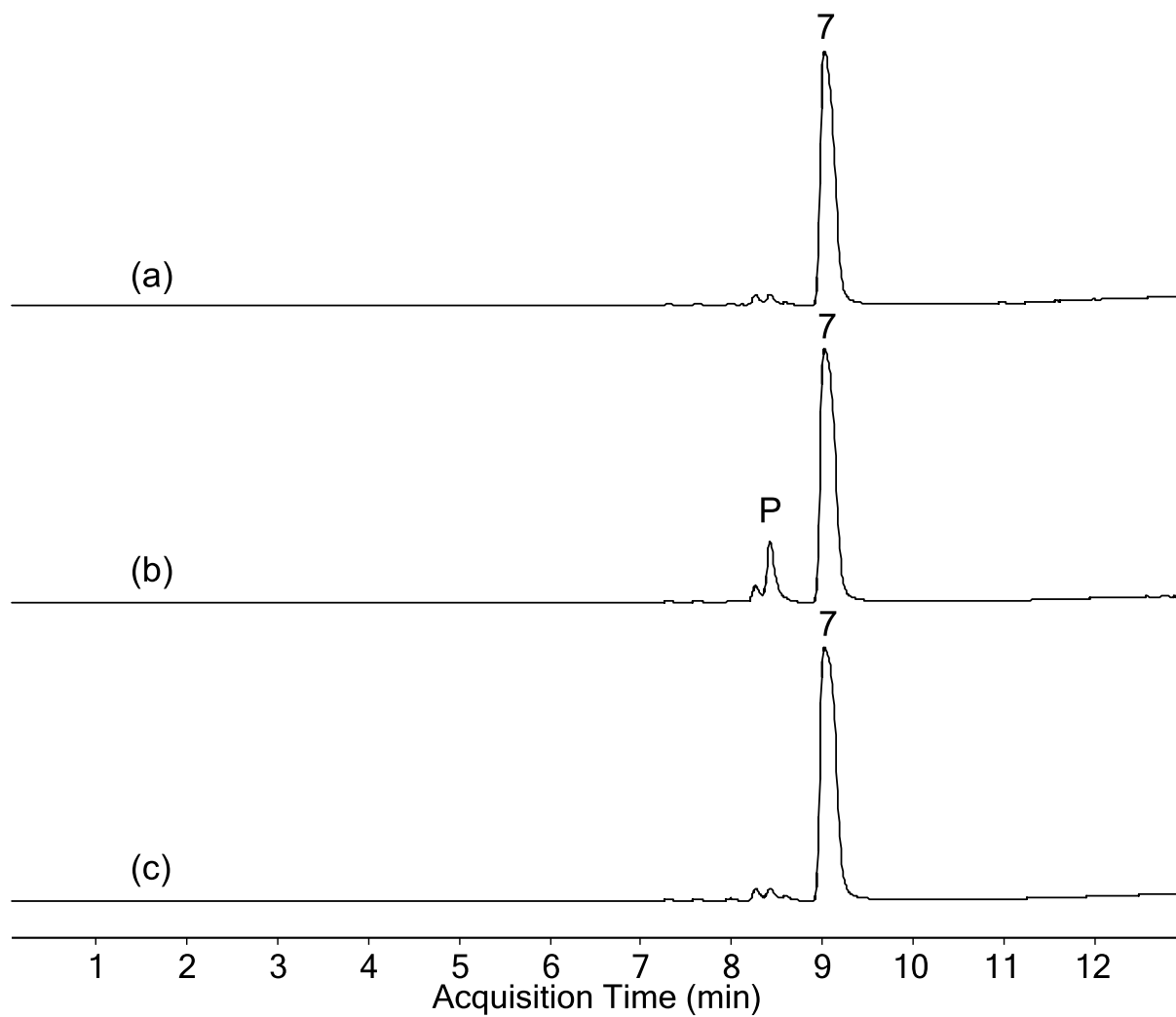


Figure 2-15. LC-MS Q-TOF analysis depicting EICs of (a) NotI' reaction with 7; (b) NotI reaction with 7; (c) authentic 7 standard. Product formed is denoted with P.

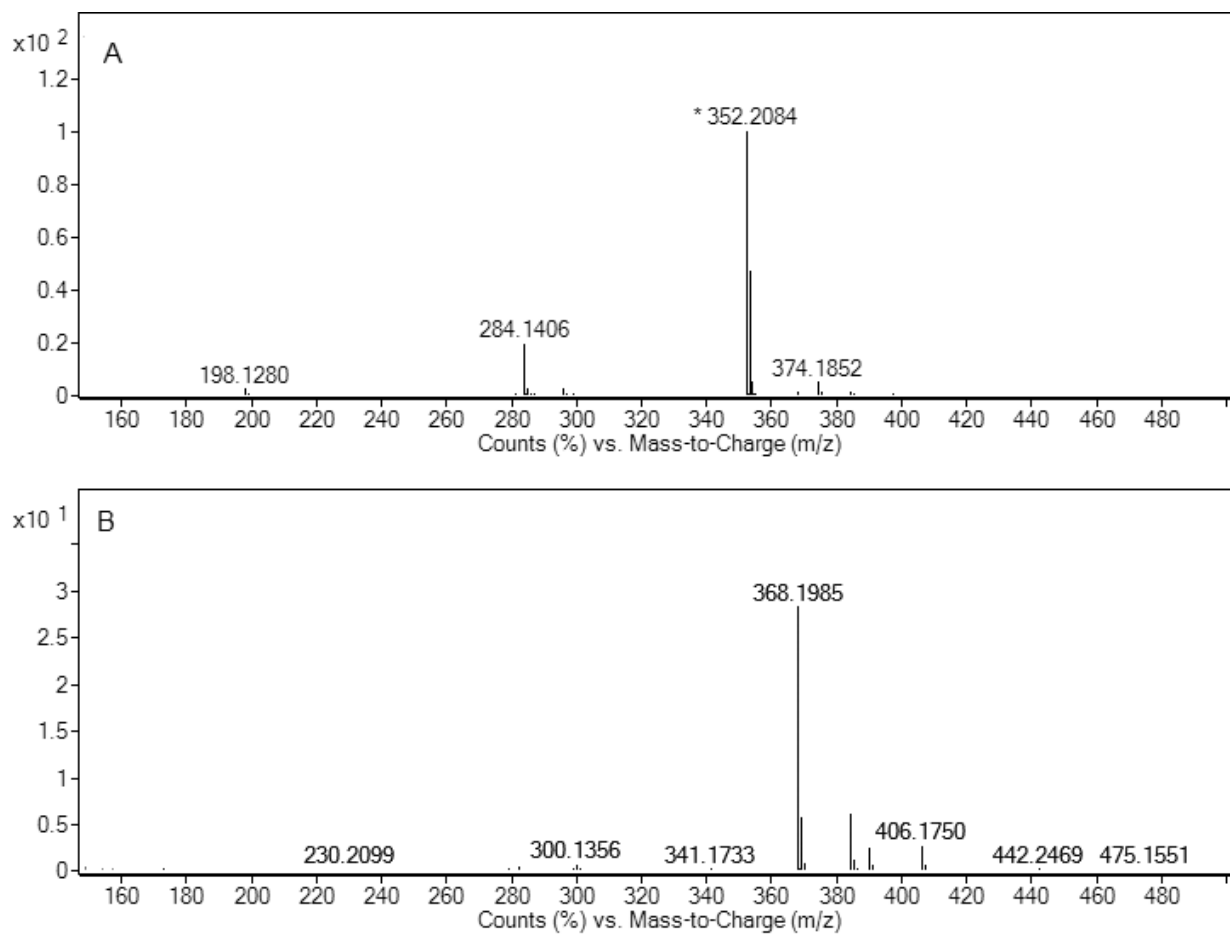


Figure 2-16. Mass spectra of (A) 7 standard; (B) Product formed from NotI + 7.

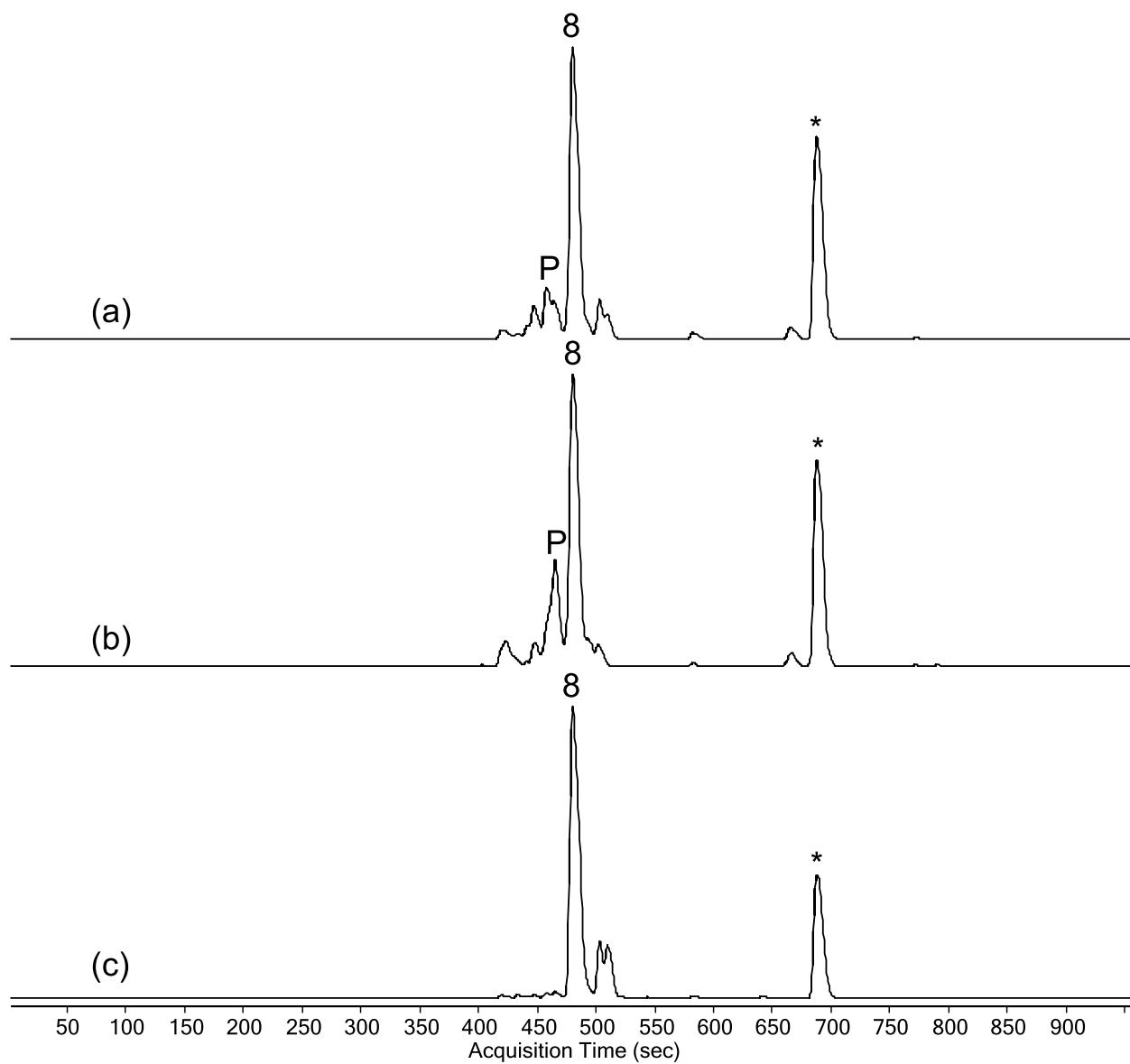


Figure 2-17. LC-MS Q-TOF analysis depicting EICs of (a) NotI' reaction with **8**; (b) NotI reaction with **8**; (c) authentic **8** standard. Product formed is denoted with P. Asterisk denotes a possible diastereomer of **8**.

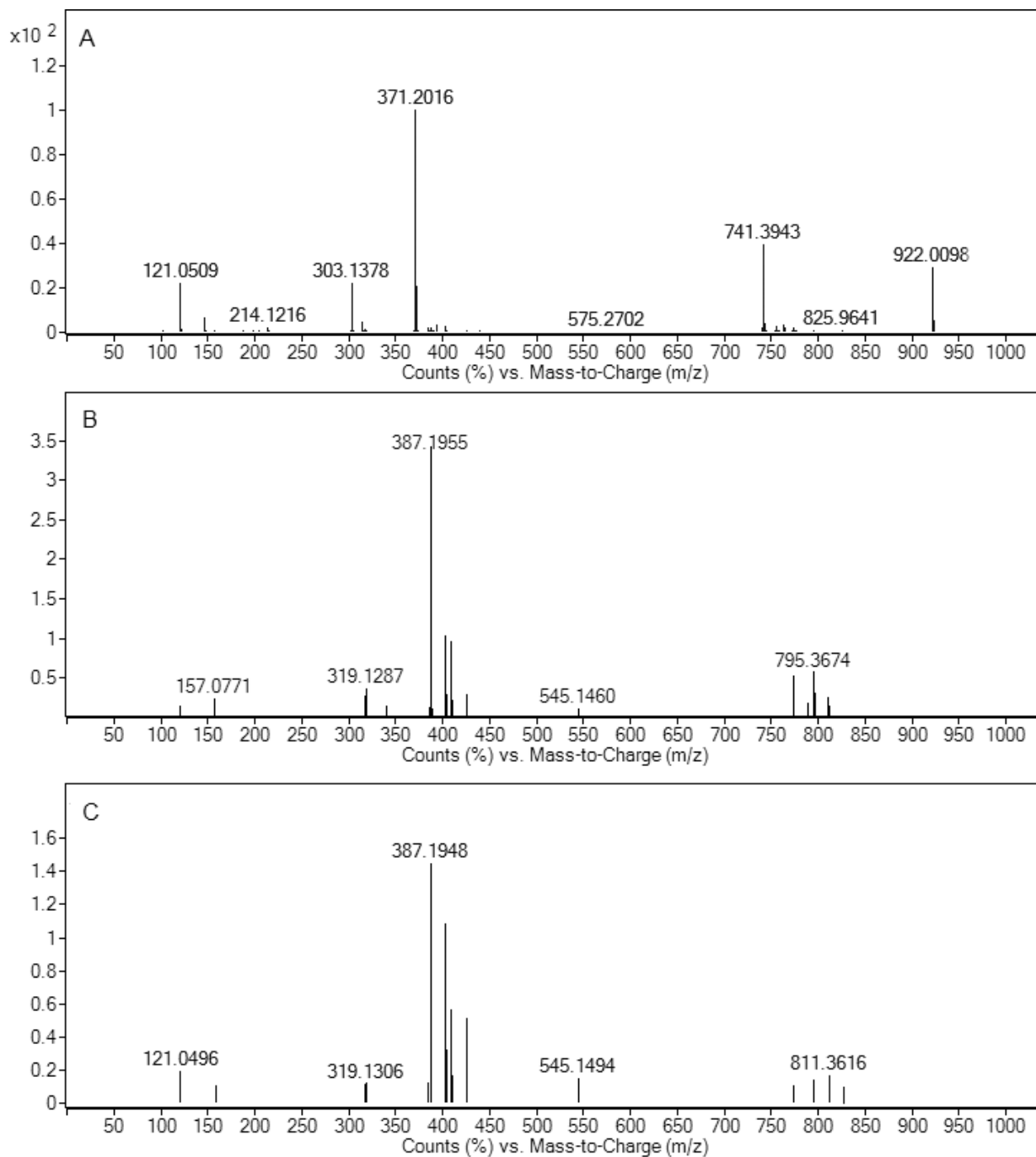


Figure 2-18. Mass spectra of (A) **8** standard with 3 ^{13}C label; (B) Product formed from NotI + **8**; (C) Product formed from NotI' + **8**.

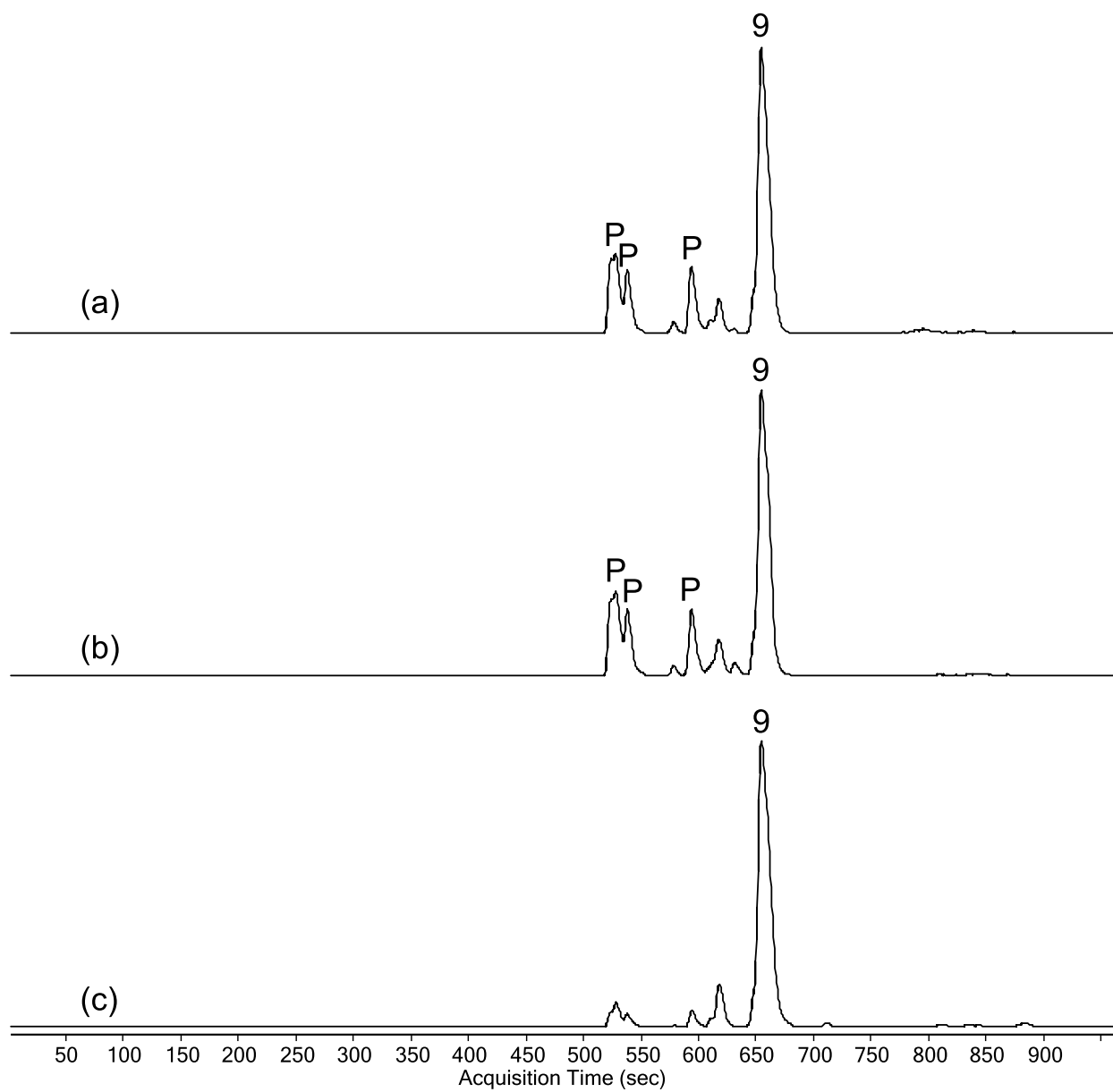
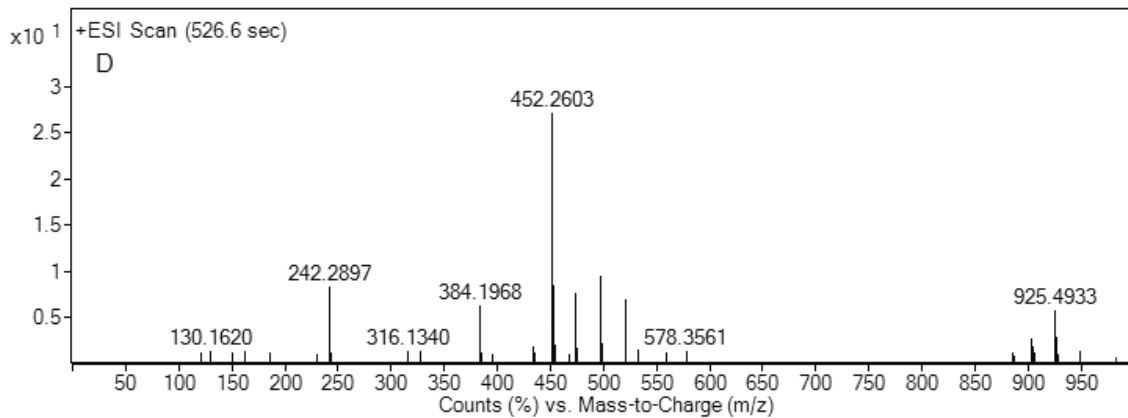
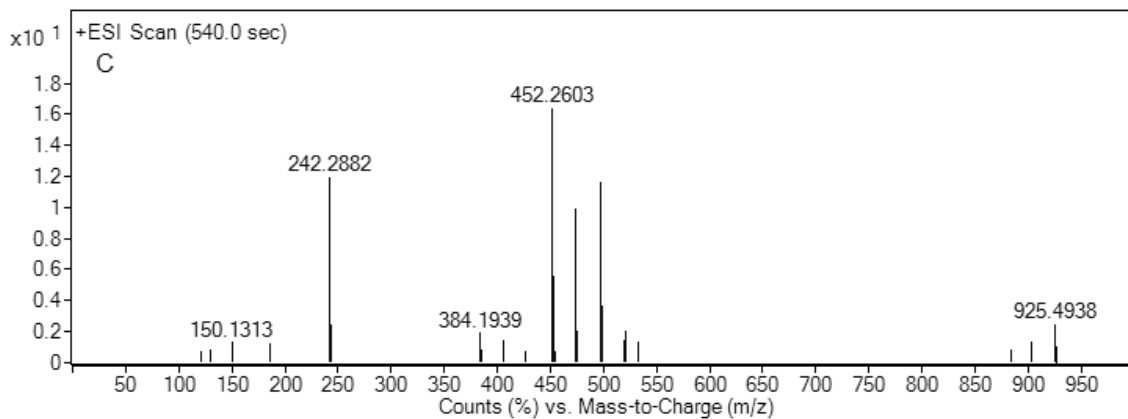
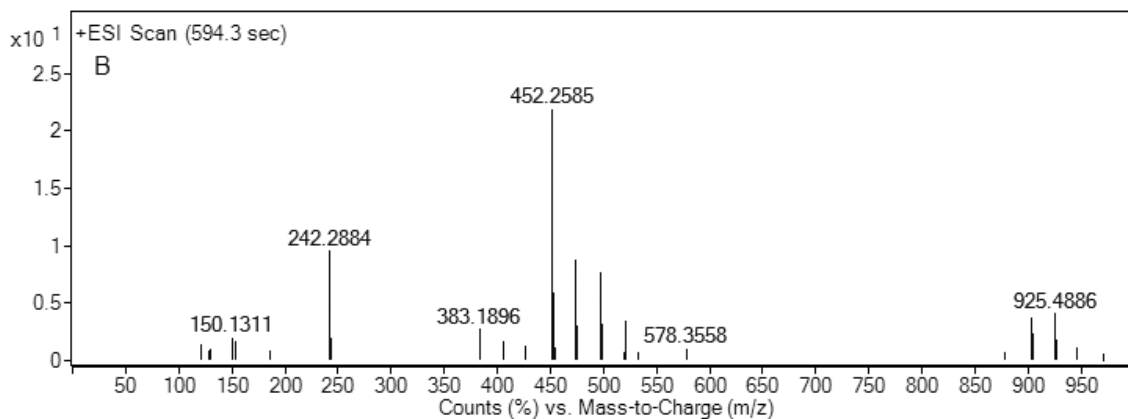
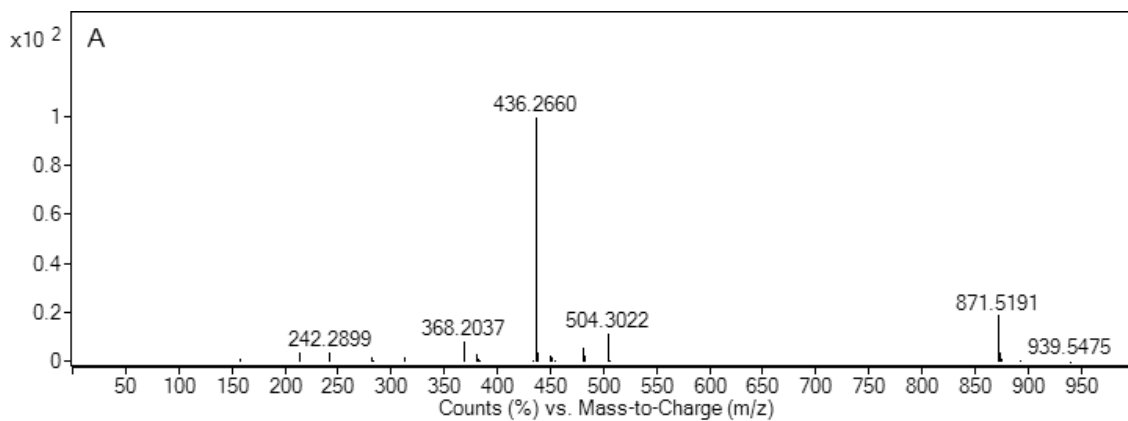


Figure 2-19. LC-MS Q-TOF analysis depicting EICs of (a) NotI' reaction with **9**; (b) NotI reaction with **9**; (c) authentic **9** standard. Product(s) formed is denoted with P.



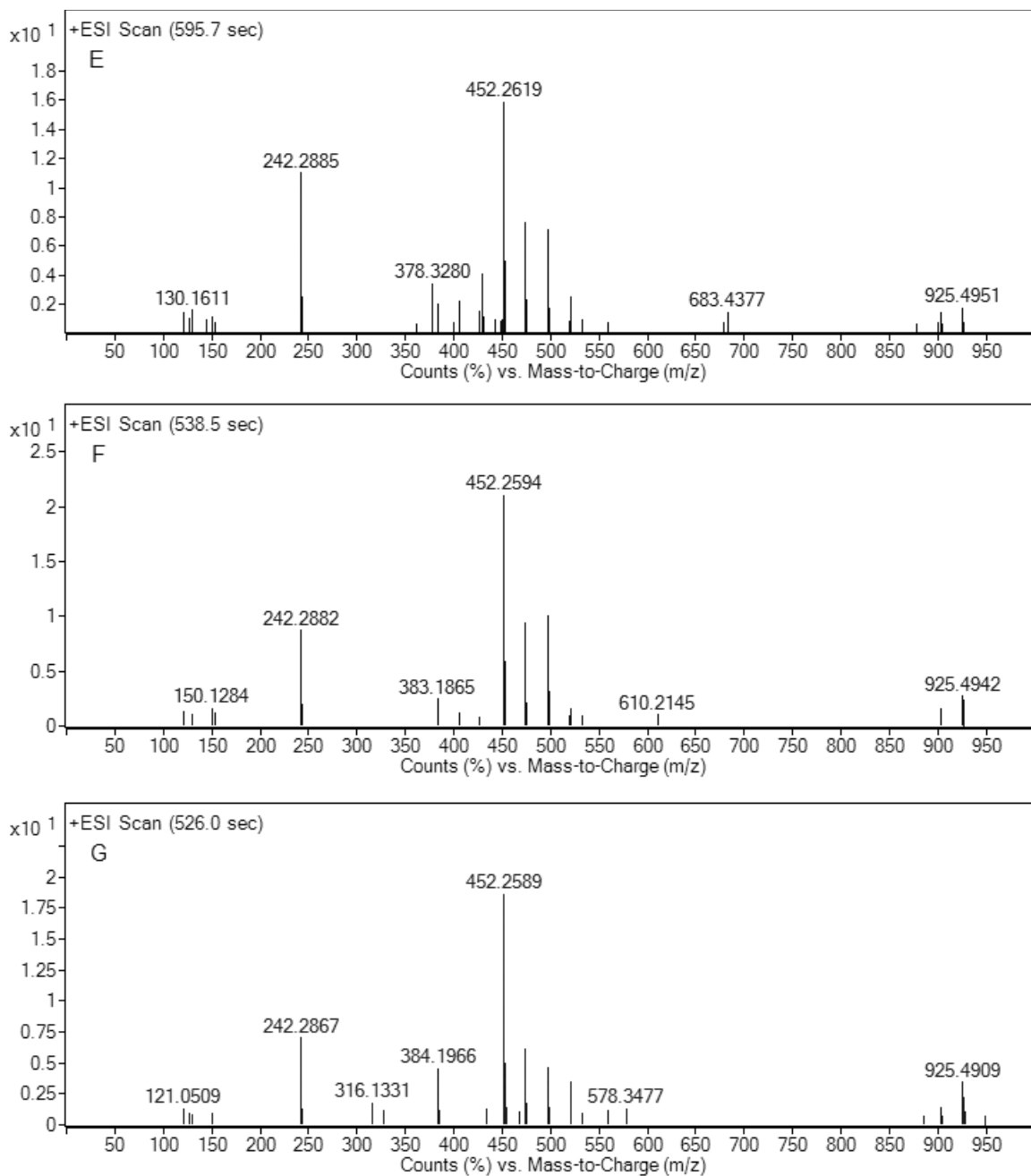


Figure 2-20. Mass spectra of (A) **9** standard; (B) Product formed from NotI + **9** observed at 594.3 seconds; (C) Product formed from NotI + **9** observed at 540.0 seconds; (D) Product formed from NotI + **9** observed at 526.6 seconds; (E) Product formed from NotI' + **9** observed at 595.7 seconds; (F) Product formed from NotI' + **9** observed at 538.5 seconds; (G) Product formed from NotI' + **9** observed at 526.0 seconds.

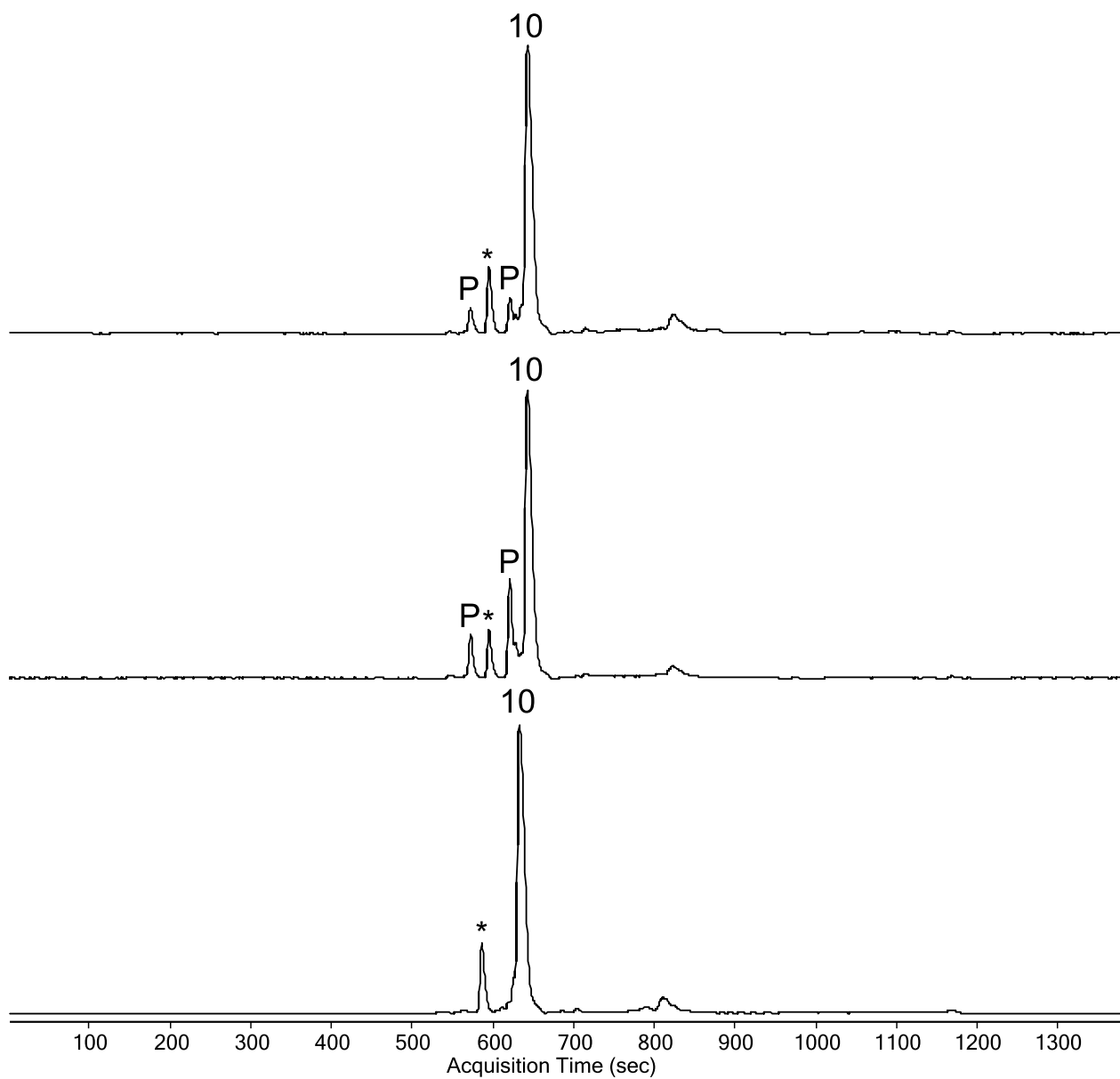
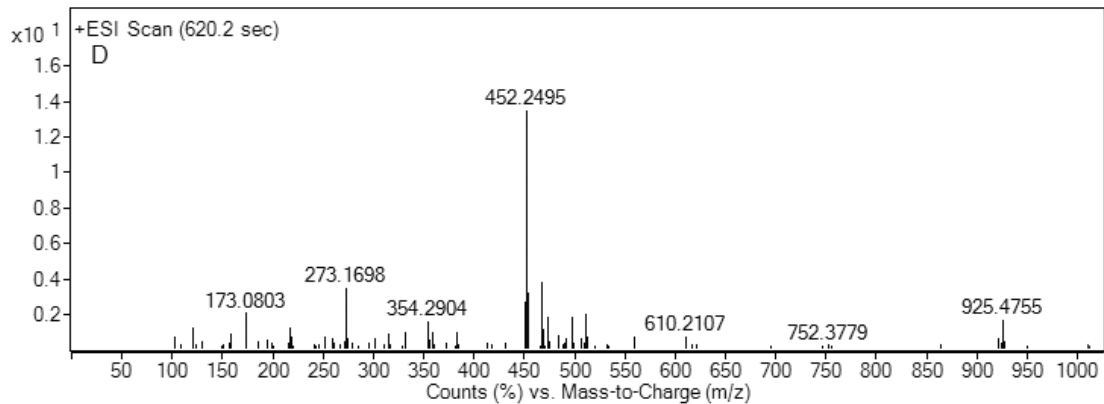
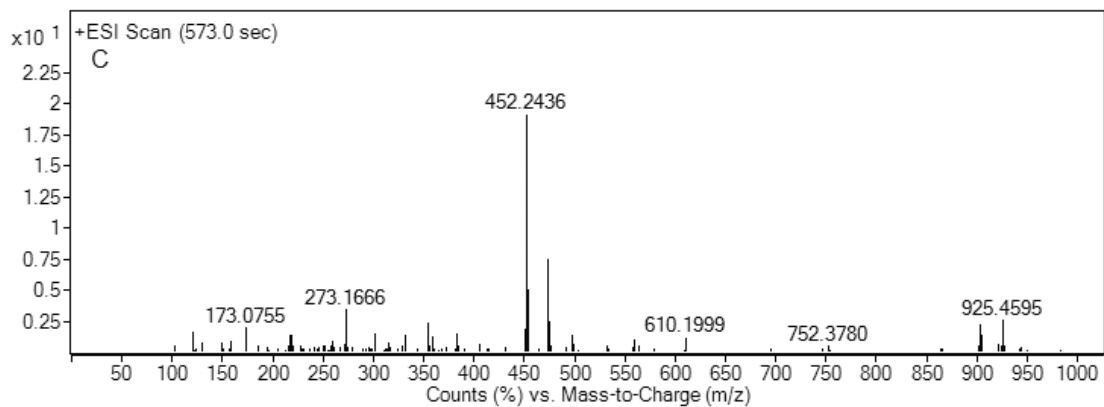
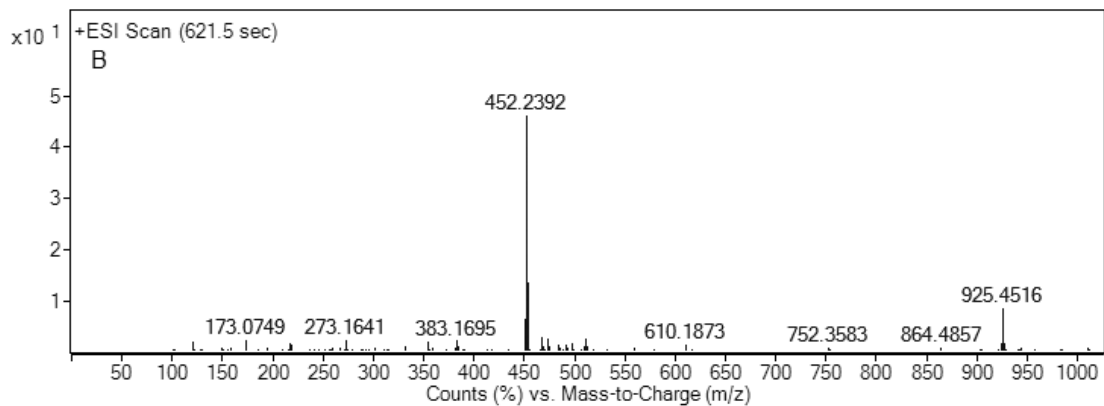
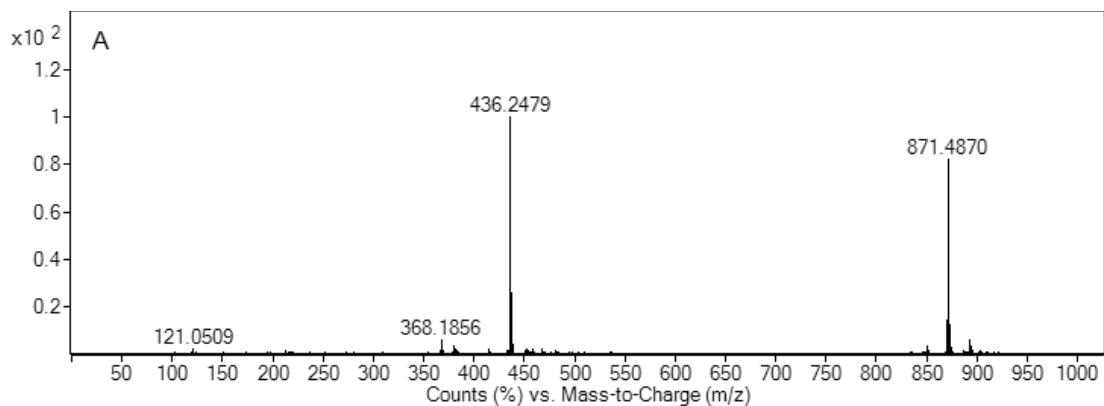


Figure 2-21. LC-MS Q-TOF analysis depicting EICs of (a) NotI' reaction with **10**; (b) NotI reaction with **10**; (c) authentic **10** standard. Product(s) formed is denoted with P. Asterisk denotes possible diastereomer of **10**.



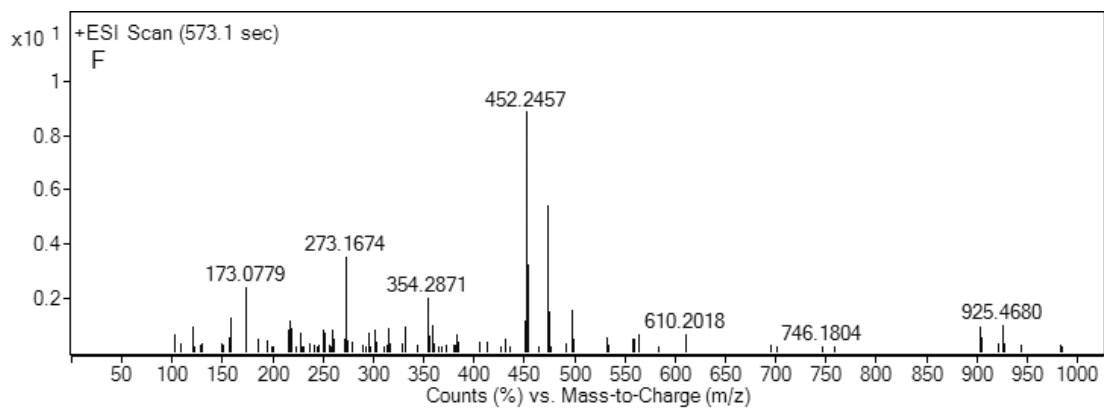


Figure 2-22. Mass spectra of (A) **10** standard with 2 ¹³C label; (B) Product formed from NotI + **10** observed at 621.5 seconds; (C) Product formed from NotI + **10** observed at 573.0 seconds; (D) Product formed from NotI' + **10** observed at 620.2 seconds; (E) Product formed from NotI' + **10** observed at 573.1 seconds.

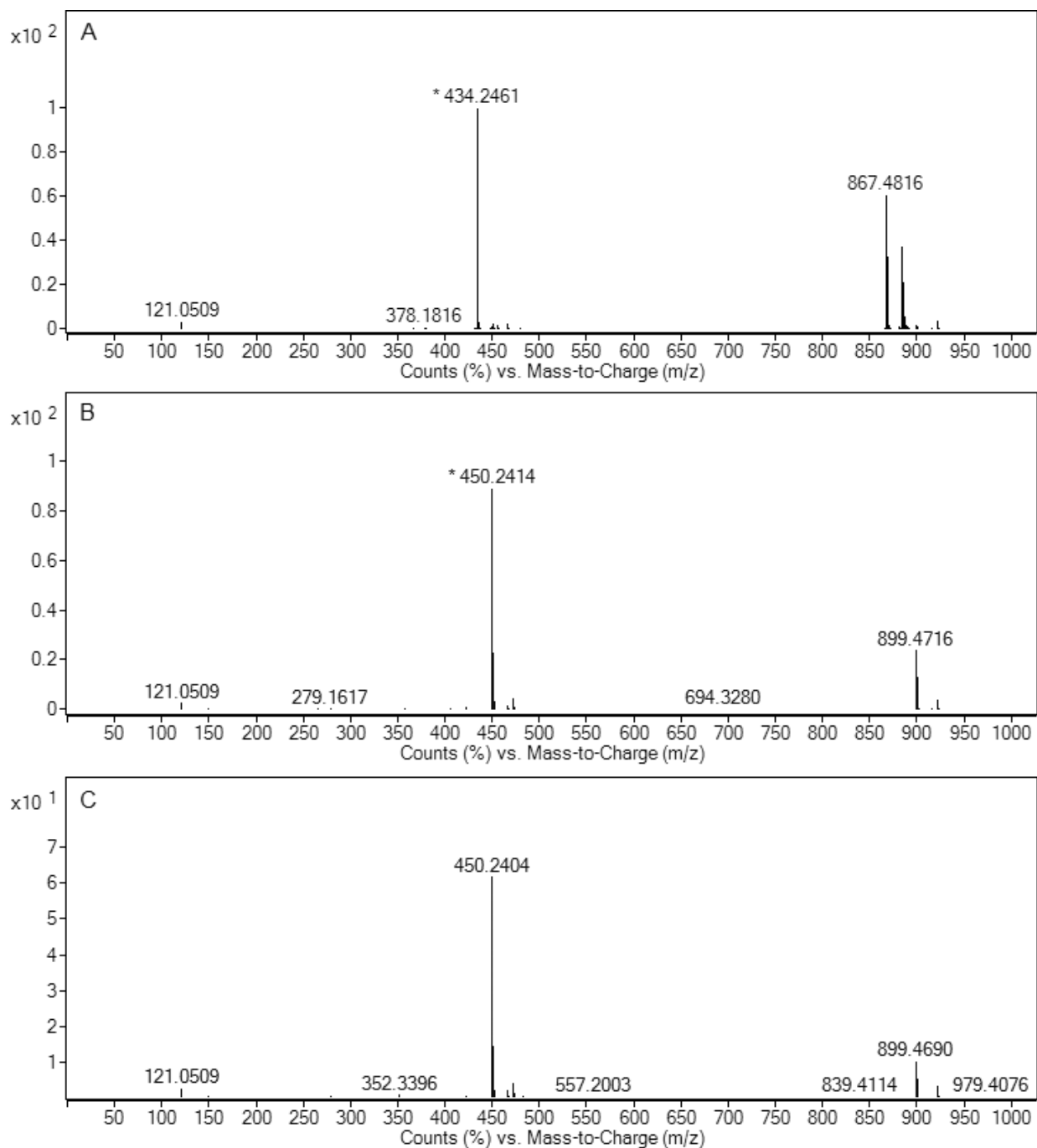


Figure 2-23. Mass spectra of (A) (\pm)-**15** standard; (B) Product formed from NotII + (\pm)-**15**; (C) Product formed from NotI' + (\pm)-**15**.

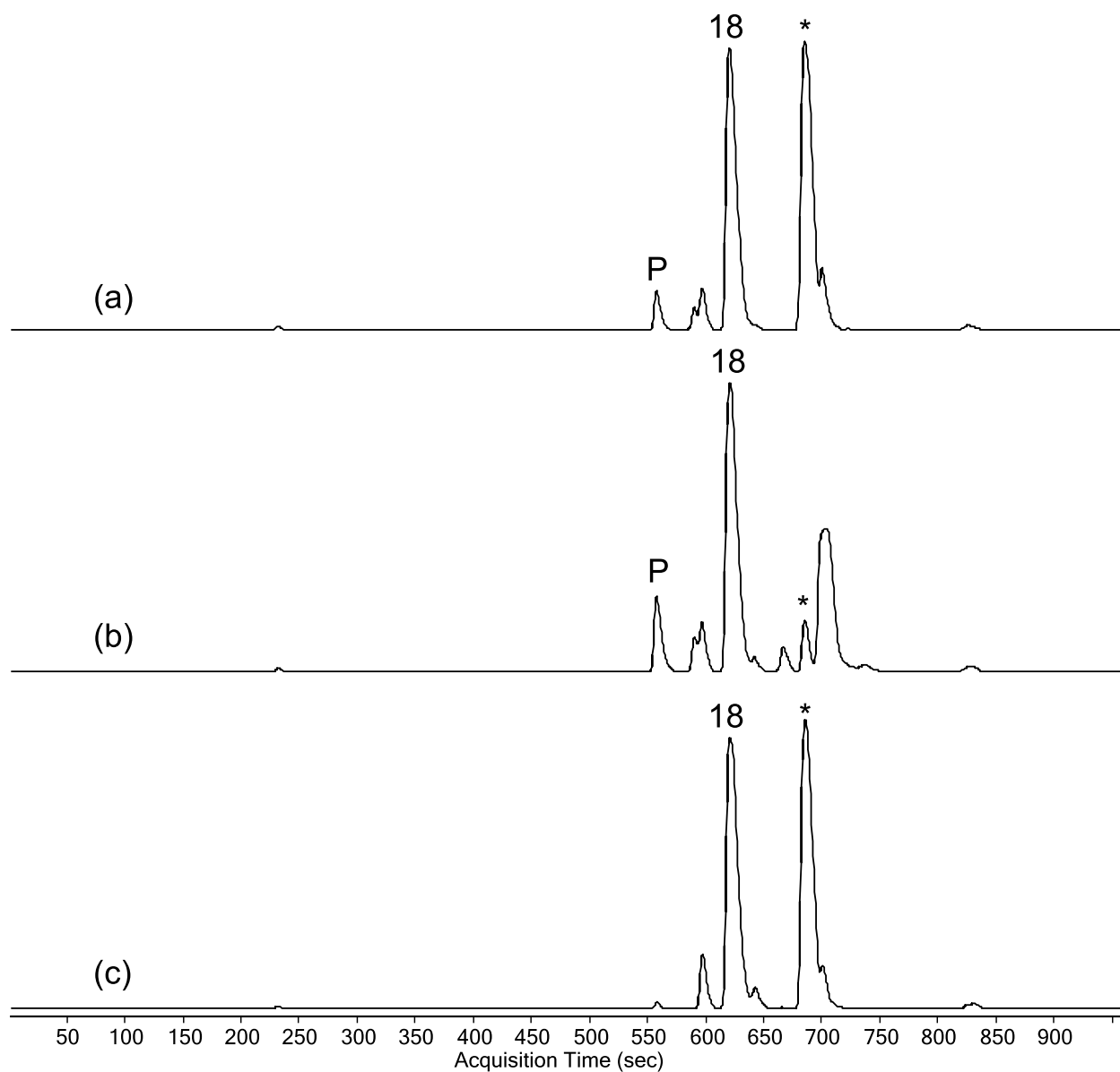


Figure 2-24. LC-MS Q-TOF analysis depicting EICs of (a) NotI' reaction with (\pm)-**18**; (b) NotI reaction with (\pm)-**18**; (c) authentic (\pm)-**18** standard. Product(s) formed is denoted with P. Asterisk denotes possible diastereomer of **18**.

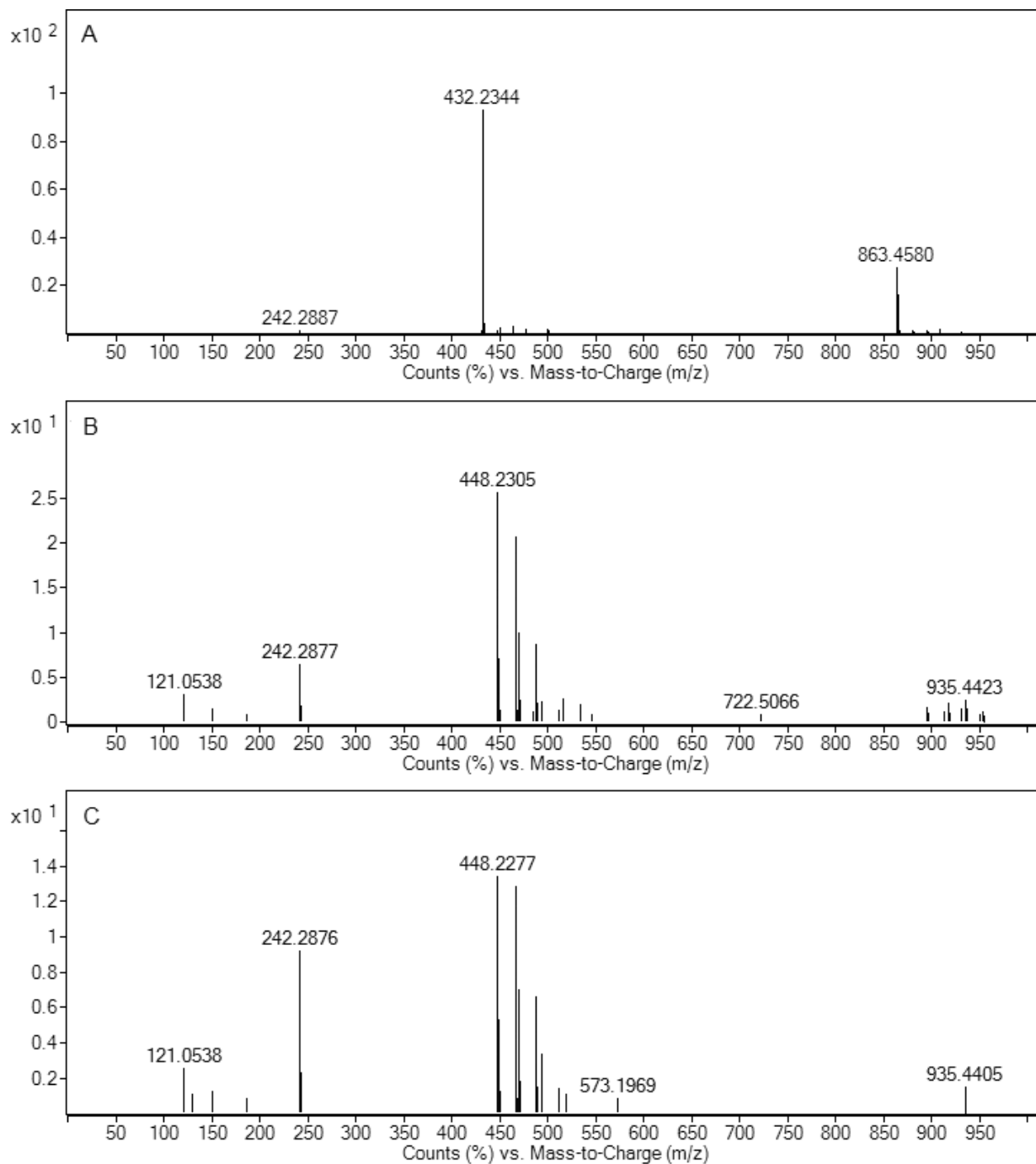


Figure 2-25. Mass spectra of (A) (\pm) -**18** standard; (B) Product formed from NotI + (\pm) -**18**; (C) Product formed from NotI' + (\pm) -**18**.

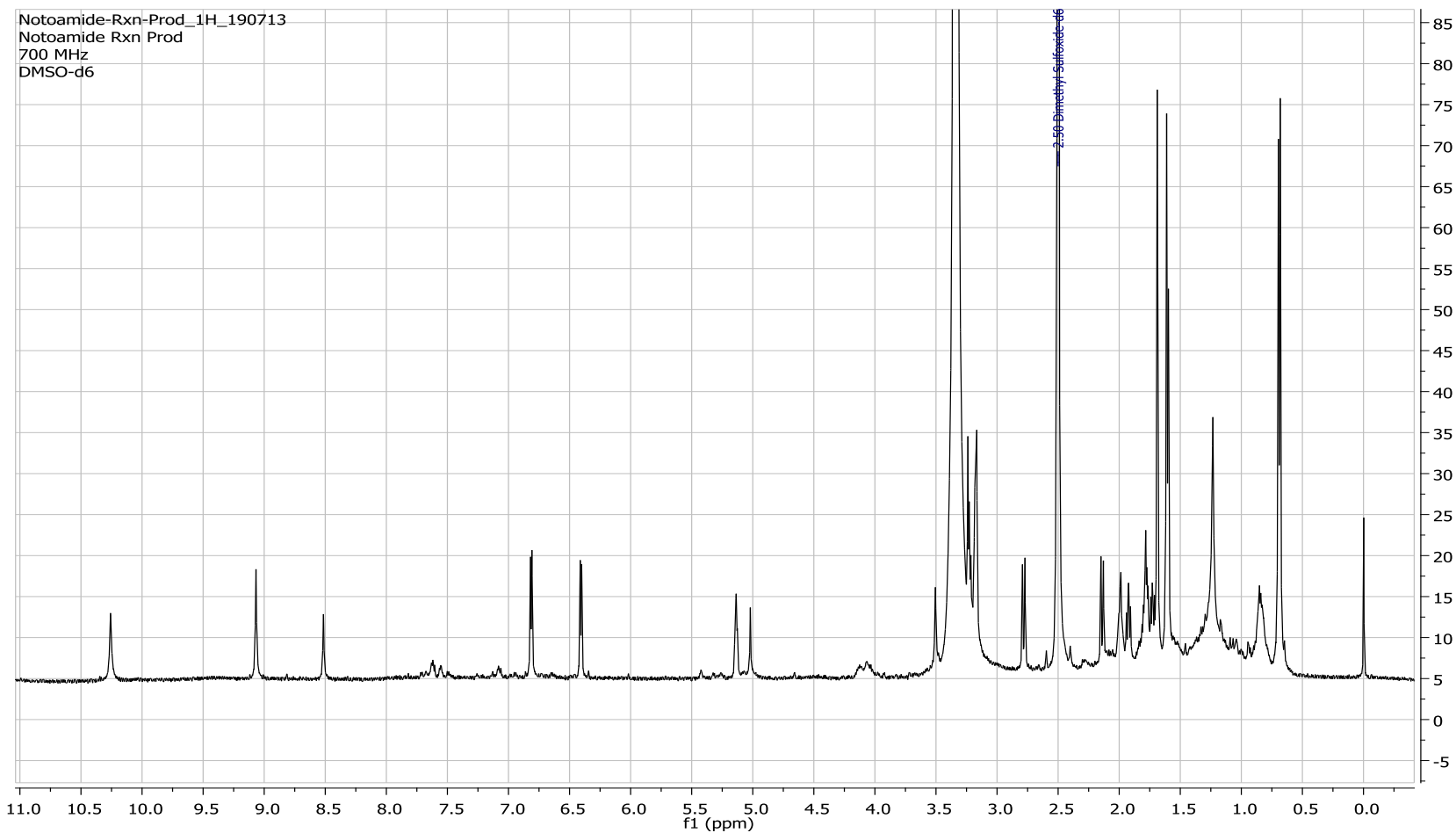


Figure 2-26. ^1H NMR spectrum of Notoamide T9 (**19**) recorded at 700 MHz (in DMSO-d_6)

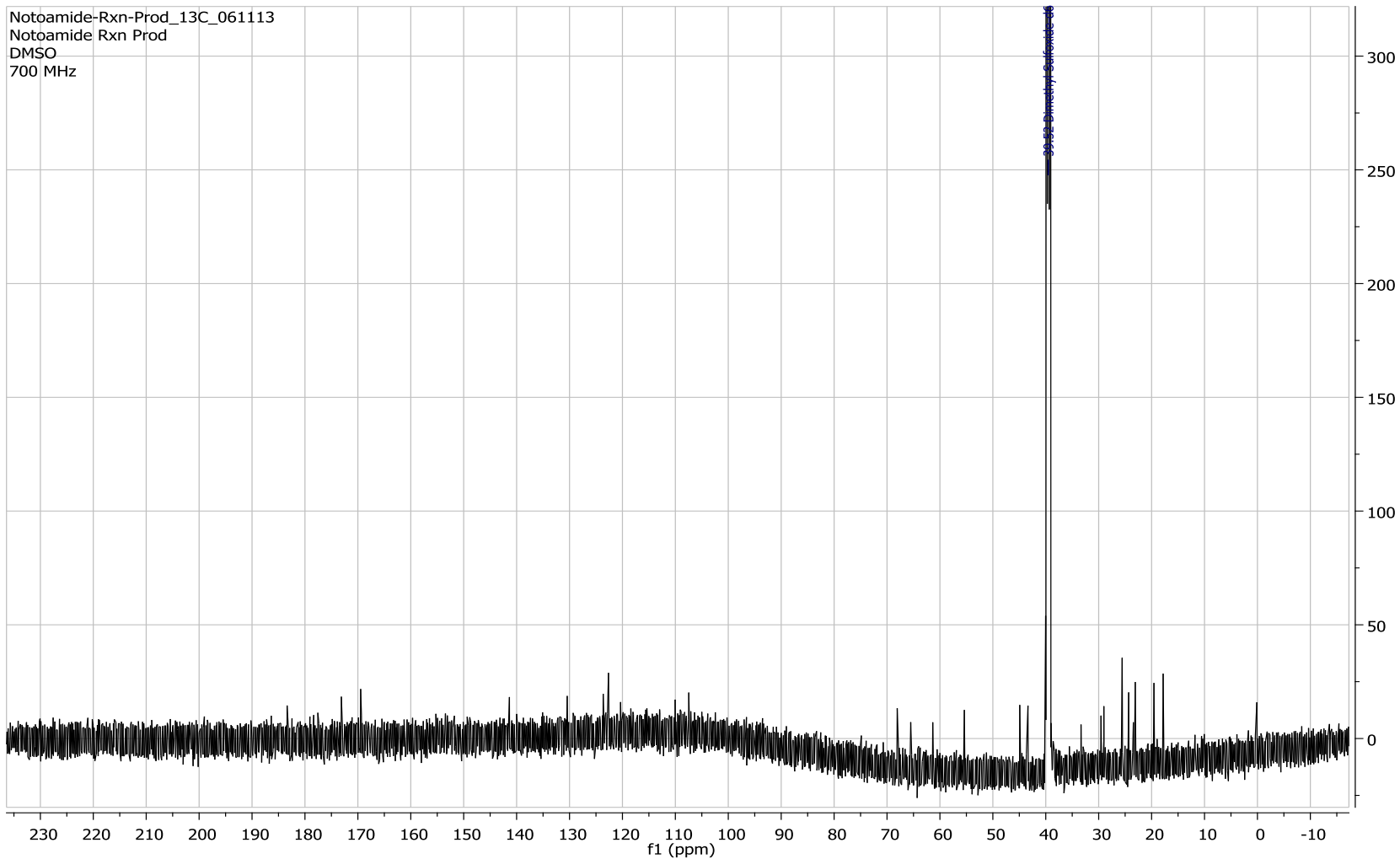


Figure 2-27. ^{13}C NMR spectrum of Notoamide T9 (**19**) recorded at 700 MHz (in DMSO- d_6)

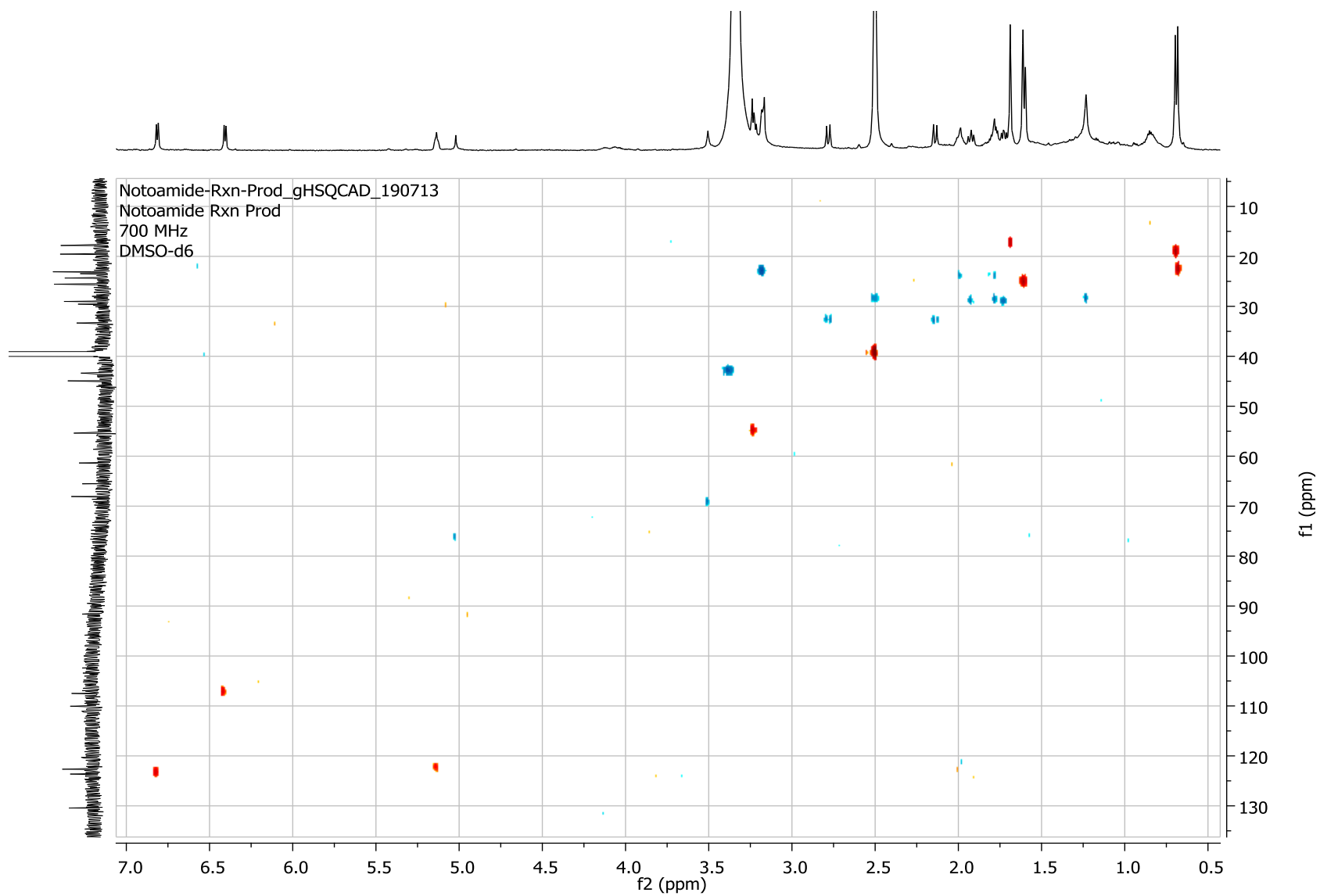


Figure 2-28. HSQCAD spectrum of Notoamide T9 (**19**) recorded at 700 MHz (in DMSO-d₆)

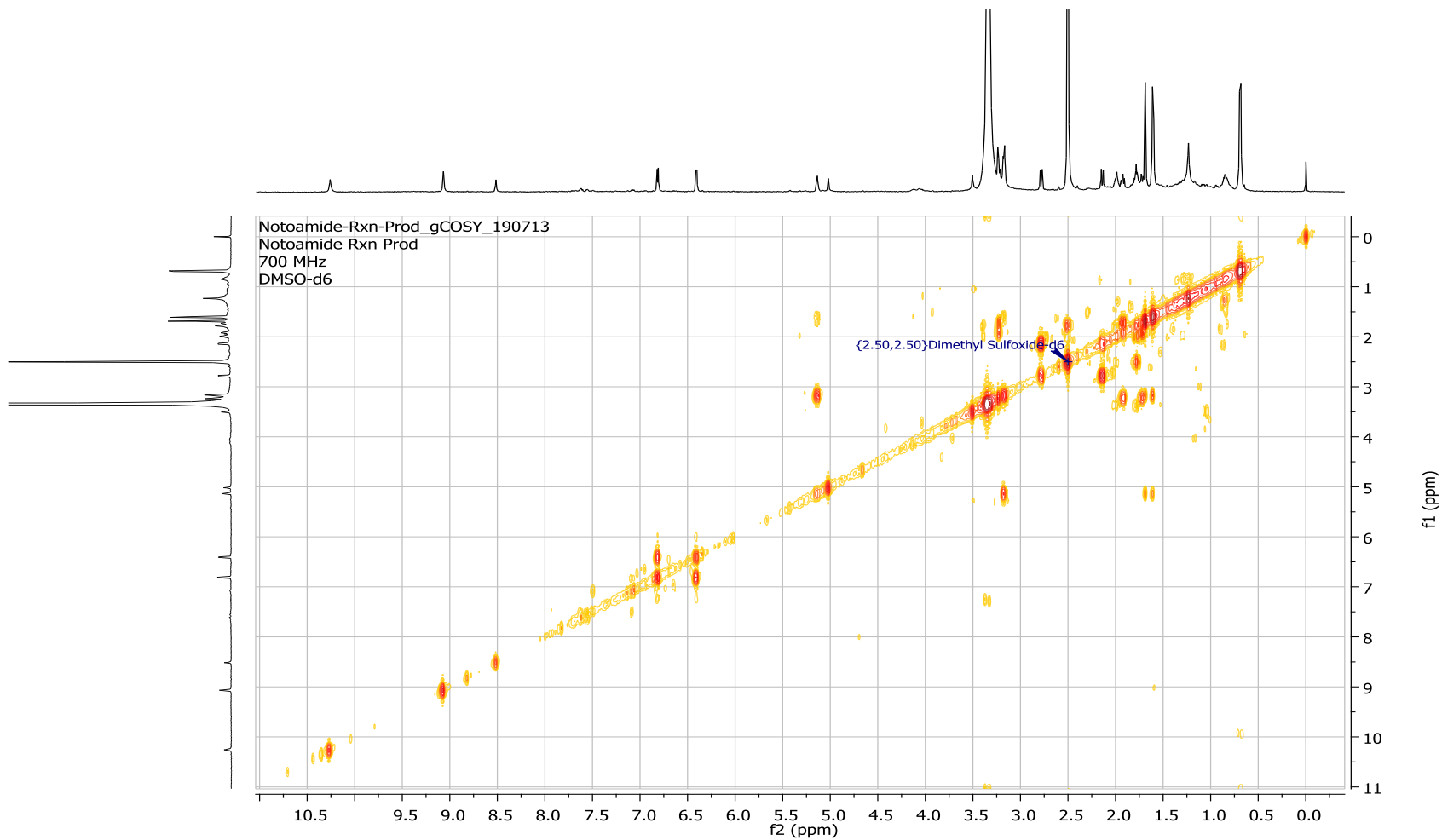


Figure 2-29. gCOSY spectrum of Notoamide T9 (**19**) recorded at 700 MHz (in DMSO-d₆)

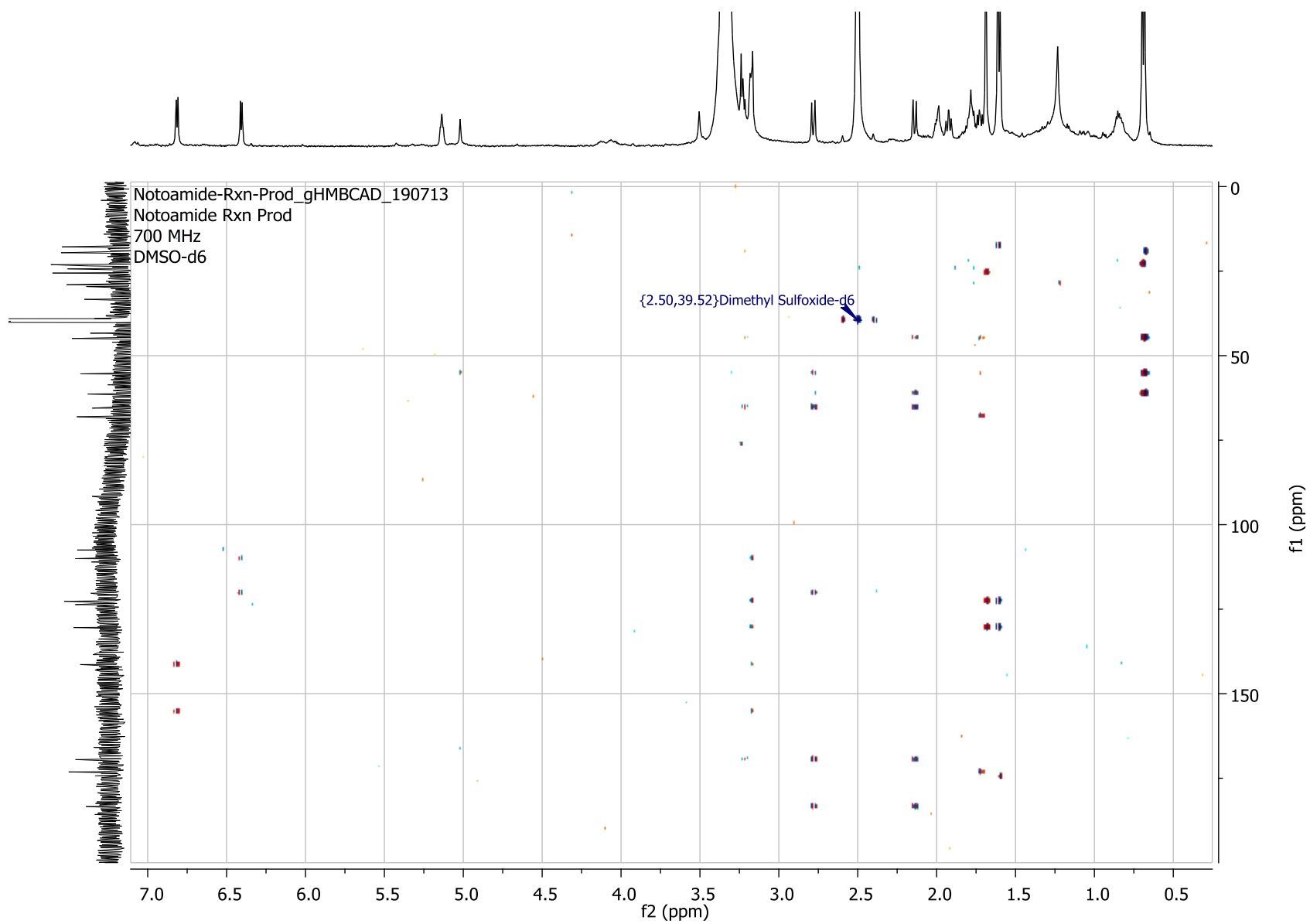


Figure 2-30. gHMBCAD spectrum of Notoamide T9 (19) recorded at 700 MHz (in DMSO-d₆)

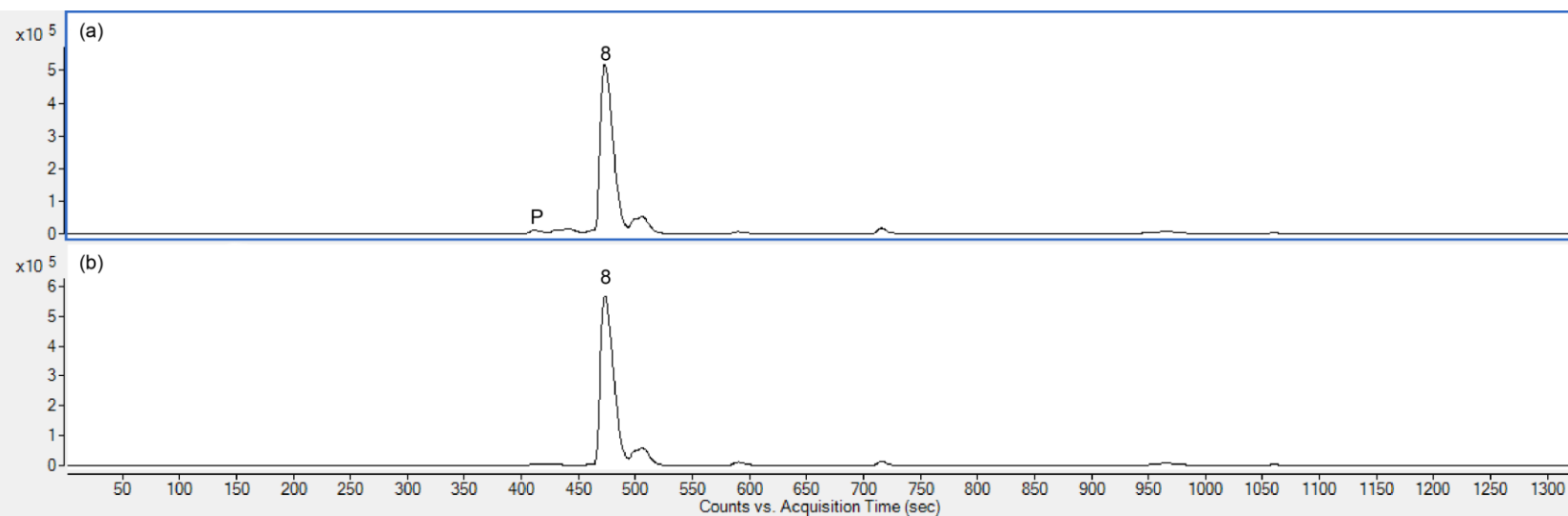


Figure 2-31. LC-MS Q-TOF analysis depicting EICs of (a) PhqK reaction with **8**; (b) authentic **8** standard. Product(s) formed is denoted with P.

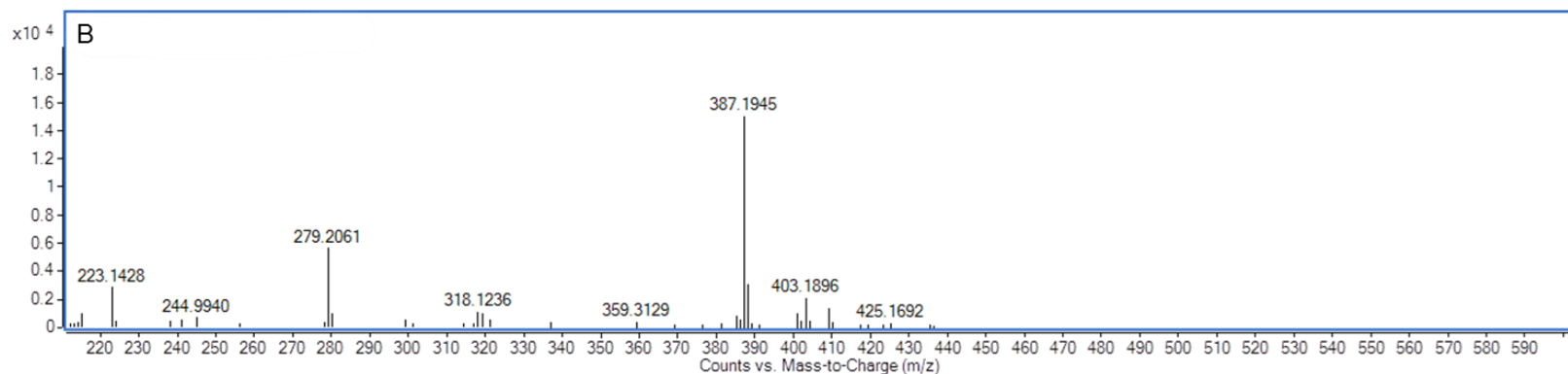
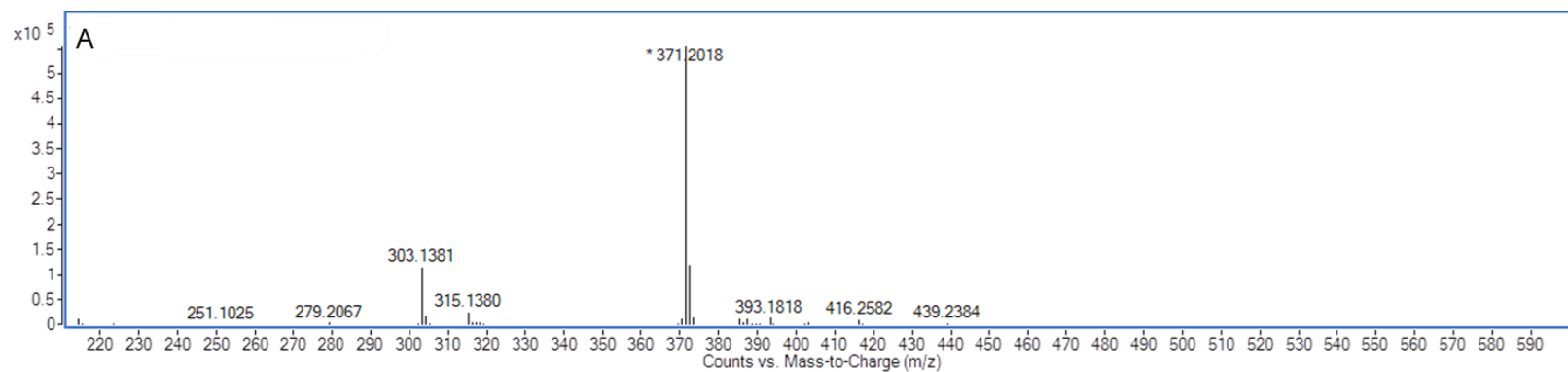


Figure 2-32. Mass spectra of (A) **8** standard with 3 ^{13}C label; (B) Product formed from PhqK + **8**.

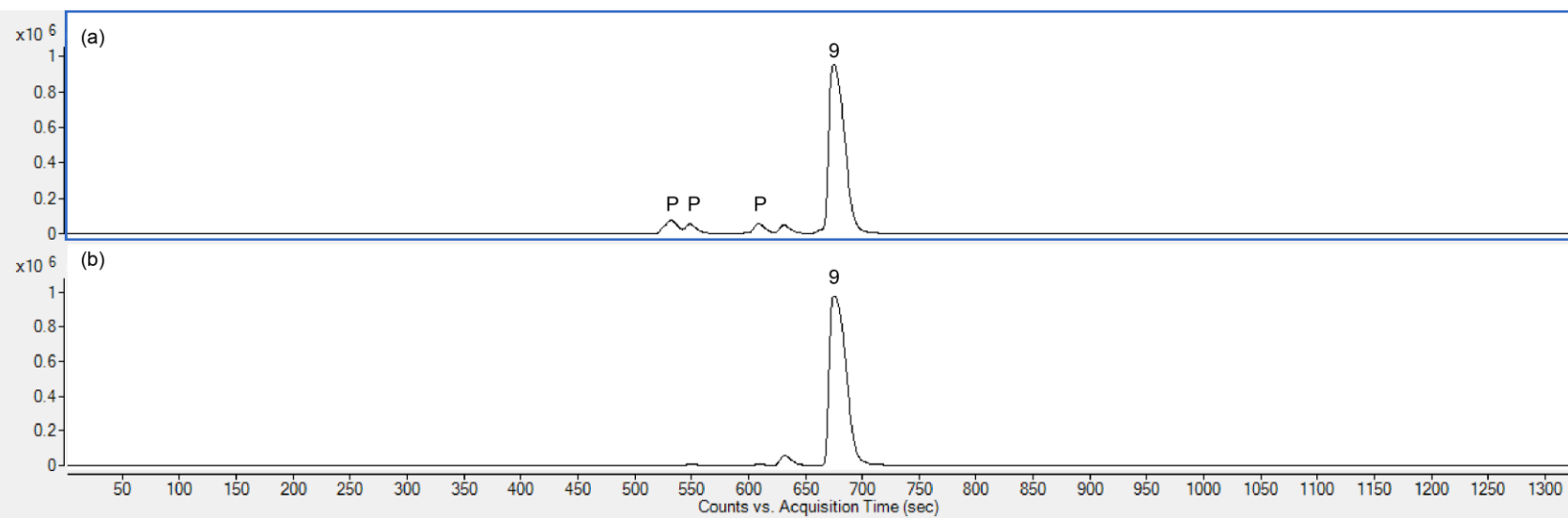


Figure 2-33. LC-MS Q-TOF analysis depicting EICs of (a) PhqK reaction with **9**; (b) authentic **9** standard. Product(s) formed is denoted with P.

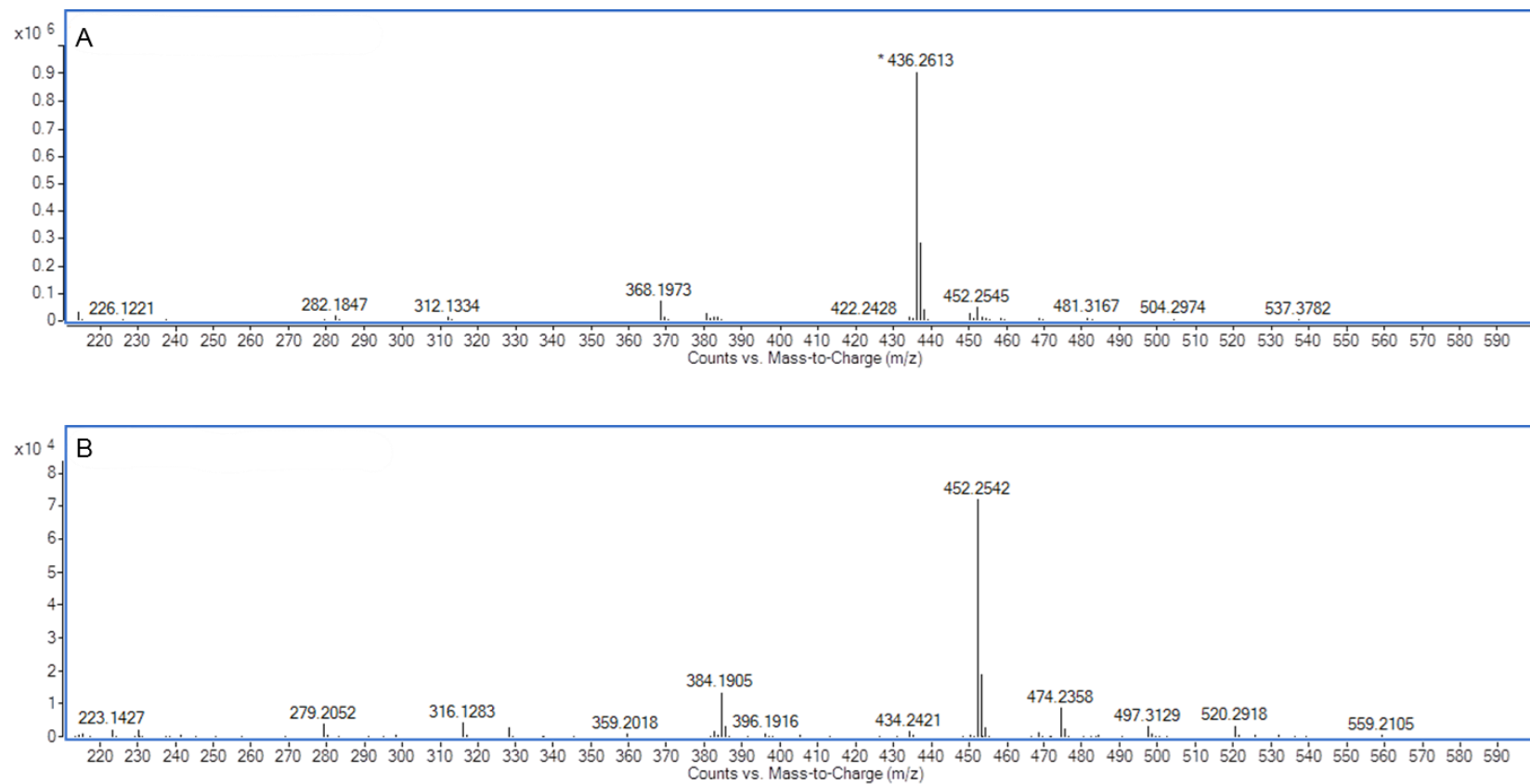


Figure 2-34. Mass spectra of (A) **9** standard; (B) Product formed from PhqK + **9**.

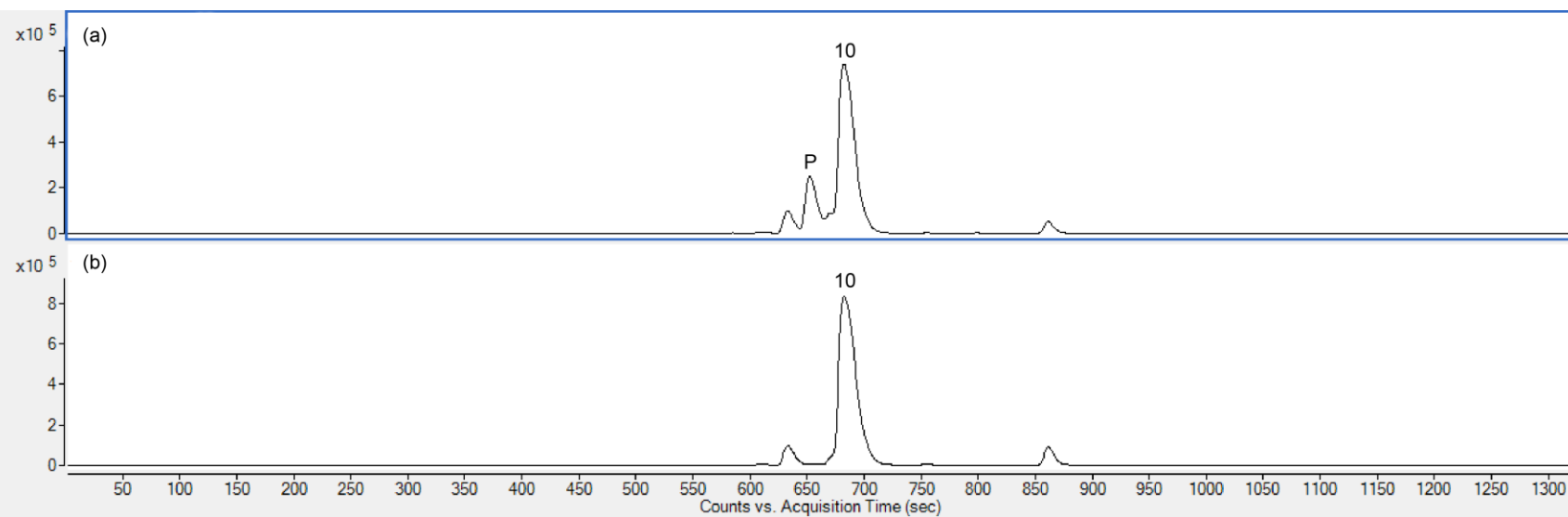


Figure 2-35. LC-MS Q-TOF analysis depicting EICs of (a) PhqK reaction with **10**; (b) authentic **10** standard. Product(s) formed is denoted with P.

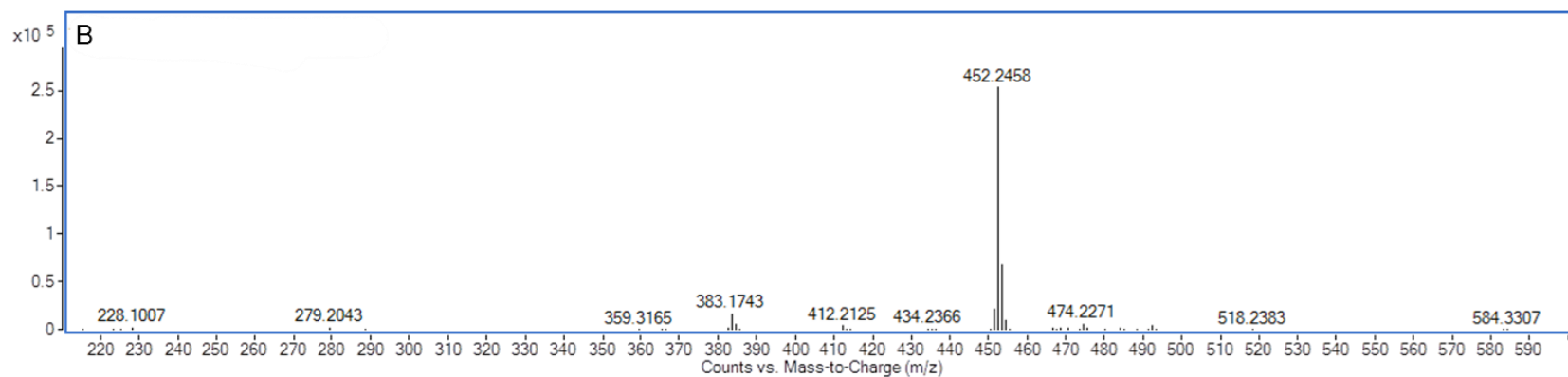
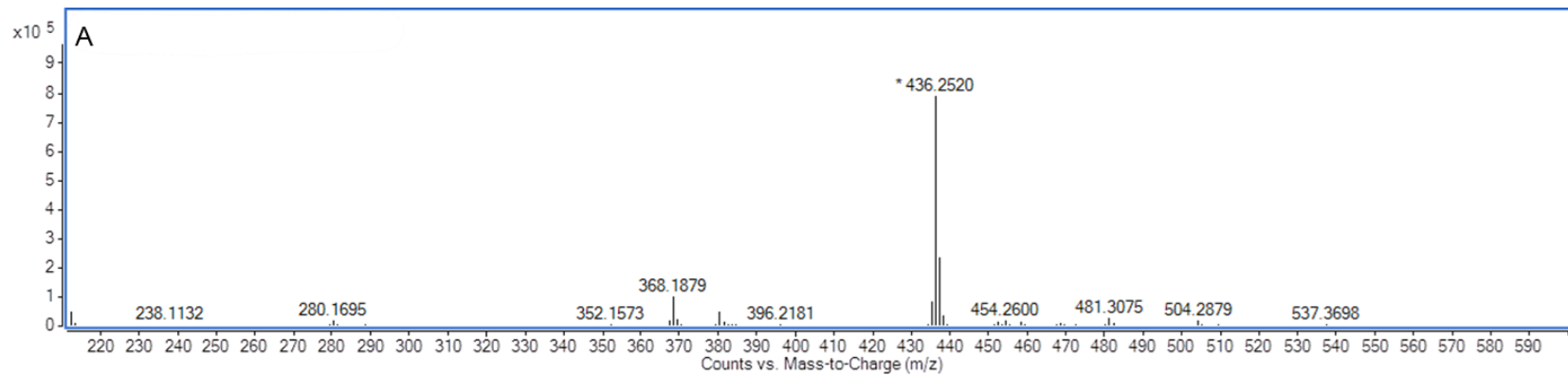


Figure 2-36. Mass spectra of (A) **10** standard with 2 ^{13}C label; (B) Product formed from PhqK + **10**.

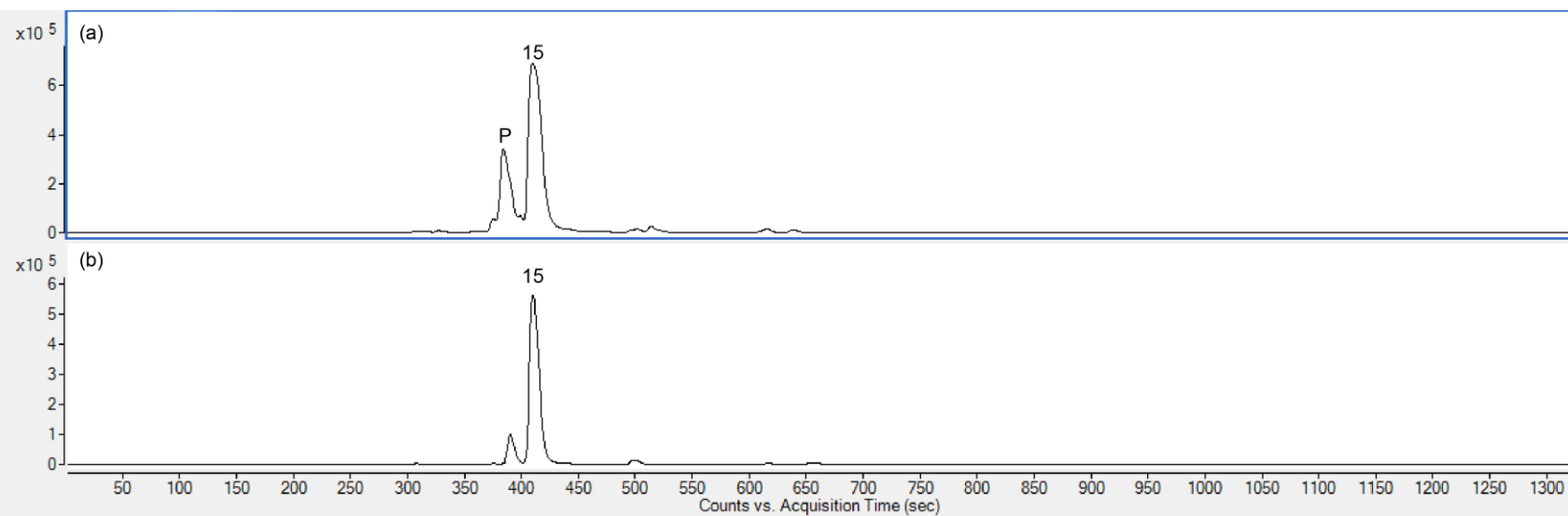


Figure 2-37. LC-MS Q-TOF analysis depicting EICs of (a) PhqK reaction with **15**; (b) authentic **15** standard. Product(s) formed is denoted with P.

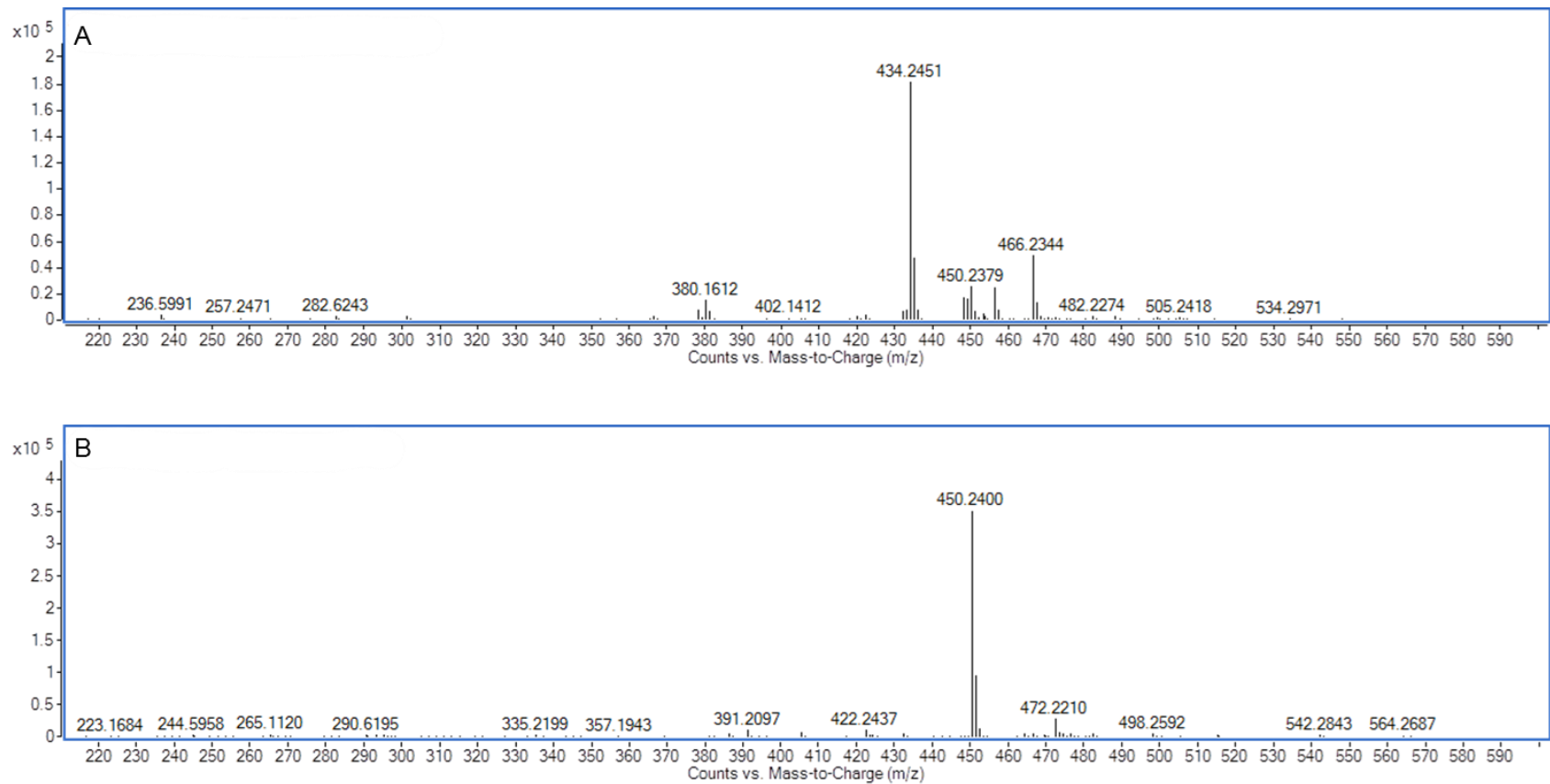


Figure 2-38. Mass spectra of (A) **15** standard; (B) Product formed from PhqK + **15**.

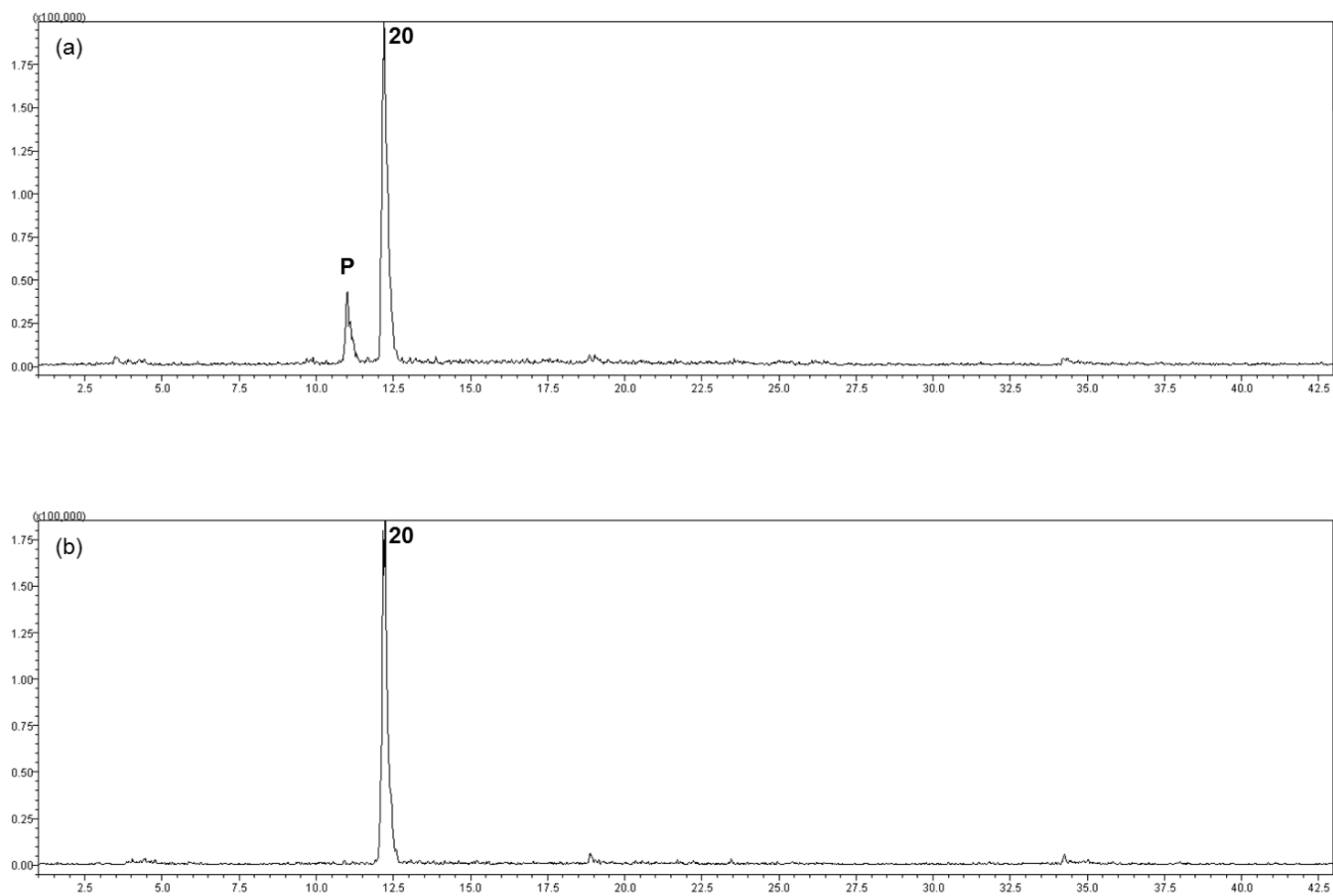


Figure 2-39. LC-MS Q-TOF analysis depicting EICs of (a) PhqK reaction with **20**; (b) authentic **20** standard. Product(s) formed is denoted with P.

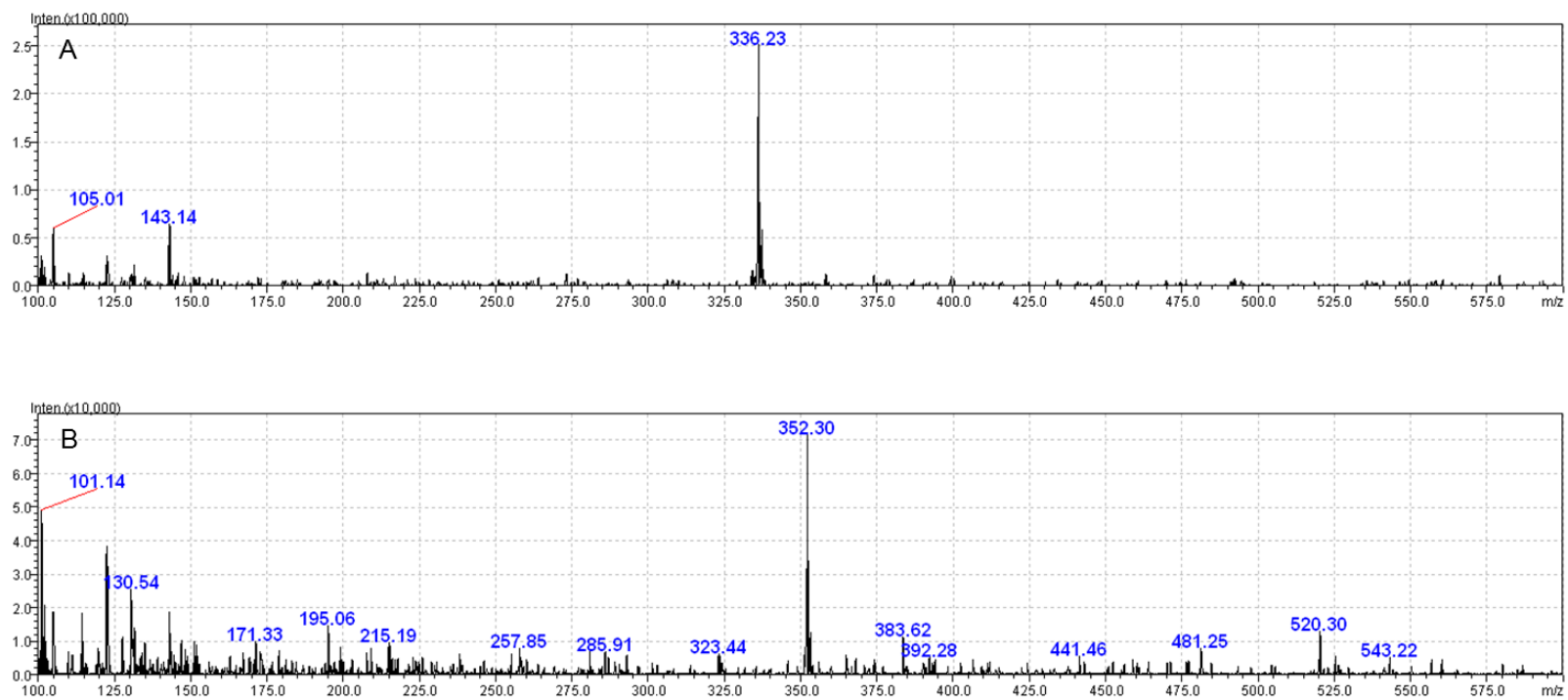


Figure 2-40. Mass spectra of (A) **20** standard; (B) Product formed from PhqK + **20**.

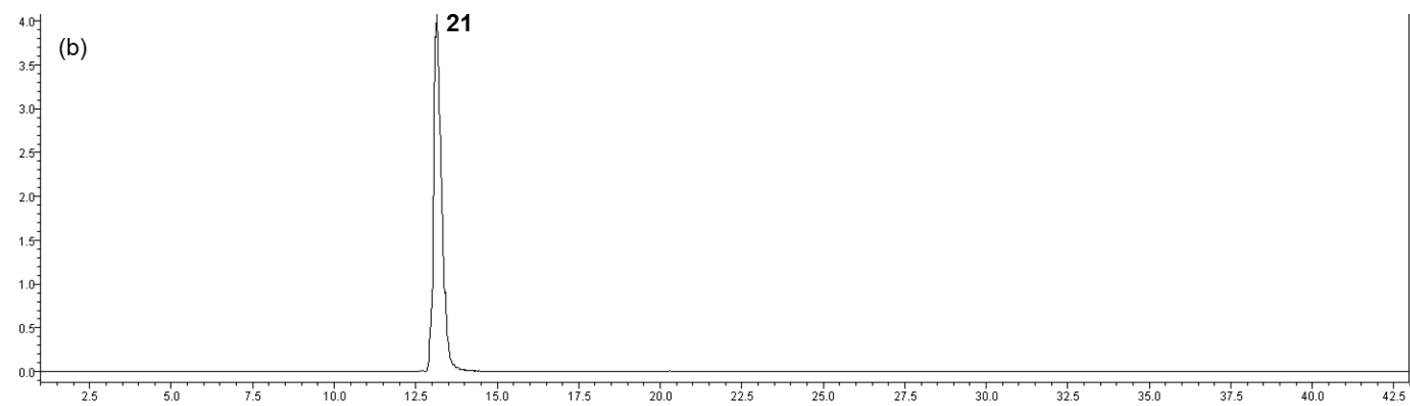
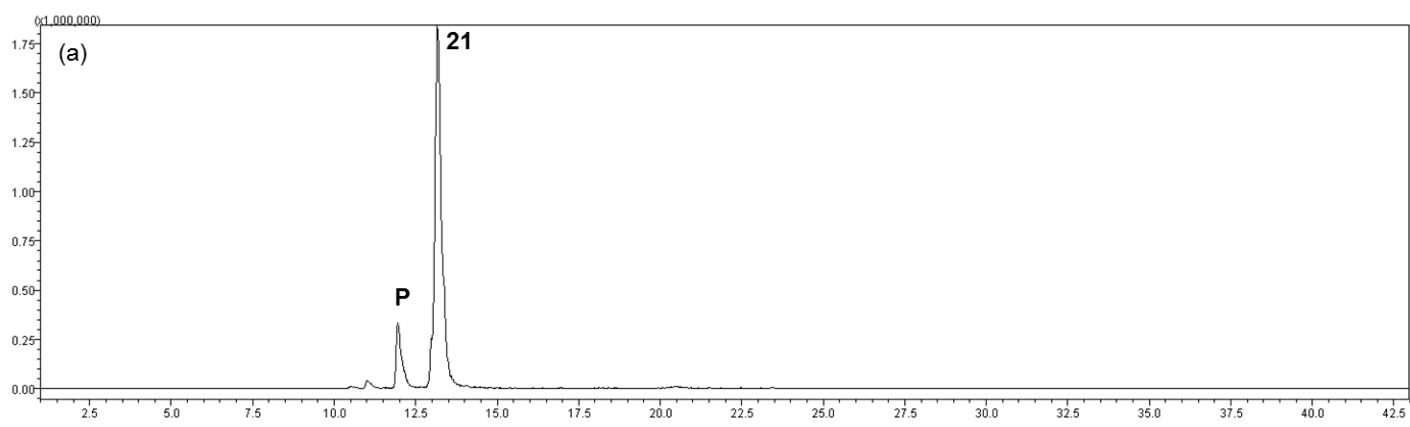


Figure 2-41. LC-MS Q-TOF analysis depicting EICs of (a) PhqK reaction with **21**; (b) authentic **21** standard. Product(s) formed is denoted with P.

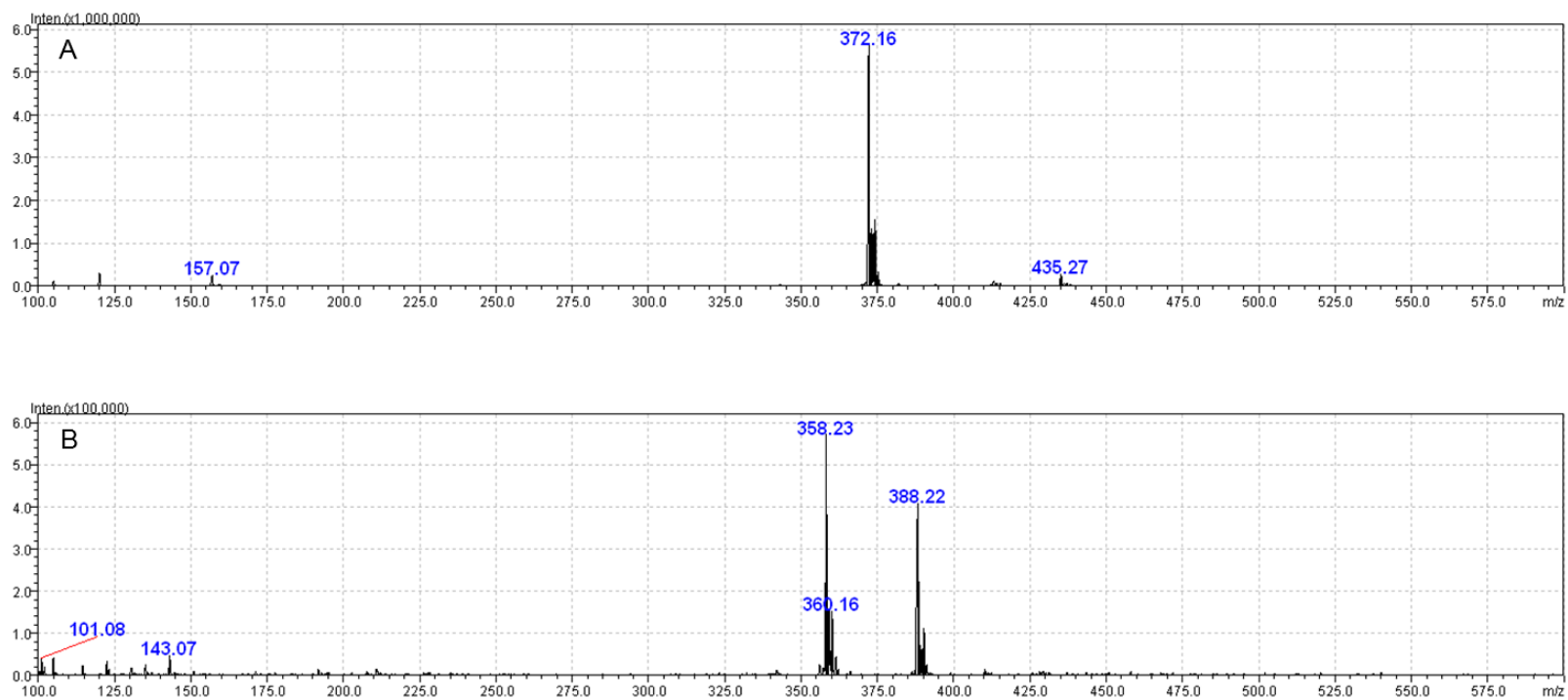


Figure 2-42. Mass spectra of (A) **21** standard with 2 ¹³C label; (B) Product formed from PhqK + **21**.

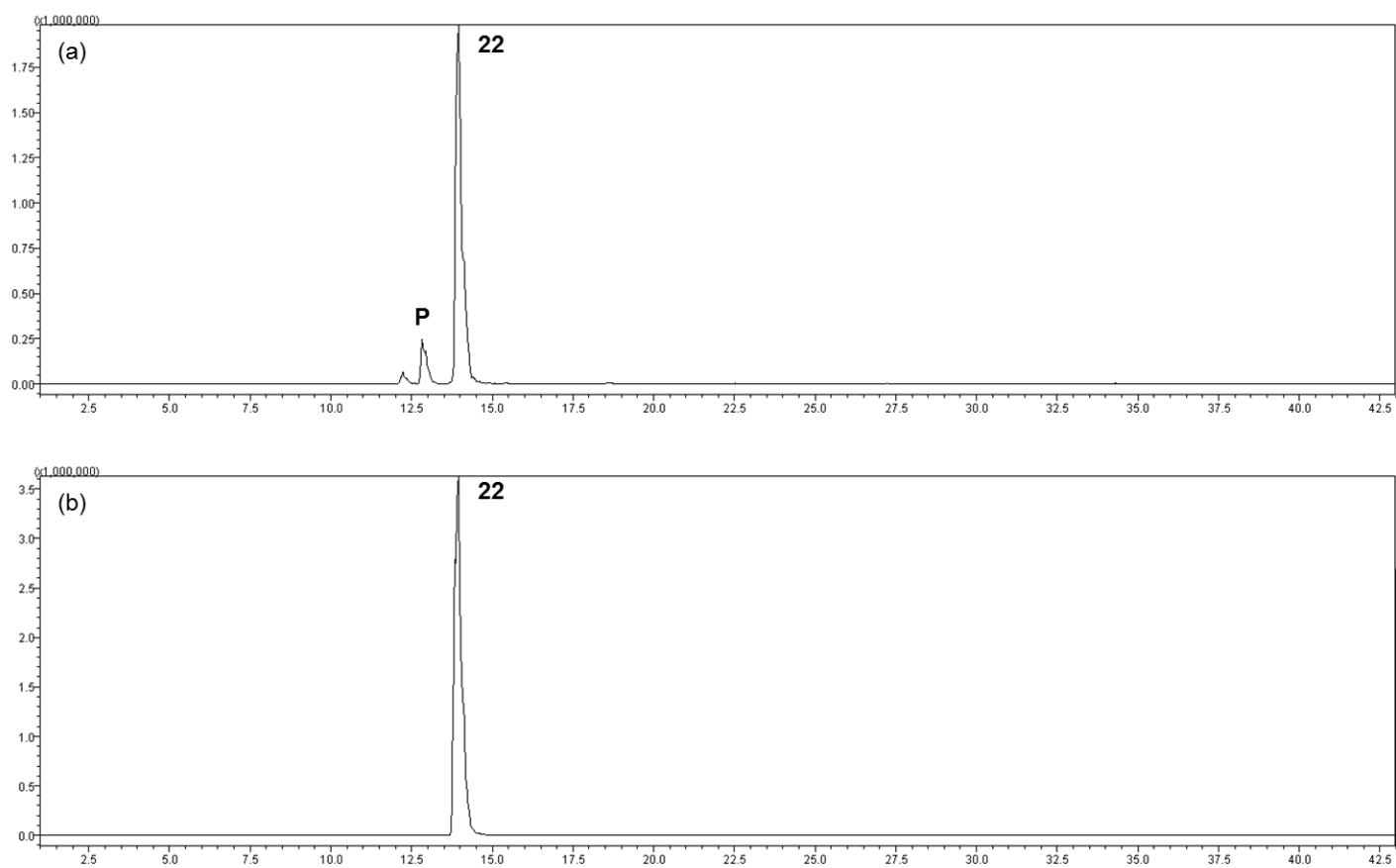


Figure 2-43. LC-MS Q-TOF analysis depicting EICs of (a) PhqK reaction with **22**; (b) authentic **22** standard. Product(s) formed is denoted with P.

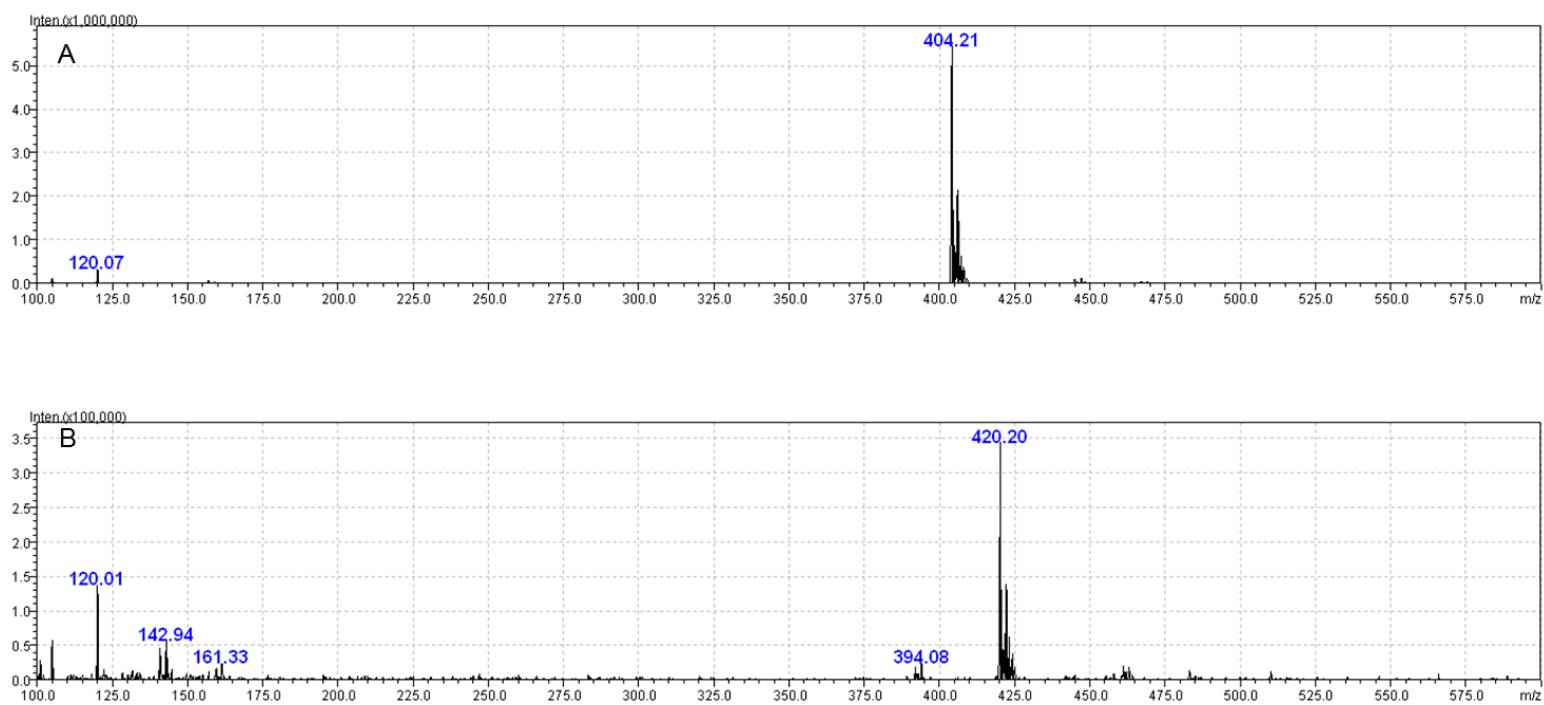


Figure 2-44. Mass spectra of (A) **22** standard; (B) Product formed from PhqK + **22**.

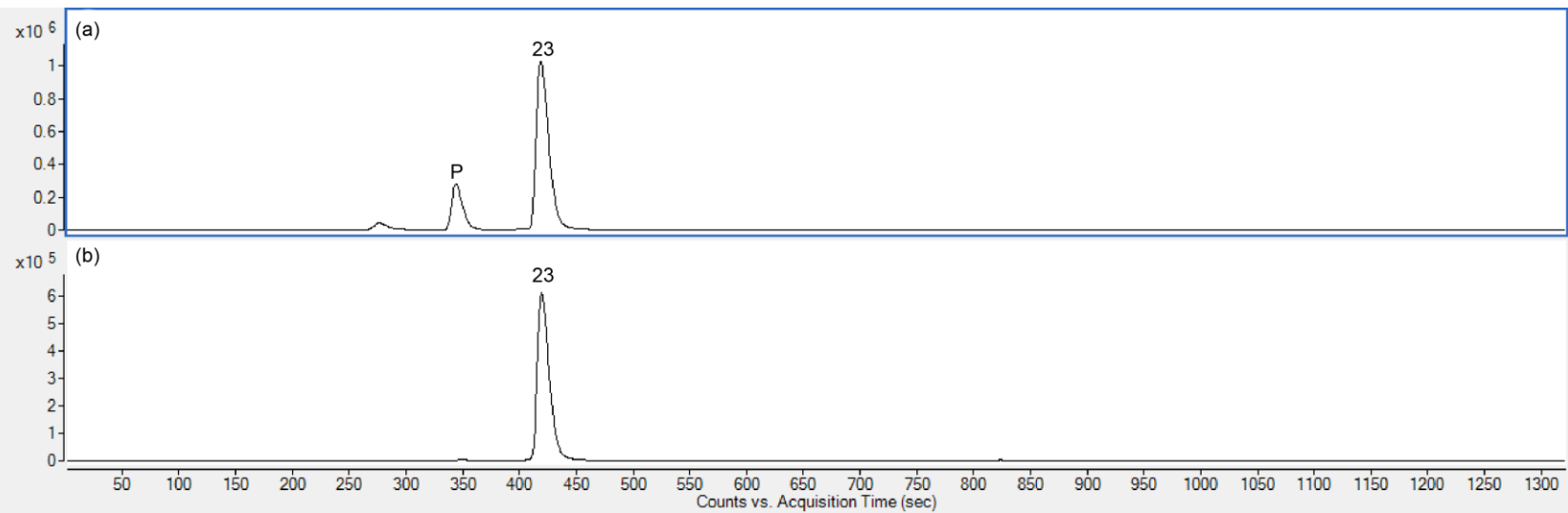


Figure 2-45. LC-MS Q-TOF analysis depicting EICs of (a) PhqK reaction with **23**; (b) authentic **23** standard. Product(s) formed is denoted with P.

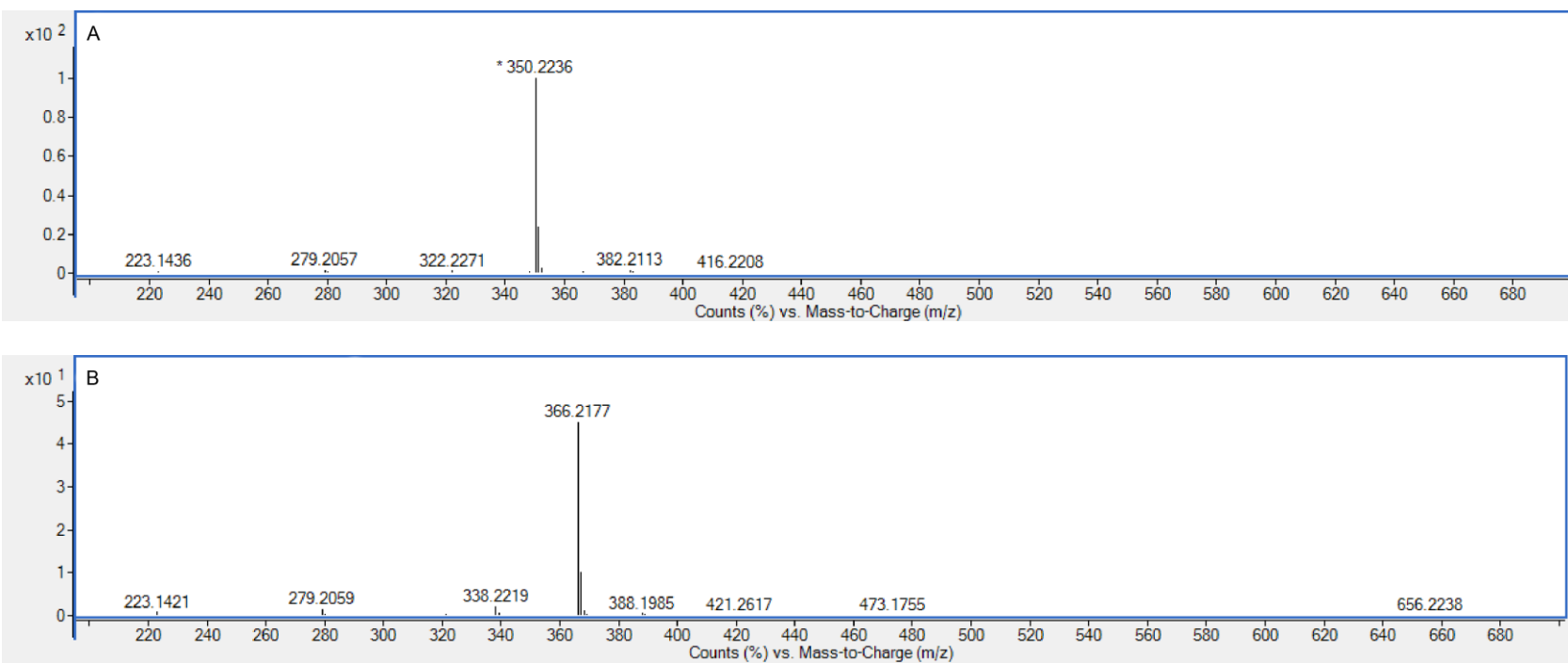


Figure 2-46. Mass spectra of (A) **23** standard; (B) Product formed from PhqK + **23**.

Author Contributions:

Hong T. Tran, Ashootosh Tripathi, Sean A. Newmister, Shengying Li, Sachiko Tsukamoto, David H. Sherman, and Robert M. Williams contributed to the experimental design. Shengying Li cloned NotI; Hong T. Tran cloned NotI', performed enzymatic reactions and analysis on proteins NotI and NotI', isolated (-)-stephacidin A for kinetics experiments, performed kinetics experiments, and scaled up and purified notoamide T9 for characterization; Sean A. Newmister performed enzymatic reactions and analysis on protein PhqK; Ashootosh Tripathi performed 2D NMR analysis of Notoamide T9. Hong T. Tran, Ashootosh Tripathi, Sean A. Newmister, Shengying Li, David H. Sherman, and Robert M. Williams evaluated the data. During the preparation of this dissertation, this body of work has been submitted to Journal of the American Chemical Society for review.

Chapter 3

Prenyltransferases

3.1 Introduction

Prenylated natural compounds have demonstrated great utility in biological activity due to the increased lipophilicity of the molecule after modification.¹⁰⁸ While the core, unmodified molecule may not exhibit activities of interest, prenylated molecules have been found to be active in most fields of pharmacological sciences.¹⁰⁹ Consequently, a better biochemical understanding of the mechanism of prenylation is desired. We seek to both understand the natural role of the prenyltransferase in the biosynthetic pathway, as well as exploring the prenyltransferases' ability to modify related compounds for the diversification of natural products and bioactive molecules.

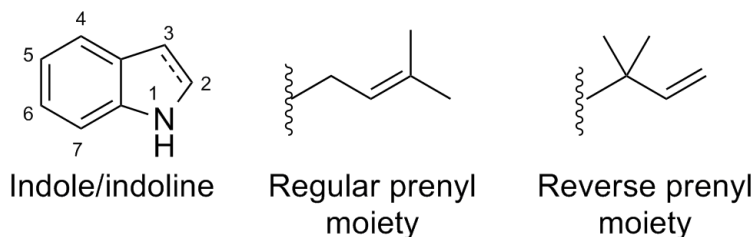


Figure 3-1. Indole ring and two types of prenyl modifications.

Prenylated indole alkaloids comprise one class of natural products that contain a prenylated aromatic moiety. These compounds are typically found in *Claviceps*, *Penicillium*, and *Aspergillus* strains.¹² The aromatic precursor is modified by an indole prenyltransferase, one major category of prenyltransferases that can be further divided into four major subcategories. Firstly, these prenyltransferases have been found to catalyze reactions on carbon atoms or nitrogen atoms, respectively named C- or N-prenyltransferases. Secondly, either the C1 or C3

atom of dimethylallyl pyrophosphate (DMAPP) will attach to the aromatic moiety, referred to as a regular or reverse prenylation, respectively (Figure 3-1).¹¹⁰ For example, if the regular prenyl moiety were added to the indole ring at position 2, it would be referred to as a regular C2-prenylation event. Examples of each type of reaction are observed within the prenylated indole alkaloid family at various positions along the indole ring, suggesting that nature has evolved many prenyltransferases for specific modifications to the indole ring.

The precursor molecule DMAPP also arises by its own biosynthetic pathway. While DMAPP is used almost universally as the building block for prenyltransferases to modify the indoles, it is more commonly known as the building block for the formation of isoprenoids, compounds that are found in all domains of life.¹¹¹ For about the past half century, the molecule was believed to be formed via the mevalonic acid (MVA) pathway, which ultimately results in the formation of isopentenyl diphosphate (IPP) that is isomerized to DMAPP.¹¹² More recently, a

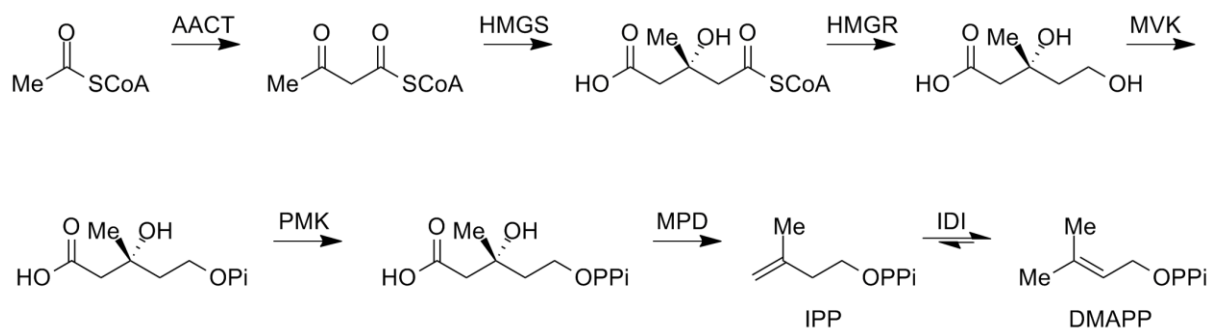


Figure 3-2. The classical mevalonate (MVA) pathway to form IPP and DMAPP.

second pathway, the methylerythritol phosphate (MEP) pathway, was discovered to also generate IPP and DMAPP.¹¹³ The MEP pathway is more frequently observed in eubacteria, green algae, and higher plants, while the MVA pathway is more commonly observed in animals, plants, fungi, and archaea.^{114,115} These molecules are thus present in most domains of life.

Indole prenyltransferases are similar to dimethylallyl tryptophan synthases from fungi, and include examples from *Aspergillus fumigatus*.¹¹⁶ Of the well characterized examples include

FgaPT2, a dimethylallyltryptophan synthase responsible for the C4 prenylation of tryptophan in fumigaclavine C biosynthesis.¹¹⁷ The structure of FgaPT2 has also previously been solved, demonstrating its similarity to ABBA bacterial prenyltransferases,¹¹⁸ which was not readily apparent from the amino acid sequence.¹¹⁹ FgaPT1 has additionally been characterized as a reverse prenyltransferase at the C2 position of the indole ring, thus converting fumigaclavine A to fumigaclavine C.¹²⁰ From the same producing organism, prenyltransferases from the fumitremorgin biosynthetic pathway were also biochemically characterized. FtmPT1 was found

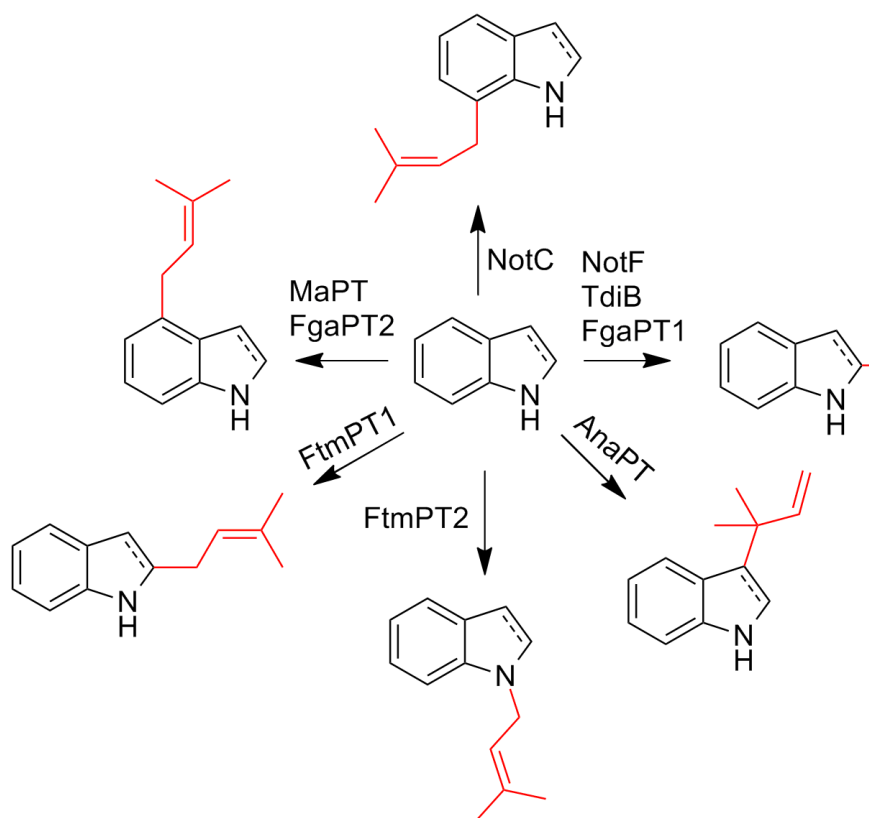


Figure 3-3. Examples of known prenyltransferases and the positions they modify along the indole ring. Actual substrate structures are not shown for simplicity.

to prenylate the indole ring of breviramide F at the C2 position,¹²¹ while FtmPT2 was demonstrated to perform a late biosynthetic step on fumitremorgin C, prenylating the indole ring on the nitrogen atom.¹²² Other fungal prenyltransferases to note include AnaPT,¹²³ which

modifies the C3 position on the indole ring to form aszonalenin, and TdiB,¹²⁴ which reverse prenylates the C2 position on the indole ring to form asterriquinone C-1.

We have also previously investigated a number of prenyltransferases from the biosynthetic gene clusters mined in our laboratory. From the notoamide biosynthetic system, NotC and NotF have previously been characterized as a regular prenyltransferase at the C7 position and a reverse prenyltransferase at the C2 position on the indole ring, respectively.⁹⁶ Additionally, a random prenyltransferase (MaPT) had been identified and characterized from the malbrancheamide pathway.¹²⁵ This gene product was mined randomly from the sequenced genome before a comparative analysis of the fungal gene clusters was available. MaPT was determined to be a regular C-prenyltransferase at the 4 position on the indole ring, which curiously does not appear in the formation of the malbrancheamide natural product at all. Also worthy to note, MaPT was reportedly inhibited by the presence of EDTA, which is an

Table 3-1. Predicted functions of gene products from the malbrancheamide gene cluster.

Gene product	Function	Size (AA)
MalA	Halogenase	667
MalB	Prenyltransferase	369
MalC	Short chain dehydrogenase	264
MalD	Negative regulator	336
MalE	Prenyltransferase	438
MalF	Oxidoreductase	590
MalG	NRPS	2345

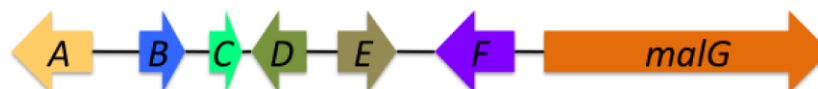


Figure 3-4. Malbrancheamide gene cluster.

unexpected finding in this class of enzymes.

When we initially investigated the malbrancheamide gene cluster (Figure 3-4), we identified two putative prenyltransferases: MalB and MalE (Table 3-1).⁹⁷ Bioinformatic analysis of each putative gene product gave no further insight to whether these gene products were regular or reverse prenyltransferases, or exactly how each would compare to the prenyltransferases from the notoamide or paraherquamide gene clusters. The inability to determine the exact reaction of a fungal prenyltransferase from the amino acid sequence has been observed in other examples,¹¹⁹ unlike findings in bacterial prenyltransferases.¹²⁶ Therefore, we decided upon an in-depth biochemical characterization of each gene product to determine the activity of MalB and MalE. Initial attempts to express and purify MalB and MalE resulted in insoluble MalB protein and soluble MalE protein. Thus, MalE was initially chosen for investigation due to its ease of accessibility.

Lastly, we hypothesized that upon prenylation of the compound **3** (Figure 3-6), the azadiene and prenyl dienophile would react to undergo the Diels-Alder construction of premalbrancheamide. To date, a natural enzyme catalyst of the Diels-Alder reaction has not yet been identified, although artificial Diels-Alderase have been designed and engineered to be effective biocatalysts for the [4+2] cycloaddition reaction.¹²⁷ However, the isolation of only the *syn*-isomers of malbrancheamide from *M. aurantiaca* strongly suggest that a stereoselective mechanism is involved in the IMDA construction of the bicyclo[2.2.2]diazaoctane core,²⁵ and that a biosynthetic enzyme is responsible for the control of the chiral center being formed.¹²⁸ Therefore, we decided to investigate the activity of MalE not only as a prenyltransferase but also as a potential Diels-Alderase.

3.2 Results

3.2.1 MalE demonstrates prenyltransferase activity

Before we began synthesizing putative substrates for use with MalE, we decided to turn to already available substrates from the Notoamide pathway. NotF has been shown to reverse prenylate Brevianamide F to form product Deoxybrevianamide E.⁹⁶ Assuming that MalE

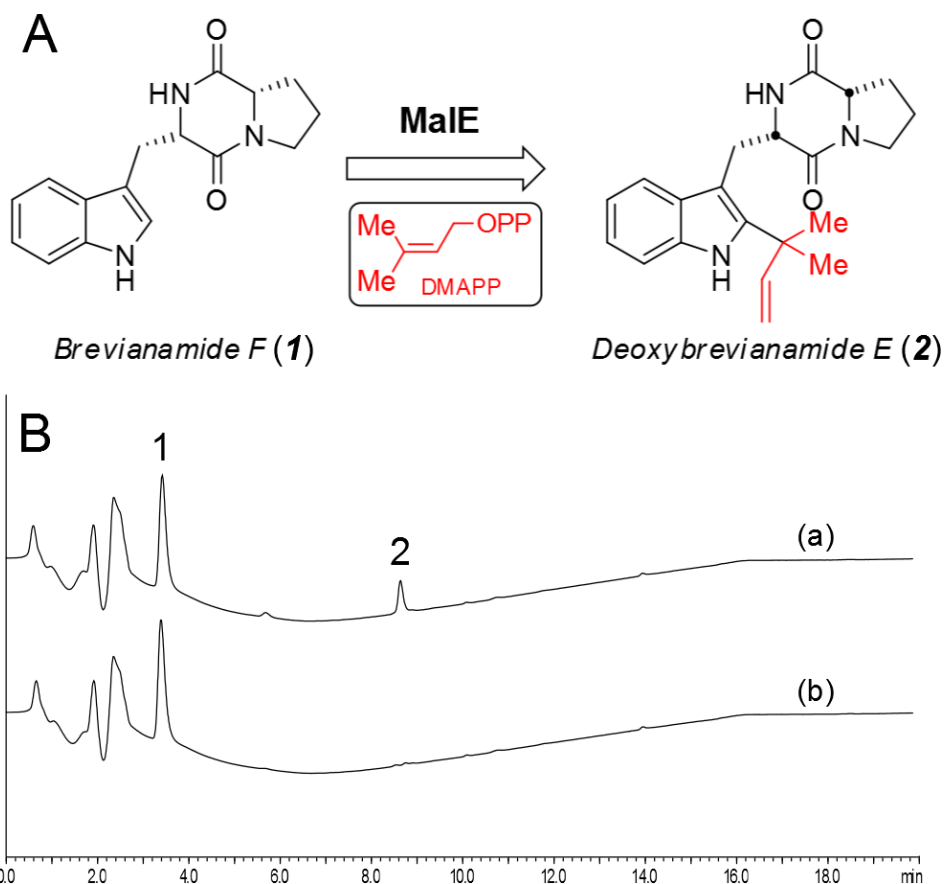


Figure 3-5. (A) Observed *in vitro* reaction containing MalE, DMAPP, and Brevianamide F. (B) HPLC traces depicting (a) Brevianamide F in reaction with MalE and (b) Brevianamide F in reaction with no enzyme.

performs the same reaction, we decided to test the activity *in vitro* with Brevianamide F as a substrate that mimics the native substrate. Deoxybrevianamide E product formation was observed after analysis with LC-MS, demonstrating that MalE was an active enzyme that accepted DMAPP as a cofactor in its prenyltransferase reaction (Figure 3-5).

3.2.2 Male substrate synthesis

In order to validate this sequence of events, my collaborators and I have pursued a biomimetic synthesis of premalbrancheamide. After consideration of the various approaches to forming premalbrancheamide, we decided that the acquisition of the intermediate **3** preceding the prenylation step would be critical to our investigation of the MalE prenyltransferase. In our consideration of compound **3**, we realized that the azadiene would require the unfavored tautomer. We then hypothesized that the enzyme may play a role in stabilizing the azadiene form and thus decided on the synthesis of compound **8**.

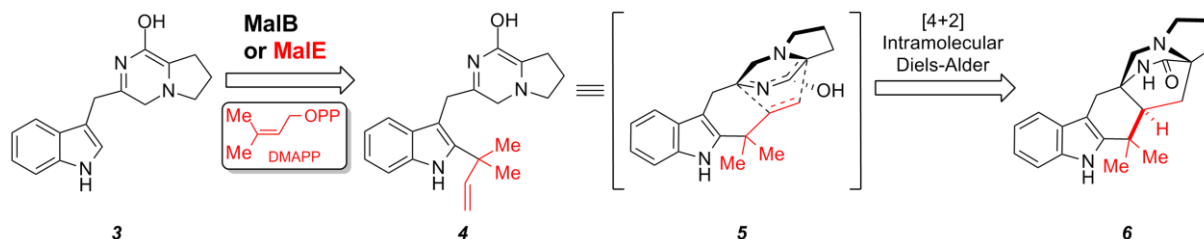


Figure 3-6. Predicted prenyltransferase reaction yielding premalbrancheamide (**6**)

During the biomimetic synthesis of pre-malbrancheamide, we discovered that compound **8** is highly unstable (See Appendix A). It rapidly degrades to form compound **9** (Figure 3-7), reason unknown. We hypothesize that a spontaneous oxidation of the compound occurs by exposure to oxygen or water, as attempts to keep the compound under neutral gas in organic solvent would typically slow the oxidation process. Extensive efforts were employed to maintain the stability of the compound, however the compound seemed to remain stable for only several hours at best. Taking this hurdle into account, it was decided that the *in vitro* reaction with MalE would need to be conducted as quickly as possible after the synthesis of compound **8**.

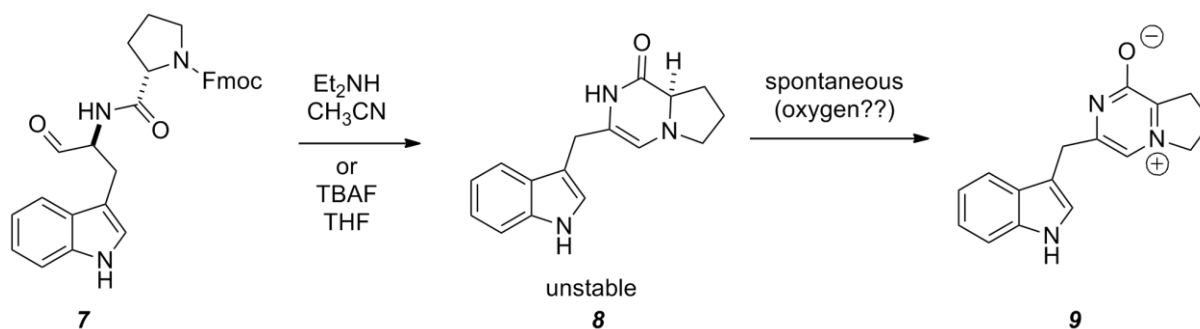


Figure 3-7. Deprotection of compound **7** will yield putative native substrate **8**, which spontaneously oxidizes to form **9**.

3.2.3 Investigation of MalE activity with biomimetic synthetic compounds

Because compound **8** was found to be unstable, stable compounds **9** and **10** were provided by collaborators in the Williams group for preliminary testing *in vitro* with MalE. As expected, compound **10** successfully reacted to form a prenylated product. Curiously, reactions with

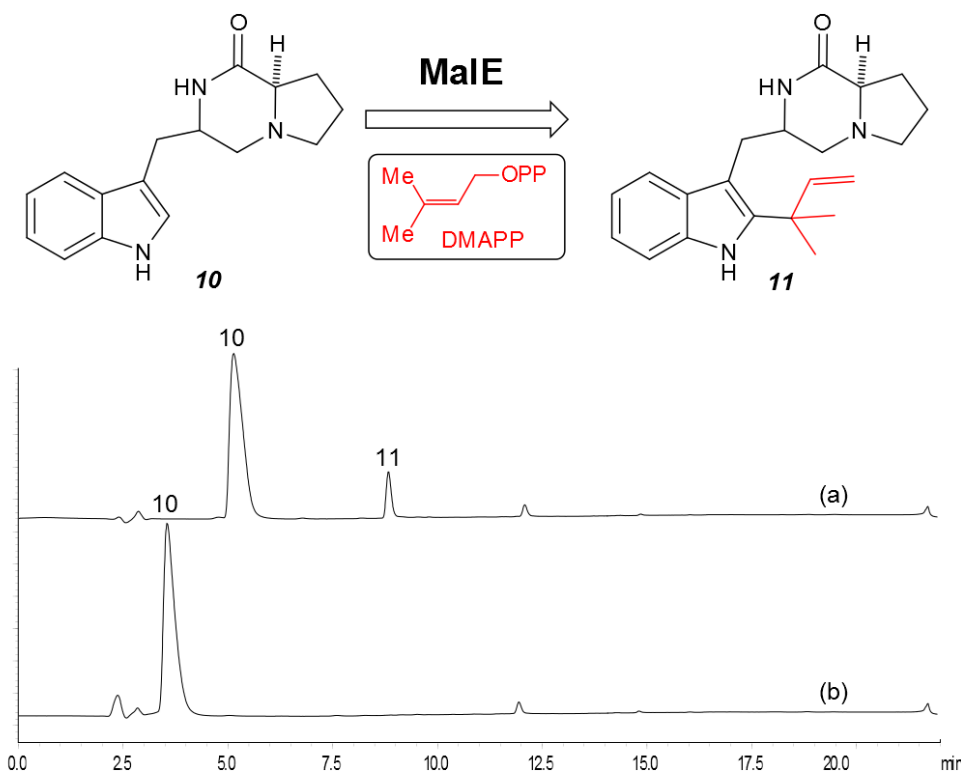


Figure 3-8. Reactions with **10** successfully generate product **11**. HPLC traces depict (a) reaction containing **10** and MalE enzyme and (b) reaction containing **10** and no enzyme. A slight shift in trace (b) was observed for substrate **10** due to possible pump error.

compound **9** showed no formation of prenylated product, indicating that compound **9** is not accepted as a substrate by MalE for prenylation.

3.2.4 Investigation of MalE activity with predicted native substrate **8**

In order to test the predicted native substrate **8**, the compound would need to be generated and

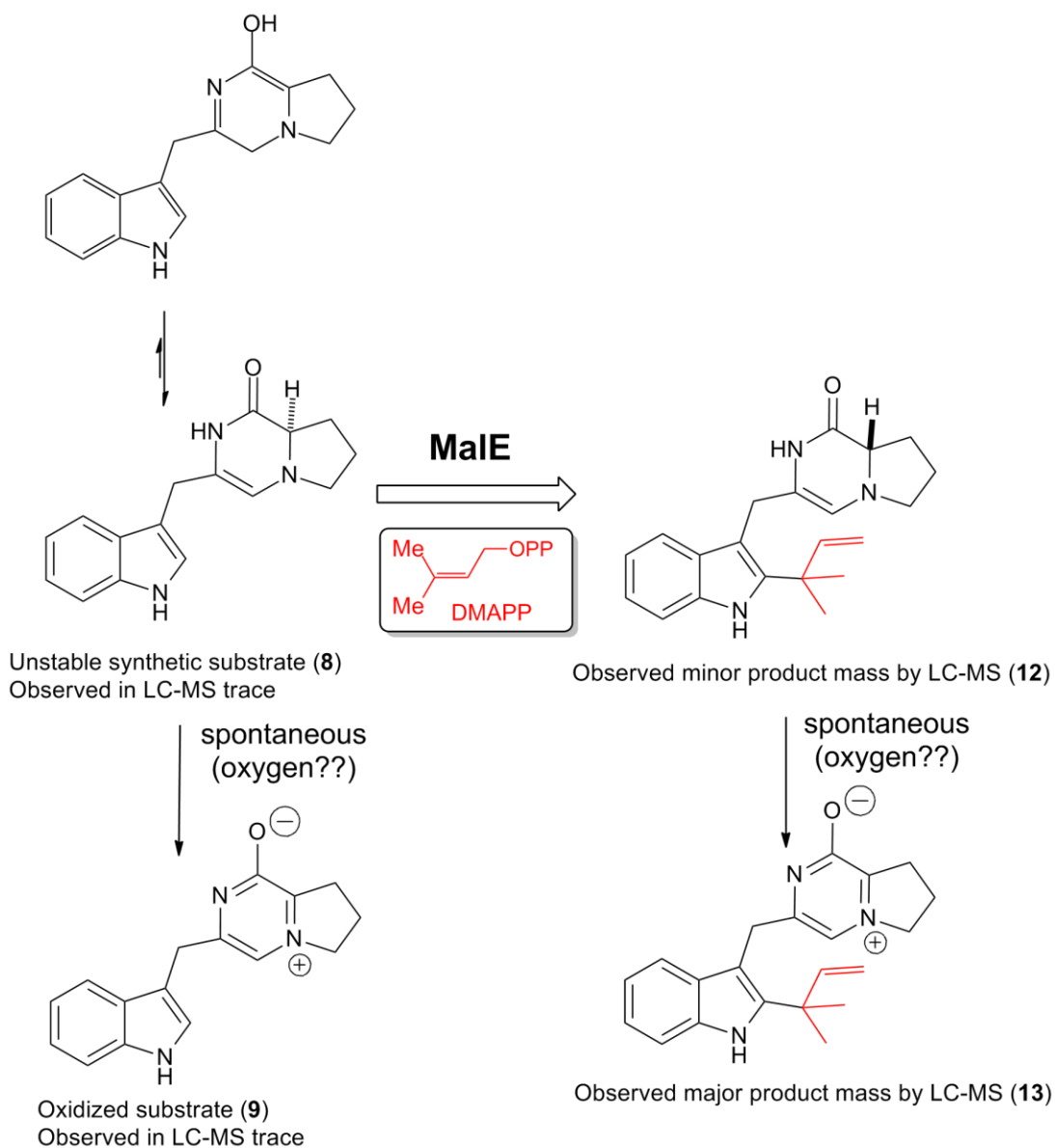


Figure 3-9. Observed enzymatic reaction containing MalE and synthesized substrate.

immediately tested *in vitro* with enzyme. To do so, the Fmoc-protected compound **7** was

provided to our lab for deprotection following established procedures (See section 3.2.2). The reaction was then dried down under argon gas and resuspended in degassed DMSO to yield a 50 mM stock solution based on the amount of starting material used. Reactions were set up containing 0.5 mM substrate mixture in DMSO, 0.1 mM DMAPP, and 50 uL MalE in degassed phosphate reaction buffer for a total reaction volume of 500 uL. Reactions were conducted on benchtop under vacuum gas and extracted after 1 hour. The analysis was conducted by LC-MS, and the results are depicted in Figure 3-9.

Prenylation was observed for unstable synthetic substrate **8**. However, the prenylated product oxidized to generate the major product **13** as observed by LC-MS (Figure 3-10). Consequently, no premalbrancheamide was observed to be formed from reactions containing MalE and **8**. According to the biomimetic synthesis (Appendix A: **Error! Reference source not found.**), upon prenylation to produce the observed minor product, treatment with TFA should push formation of premalbrancheamide. The synthesis and enzymatic prenylation was thus repeated, followed by addition of TFA to the reaction mixture to simulate biomimetic synthetic procedures. Formation of premalbrancheamide was not observed from these reactions. Additionally, reactions were carried out under various pH conditions between 4.0 and 10.0, with no observable premalbrancheamide formation.

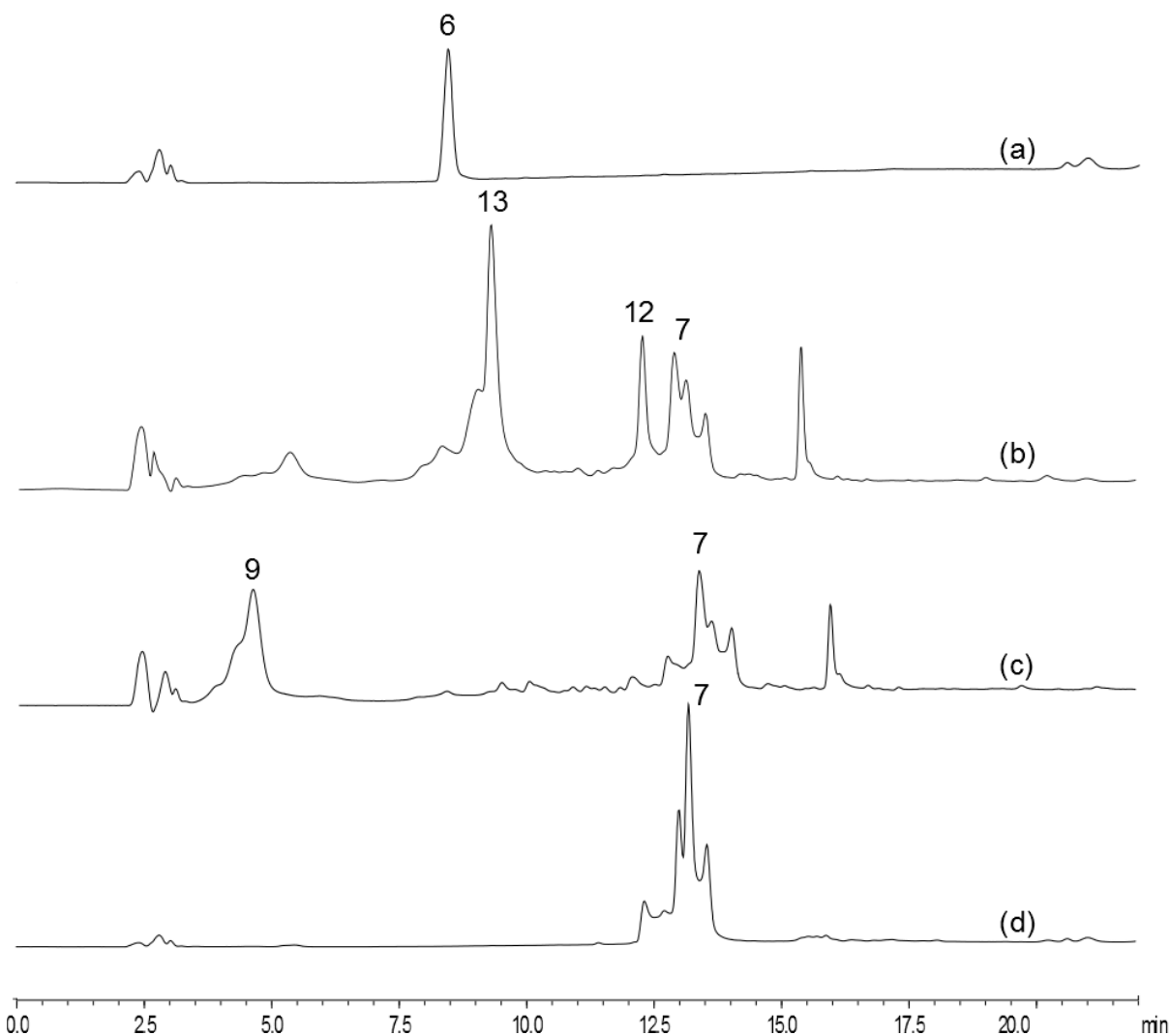


Figure 3-10. Reactions containing **8**. HPLC traces of (a) authentic premalbrancheamide standard, (b) MalE with synthetic product **8**, (c) synthetic product **8** (seen as **9**) from deprotection of **7**, and (d) **7** standard.

3.3 Discussion

MalE, a putative prenyltransferase identified in the malbrancheamide biosynthetic gene cluster, was determined to be an active protein able to prenylate not only its expected substrate monooxopiperazines but also some dioxopiperazines from the notoamide pathway. From the observed *in vitro* reactions, MalE is able to use DMAPP to prenylate various indole alkaloid derivatives in a similar fashion to NotF from the notoamide pathway.⁹⁶ The only substrate that was not accepted by MalE for reaction was compound **9**, the oxidized form of the predicted native substrate.

We were expecting the IMDA reaction to occur upon introduction of the prenyl dienophile. Based on previous investigations of Diels-Alder biosynthetic enzymes, we predicted that MalE would similarly act as a chaperone-like protein, providing a scaffold to lower the activation energy of the IMDA reaction. Instead, the data suggest that MalE catalyzes a prenylation reaction and releases the prenylated product. Interestingly, the lack of premalbrancheamide formation suggests that an additional catalyst may be needed for the IMDA reaction to occur. In other words, the lack of spontaneous cyclization supports the theory that a biocatalyst is needed for the Diels-Alder reaction, and that a different enzyme may be involved in this step of malbrancheamide biosynthesis. These findings are presented in contrast to the formation of spinosyn A, which forms with or without enzyme but increases catalytic activity in presence of enzyme.⁸⁰ On the other hand, it is possible that the IMDA reaction in malbrancheamide biosynthesis is instead dependent upon the biosynthetic enzyme for catalysis and will not proceed without it.

It is important to note that the identity of the product being formed was only verified using LC-MS experiments. An authentic synthetic standard of **13** was provided and analyzed for comparison, demonstrating that the compound generated from *in vitro* reactions containing MalE and **8** was indeed **13** (data not shown). However, if this investigation is to be continued, it would be highly advised to obtain structural data for the product compound to determine whether the prenyltransferase reaction is indeed a reverse prenylation at the C2 position of tryptophan. It is unclear the degree to which the retention times may differ if the prenylation reaction occurred at a different position, or if the prenylation reaction occurred in the normal direction. Therefore, the exact product being formed by MalE has not yet been investigated to 100% certainty.

As the investigation for the Diels-Alderase continues, we have begun to turn to other

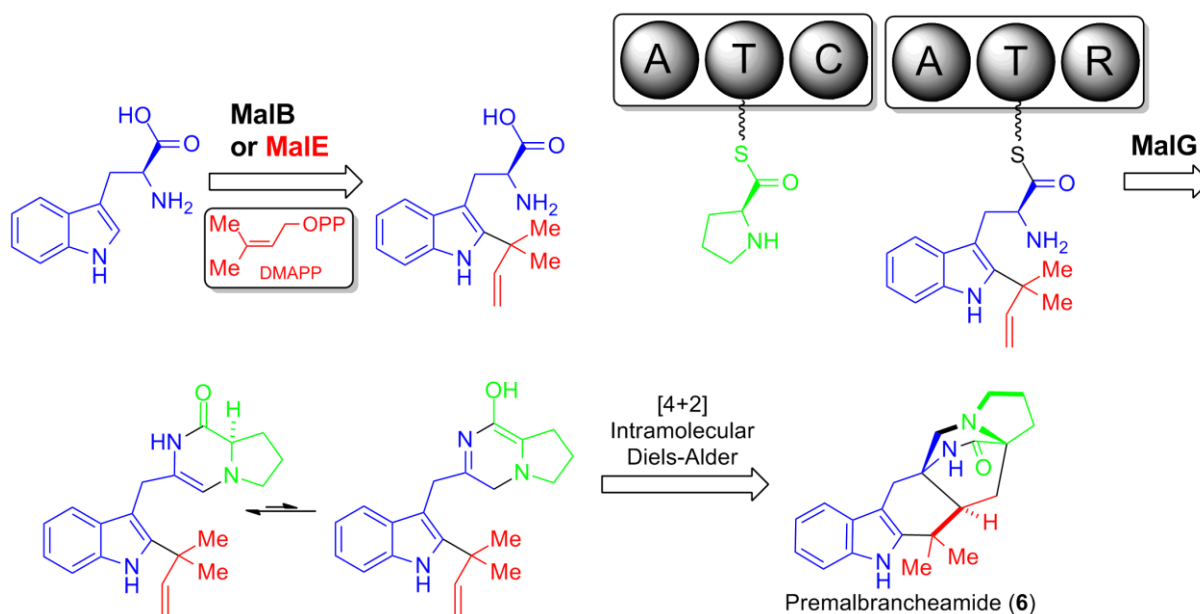


Figure 3-11. Alternative order of biosynthesis where prenylation occurs before loading onto the NRPS.

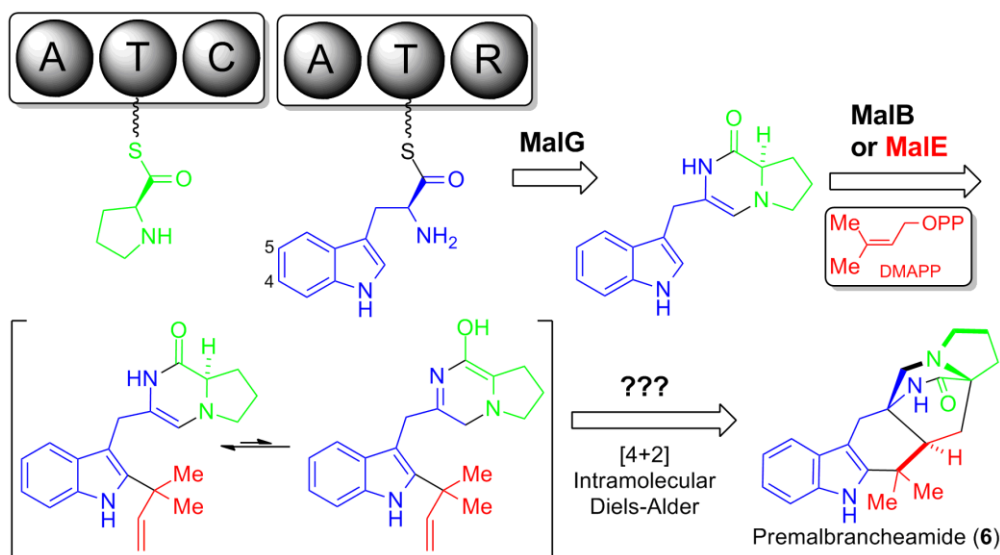


Figure 3-12. Alternative order of biosynthesis where a separate enzyme is responsible for the stabilization of the prenylated intermediate and Diels-Alder reaction.

biosynthetic enzymes present within the gene cluster. The instability of compound **8** suggests that it is unlikely to exist as an intermediate within the organism. This finding suggests a few options could be viable: (a) the prenylation event occurs before tryptophan is loaded onto the

NRPS (Figure 3-11) or (b) a separate protein is responsible for stabilizing the intermediate (Figure 3-12). In the former case, the NRPS MalG would be acting as the Diels-Alderase, and the prenyl dienophile is introduced before the azadiene is formed. In the latter case, the protein may be acting as a chaperone or scaffold to stabilize the intermediate, or it could be interacting with prenyltransferase MalE to perform the IMDA reaction.

In summary, we have identified the biochemical activity of MalE, a prenyltransferase from the malbrancheamide biosynthetic gene cluster. MalE is able to prenylate dipeptides similar to and including brevianamide F, appearing to catalyze the same reaction as NotF from the notoamide pathway. This body of work was conducted in order to address our hypothesis that the IMDA reaction occurs immediately after prenylation in the malbrancheamide pathway. The collected evidence do not support the hypothesis that MalE can form the IMDA product, premalbrancheamide. However, the lack of premalbrancheamide formation also suggests that a separate catalyst may be necessary for the Diels-Alder reaction. In future work, MalE will be investigated alongside the remaining malbrancheamide biosynthetic enzymes for its possible role in IMDA synthesis. Overall, the findings in this investigation have puzzling yet exciting implications for bicyclo[2.2.2]diazaoctane biosynthesis.

3.4 Methods

1. Fungal strains and culture conditions

Malbranchea aurantiaca spores were generated on YPD agar plates over the course of 7 days. Spores were harvested into 5 mL sterile water per plate by gently scraping the surface of the culture with a sterile inoculating loop. Spores were stored at -80°C until ready to use. Genomic DNA was harvested using Wizard Genomic DNA Purification Kit from Promega.

2. cDNA preparation and cloning of *malE*

Total RNA was extracted from a sample of fungal mycelia collected on the 15th day of culture grown in liquid medium (Difco Potato Dextrose Broth) with 160 rpm agitation at 28°C, using Invitrogen PureLink RNA Mini Kit by following the plant tissue processing protocol. RNA was treated using DNase I. cDNA was generated using Invitrogen Superscript First Strand Synthesis. PCR was used to amplify *malE* from the cDNA template. The amplified gene was then cloned into pET28b vector using restriction enzyme digest and ligation. Plasmids were transformed into *E. coli* DH5 α for screening and plasmid maintenance.

3. Overexpression and purification of protein for enzymology

The *Escherichia coli* BL21 pRARE transformant containing pET28b-*malE* was grown at 37°C overnight in LB media containing 50 μ g/mL of kanamycin and 100 μ g/mL of spectinomycin. 25 mL of culture was used to inoculate 1 L of TB media containing the aforementioned concentrations of antibiotic and 4% glycerol. Cells were grown at 37°C for roughly 4 hours until A_{600} reached 0.6-1.0, and isopropyl β -D-thiogalactoside (IPTG, 0.2 mM) was added to induce protein overexpression overnight at 18°C.

All purification steps were conducted at 4°C. Briefly, 2 L of expression culture were spun down at 5,500 xg to yield approximately 20 mL of cell pellet volume. Harvested cell pellets were resuspended in 60 ml of lysis buffer (10 mM imidazole, 50 mM NaH₂PO₄, 300 mM NaCl, 10% v/v glycerol, pH 8) and lysed by sonication. Insoluble material was removed by centrifugation at 38,000 xg for 30 min, and the supernatant was batch-bound for 1 hour to 4 mL of Ni²⁺-NTA

slurry (Novagen) that was equilibrated in lysis buffer. This batch-binding mixture was poured through a 50 ml fritted glass column where the retained resin was washed with 100 mL of lysis buffer, 50 mL of wash buffer (20 mM imidazole, 50 mM NaH₂PO₄, 300 mM NaCl, 10% v/v glycerol, pH 8), and finally 10 ml of elution buffer (250 mM imidazole, 50 mM NaH₂PO₄, 300 mM NaCl, 10% v/v glycerol, pH 8). Protein in the eluate was exchanged into storage buffer (50 mM NaH₂PO₄, 1 mM EDTA, 0.2 mM DTT, 10% v/v glycerol, pH 7.3) using PD-10 columns. Samples were then flash frozen with liquid N₂ and stored at -80°C.

4. Enzyme assays and LC-MS analysis

The standard enzyme assay containing 0.5 mM substrate mixture in DMSO, 0.1 mM DMAPP, and 50 uL MaleE in 500 µL total volume reaction buffer (50 mM NaH₂PO₄, 1 mM EDTA, 0.2 mM DTT, 10% v/v glycerol, pH 7.3) was performed on benchtop under vacuum for one hour. 100 uL of each reaction was then transferred to a new eppendorf tube, extracted 3 times with 200 µL chloroform, and the extract was dried down under N₂ gas. The product was then resuspended in 100 µL methanol for LC-MS Q-TOF analysis. Analysis was conducted on a LCMS-2010 EV outfitted with a Waters XBridge C18 3.5 µm, 2.1x150 mm column. HPLC conditions: monitoring wavelengths 240 nm and 280 nm; scanning 200 to 1200 *m/z*; solvent A: water + 0.1% formic acid, solvent B: acetonitrile + 0.1% formic acid; flow rate: 0.2 mL/min; mobile phase: 20% B over 2 min, 20-100% B over 10 min, 100% B over 5 min, 100-20% B over 1 min, 20% over 7 min.

3.5 Appendix A*

*Adapted from manuscript in progress written by James D. Sunderhaus, Jennifer M. Finefield, Amber D. Somoza, Timothy J. McAfoos, Hong Tran, David H. Sherman, and Robert M. Williams.

Chemical validation of the proposed IMDA construction of monooxopiperazine prenylated indole alkaloids.

The ever expanding family of prenylated indole alkaloids produced by various genera of fungi, has attracted considerable interest due to their wide spectrum of biological activities, and serve as provocative targets for chemical synthesis and biosynthetic studies.¹⁰ Family members include the anticancer agents stephacidin A,³² the anthelmintic paraherquamide A,¹²⁹ calmodulin-inhibitor malbrancheamide,⁵¹ neuroprotective agent chrysogenamide A among a growing number of related novel bioactive metabolites.¹⁰

Of particular interest to our laboratories, is the mechanism by which Nature constructs the bicyclo[2.2.2]diazaoctane ring nucleus that is common to this family of prenylated indole alkaloids. It is noteworthy that, the paraherquamides, asperparalines, malbrancheamides, marcfortines and chrysogenamide A, are all constituted of a monooxopiperazine-based bicyclo[2.2.2]diazaoctane system, whereas the stephacidins, notoamides, brevianamides, aspergamides, and avrainvillamide, are all constituted of a dioxopiperazine-based bicyclo[2.2.2]diazaoctane system. Structures of a few representative members of both sub-families are depicted in Figure 3-13. The unique bicyclo [2.2.2] diazaoctane core of these naturally occurring fungal metabolites, has been proposed to arise from an intramolecular Diels-Alder (IMDA) reaction. An additional fascinating element in the biosynthesis of the notoamides and stephacidins is the discovery that the marine-derived *Aspergillus* sp. MF297-2 exclusively produces the enantiomers of (+)-stephacidin A, and (-)-notoamide B, whereas the terrestrial A.

versicolor NRRL 35600 generates the antipodal products (-)-stephacidin A, and (+)-notoamide B. This implies the biosynthetic enzymes involved in assembly and tailoring might have evolved to catalyze an “identical” reaction to give an enantiomerically distinct product.

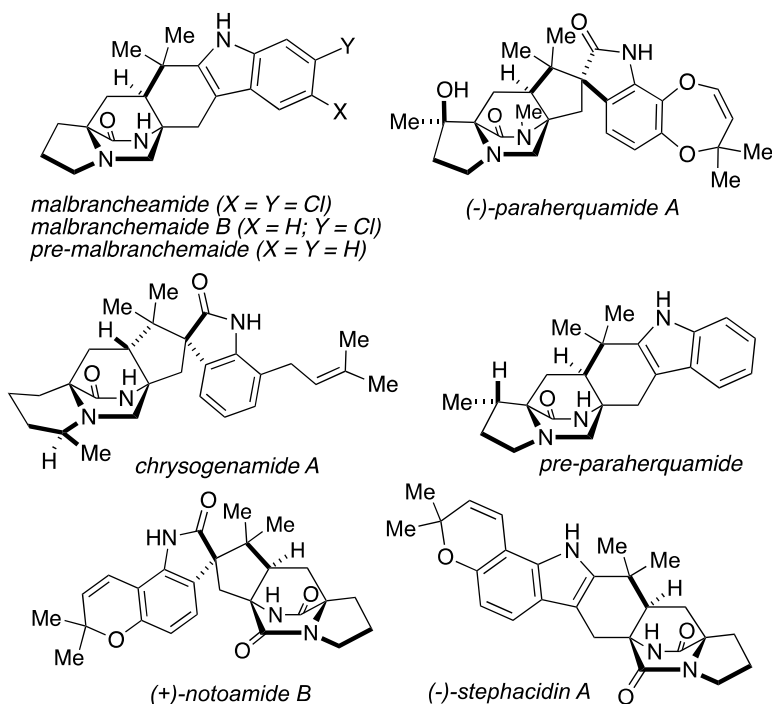
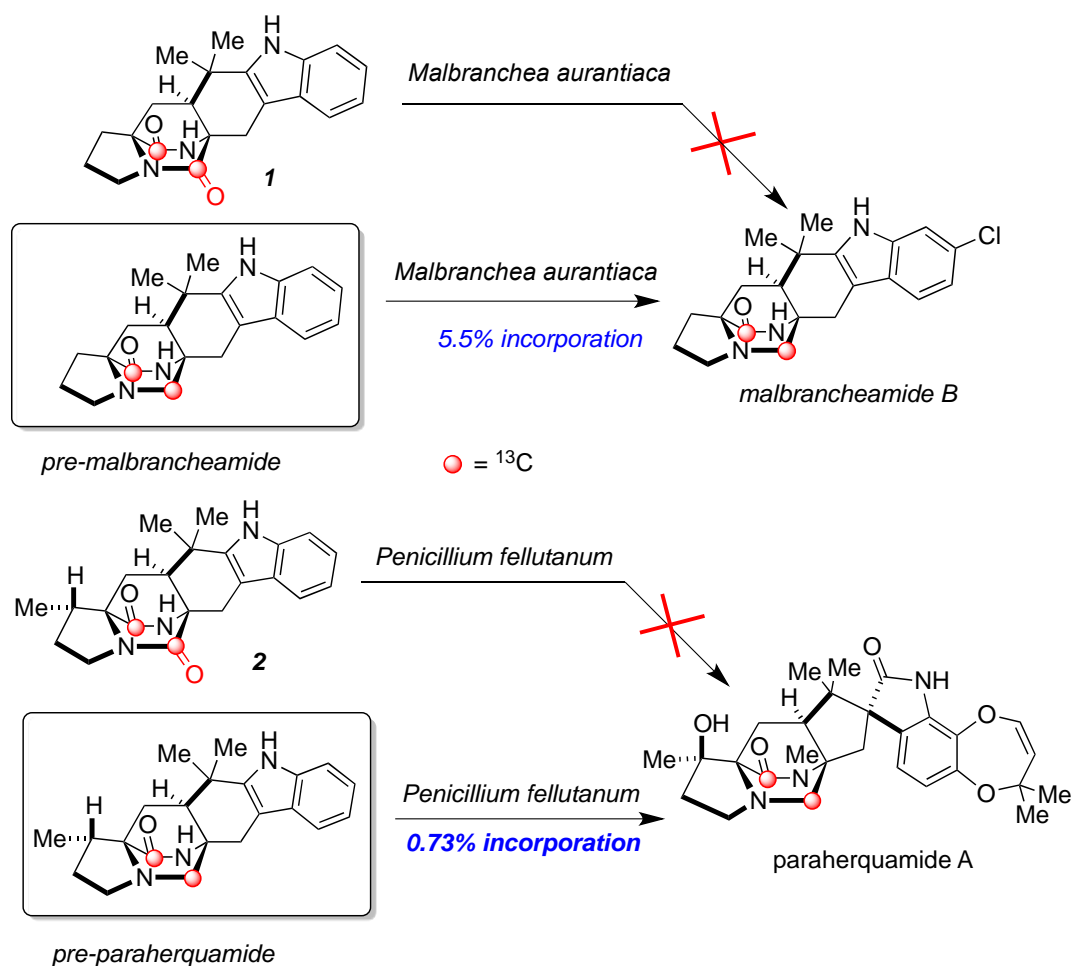


Figure 3-13. Representative fungal prenylated indole alkaloids.

The monooxopiperazine-based members of this family, such as paraherquamide and malbrancheamide, have been the subject of intensive study in our laboratories with respect to the identification of early pathway metabolites that contain the bicyclo[2.2.2]diazaoctane ring system. In both the case of paraherquamide and malbrancheamide biosynthesis, we have synthesized the double ^{13}C -labeled putative progenitors “pre-malbrancheamide” and “pre-paraherquamide”. In both instances, precursor incorporation experiments with the respective producing fungi, revealed that both “pre-malbrancheamide” and “pre-paraherquamide” were incorporated intact into malbrancheamide B and paraherquamide A, respectively. Curiously, in both instances, the synthetic, double ^{13}C -labeled dioxopiperazines from which “pre-

malbrancheamide” and “pre-paraherquamide” were prepared by recution of the tryptophan-derived carbonyl group, were found not to incorporate into the respective natural products in parallel precursor incorporation experiments as illustrated in Scheme 3-1. This raised the obvious question as to the timing of the reduction of the tryptophan-derived carbonyl group, by a net four-electrons, down to the oxidation state of a CH₂ group as this position exists in the natural products.



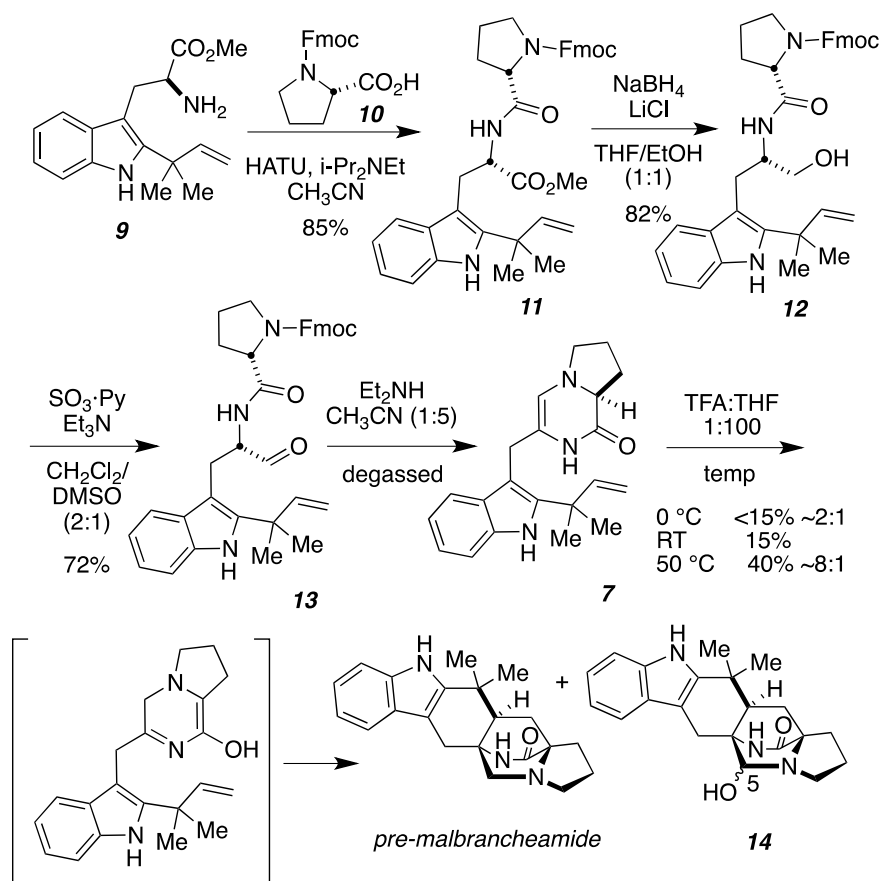
Scheme 3-1. Precursor incorporation experiments of monooxpiperazine and dioxopiperazine substrates.

To address these biosynthetic questions, we recently sequenced the genome of *Penicillium fellutanum* and *Malbranchea aurantiaca* and identified the malbrancheamide and paraherquamide biosynthetic gene clusters through *in silico* sequence database mining.⁹⁷ We

found that in both the malbrancheamide and paraherquamide NRPS modules, the terminal end of the tryptophan unit, is constituted with a *reductase domain*, as opposed to a *condensation domain* which is evident in the stephacidin and notoamide biosynthetic geneclusters. This remarkable finding led us to suggest that the bicyclo[2.2.2]diazaoctane ring system is directly produced in the monooxopiperazine oxidation state, via the cascade of events depicted in Scheme 3-2, following the reductive cleavage of the tryptophan thiol ester by the NADPH-dependent reductase domain. Although we do not yet know the exact timing of the reverse prenylation, all available evidence suggests that the most likely sequence is at the stage of one of the reduced dipeptide intermediates (5-8).

In order to validate this sequence of events, we have prepared amino-aldehyde 5 (R=H), and have found that this substance spontaneously undergoes the cascade of ring closure (6), dehydration (7), tautomerization (8) and intramolecular Diels-Alder cycloaddition to give pre-malbrancheamide as an isolable product as illustrated in Scheme 3-3.

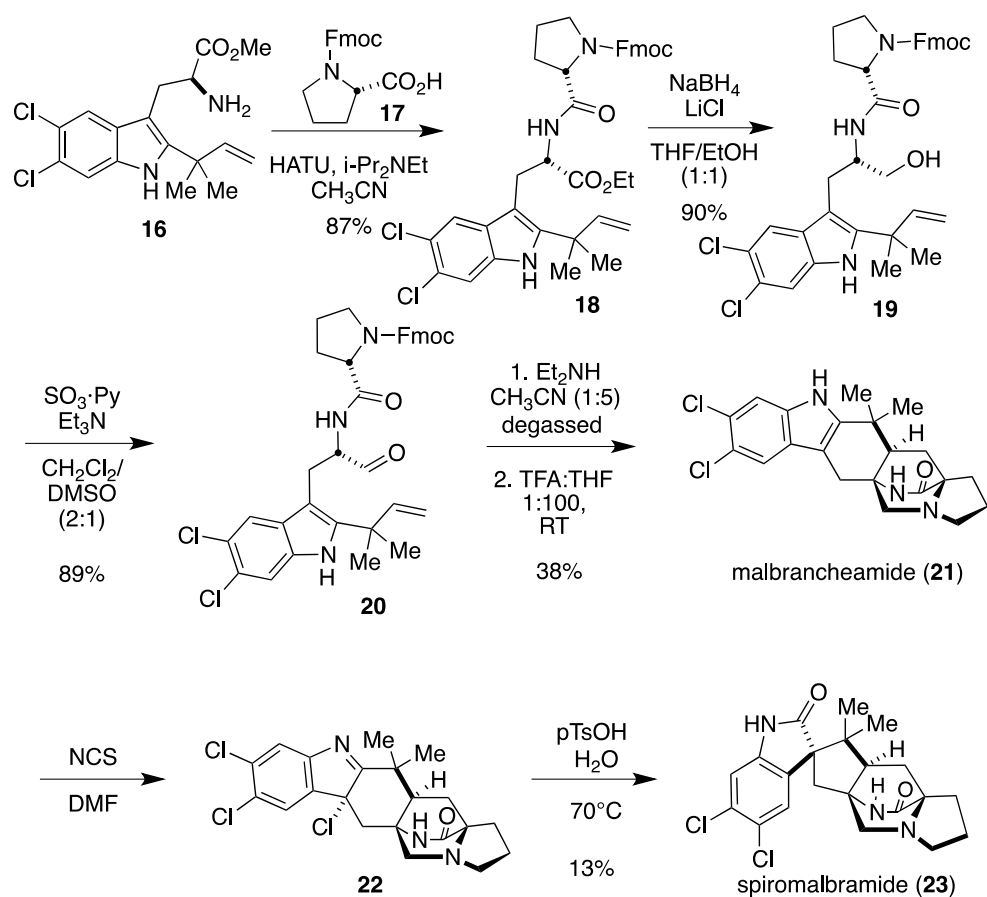
The key, Fmoc-protected amino aldehyde (13), corresponding to putative species 5 was prepared through the peptide coupling of *N*-Fmoc proline (10) with the C2-reverse-prenylated



tryptophan methyl ester (9) through the agency of HATU in acetonitrile in 85% yield. Reduction of the methyl ester with sodium borohydride (82% to 12) followed by a Doering-LaFlamme oxidation, furnished the *N*-Fmoc aldehyde 13 in 72% yield. Removal of the *N*-Fmoc residue with diethylamine furnished the di-enamine 7, which could be isolated and characterized. Treatment

of this substance with TFA in THF at temperatures between 0 °C and 50 °C, resulted in the formation of pre-malbrancheamide, and the unexpected carbinolamine oxidation congener 14 as a minor product. At 50 °C, pre-malbrancheamide was produced in an 8:1 ratio with 14 (inseparable) in 40% combined yield.

As further proof to our proposal, we applied an analogous synthesis to an additional member of the malbrancheamide family, spiromalbramide (23). Likewise, the key halogenated Fmoc-protected amino aldehyde (20) was prepared by peptide coupling of the reverse prenylated tryptophan ethyl ester (16) with Fmoc-protected proline amino acid (17) using HATU afforded an 87% yield. The ethyl ester was reduced with sodium borohydride (19 in 90%) and followed by an oxidation to provide the N-Fmoc aldehyde 20 in 89% yield. The Fmoc group was removed with diethylamine, and the crude product was directly treated with a degassed solution of TFA in THF at room temperature to provide the *syn* cycloadduct of malbrancheamide (21) in 38% yield. Malbrancheamide was treated with N-chlorosuccinimide to form the chloroindoline intermediate (22), which was directly hydrated under acidic conditions to undergo a pincol-type rearrangement and form spiromalbramide in 13% yield.



Scheme 3-3. Biomimetic synthesis of spiromalbramide.

We presume in the biosynthesis of pre-malbranchemide, that it is the reverse-prenyltransferase, that likely catalyzes the tautomerization and intramolecular Diels-Alder reaction of the putative azadiene 8, which in the case of pre-malbranchemide, is *achiral*. The fact that malbranchemide and malbranchemide B are produced as single, optically pure enantiomers, provocatively suggests that the reverse-prenyltransferase, must orient the azadiene and pendant isoprene-derived vinyl residue in a single conformational disposition that concomitantly controls the enantiofacial bias and the diastereoselectivity of this cycloaddition that proceeds to give only the *syn*-stereochemistry.

3.6 Appendix B

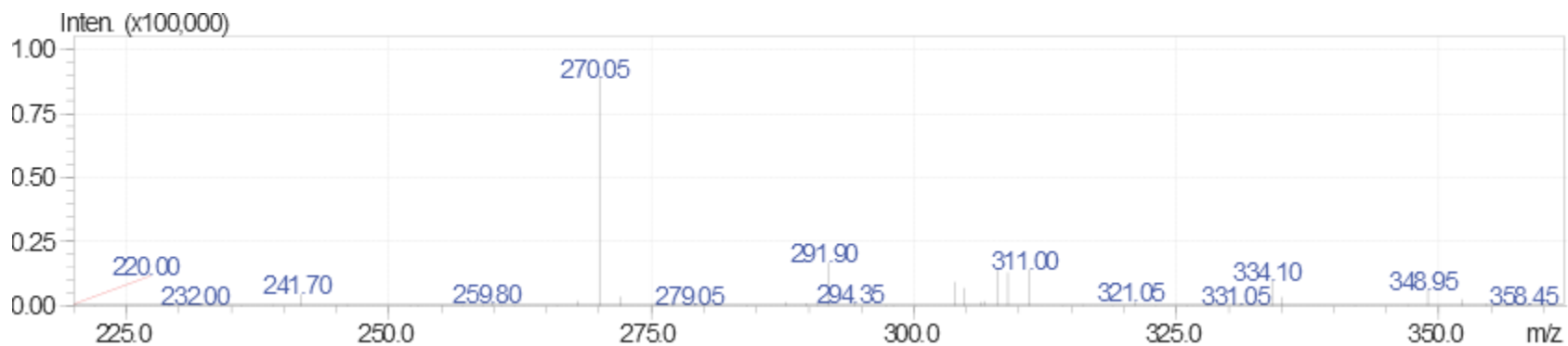


Figure 3-14. Mass spectrum of substrate 10 with [M+H] peak at 270.05 m/z.

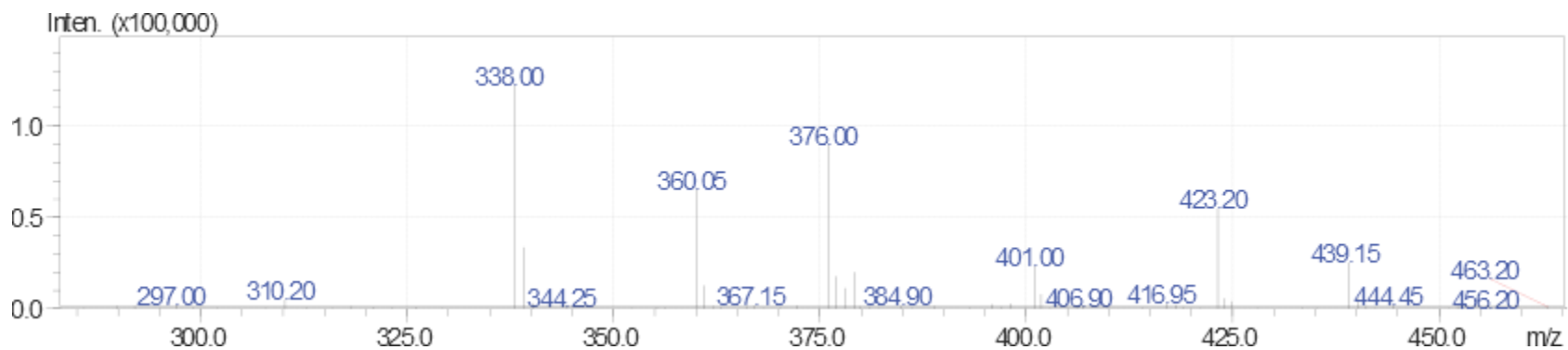


Figure 3-15. Mass spectrum of product 11 with [M+H] peak at 338.00 m/z.



Figure 3-16. Mass spectrum of compound 9 with [M+H] peak at 265.80 m/z .

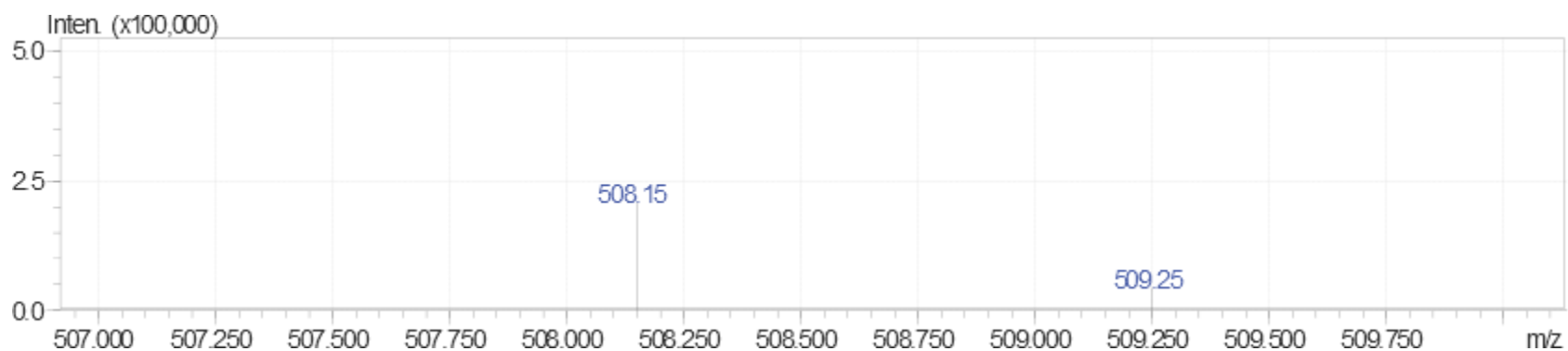


Figure 3-17. Mass spectrum of compound 7 with [M+H] peak at 508.15 m/z .

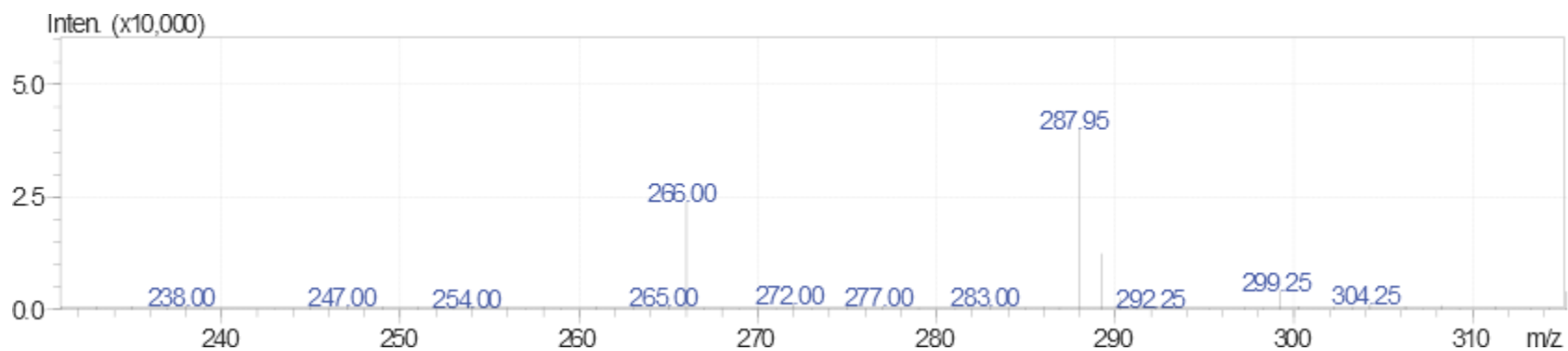


Figure 3-18. Mass spectrum of deprotected 7 appears as 9 with [M+H] peak at 266.00 m/z .

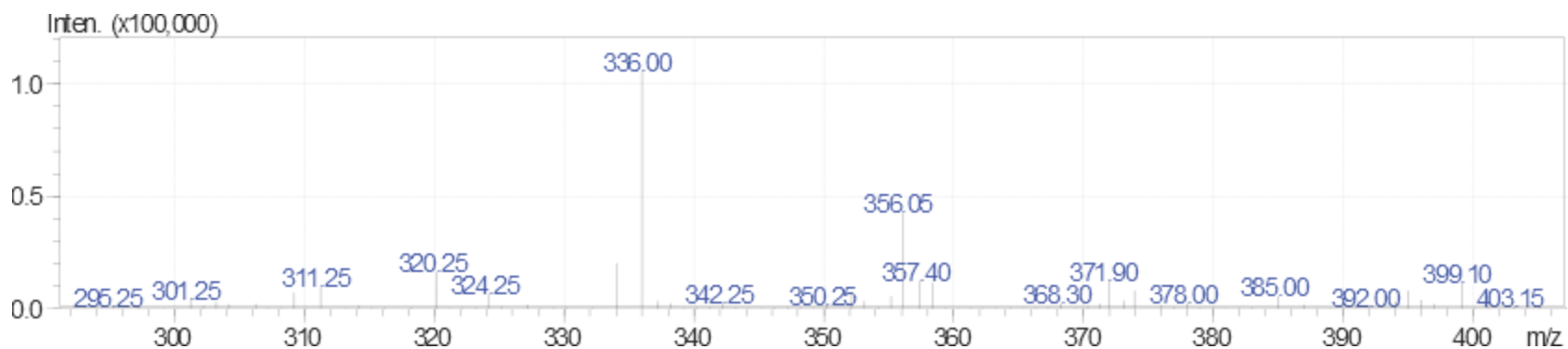


Figure 3-19. Mass spectrum of compound 12 with [M+H] peak at 336.00 m/z.

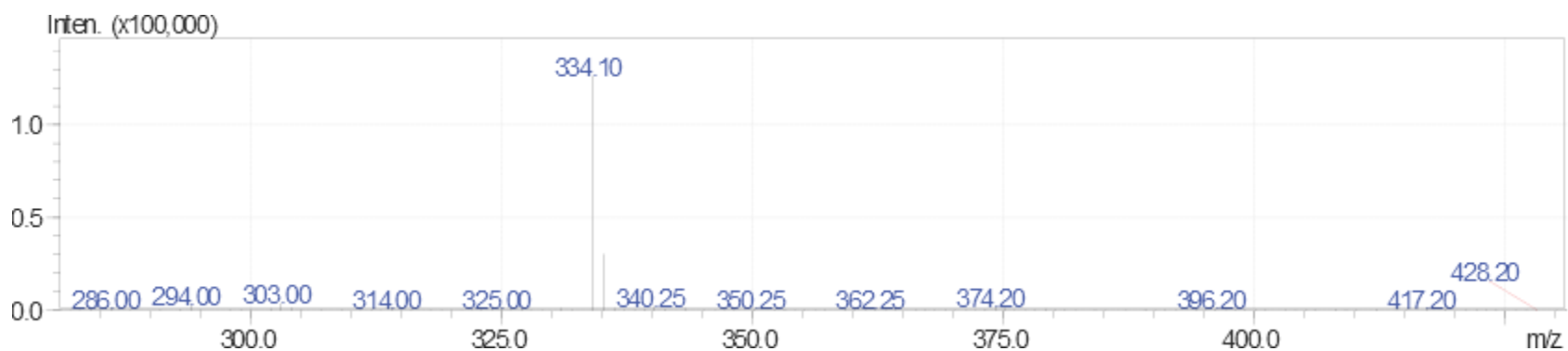


Figure 3-20. Mass spectrum of compound 13 with [M+H] peak at 334.10 m/z.

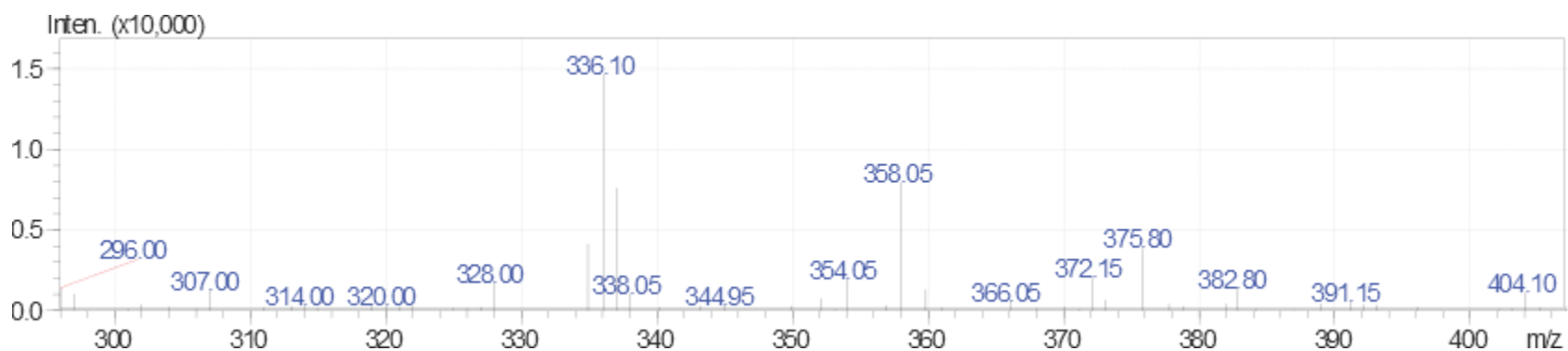


Figure 3-21. Mass spectrum of standard premalbrancheamide 6 with [M+H] peak at 336.10 m/z.

Author Contributions:

Hong T. Tran, James D. Sunderhaus, Jennifer M. Finefield, Amber D. Somoza, Timothy J.

McAfoos, David H. Sherman, and Robert M. Williams contributed to the experimental design.

Hong T. Tran performed the enzymatic reactions and analysis; James D. Sunderhaus synthesized, confirmed, and provided substrates. Hong T. Tran, James D. Sunderhaus, Jennifer M. Finefield, Amber Somoza, David H. Sherman, and Robert M. Williams evaluated the data.

Chapter 4

Halogenation

4.1 Introduction

Halogenated natural products have demonstrated great utility as antibiotics, including the well-known vancomycin and chloramphenicol.^{130,131} In regards to the importance of the halogens, the two chlorine substituents on vancomycin, for example, are required for clinical activity of the compound.¹³² Today, this vast group of naturally occurring organohalogenes exceeds 5000 in number, with roughly 25% of that number being constituted of halogenated alkaloids.¹³³ In terms of origin, the compounds are produced by bacteria, fungi, lichens, marine algae, higher plants, insects, invertebrates, vertebrates, and mammals, demonstrating the wide spread of halogenases in nature.⁵⁵ Chlorinated compounds are frequently observed in terrestrial environments, while brominated compounds are abundant in the marine environment, and fluorinated compounds are incredibly rare.¹³⁴ Halogenases are typically found to be able to perform both chlorination or bromination reactions, and the incorporation of chlorine versus bromine is usually dependent upon which halogen is supplied by the environment or medium of the organism.¹³⁵

Halogenases can currently be divided into five major categories: heme iron-dependent haloperoxidases, vanadium-dependent halo peroxidases, flavin-dependent halogenases, non-heme iron-dependent halogenases, and nucleophilic halogenases.⁵⁶ While haloperoxidases were previously believed to be the primary halogenase enzymes, research in the field has led us to the understanding that naturally halogenated compounds are more often produced by flavin-dependent halogenases.¹³⁶ These flavin-dependent halogenases are also dependent upon a flavin

reductase for the supply of reduced flavin necessary to conduct its halogenation reaction. Of these flavin-dependent halogenases, they can be further subdivided into two major groups: enzymes that halogenate small-molecule substrates and enzymes that react with substrates bound to the thiolation of an NRPS system.¹³⁷ For halogenating indoles, tryptophan halogenases are included in the former of the two categories and have been well-characterized, including but not

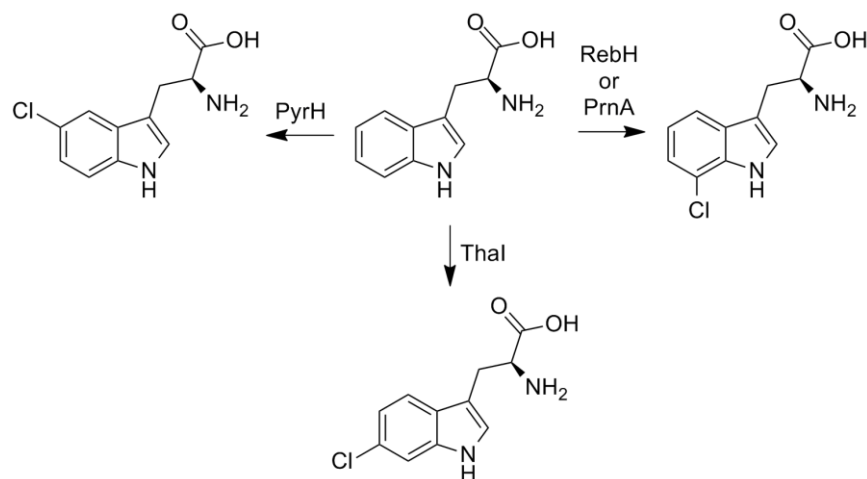


Figure 4-1. Characterized tryptophan halogenase reactions.

limited to rebeccamycin's RebH^{138,139} and pyrrolnitrin's PrnA^{140,141}. PyrH and Thal round out the other tryptophan halogenases that chlorinate at the C5 and C6 positions, respectively (Figure 4-1).^{57,142}

In the malbrancheamide natural product, we observe two chlorine atoms at the C5 and C6 positions on the tryptophan moiety.¹⁷ Additionally, the two monochlorinated intermediates

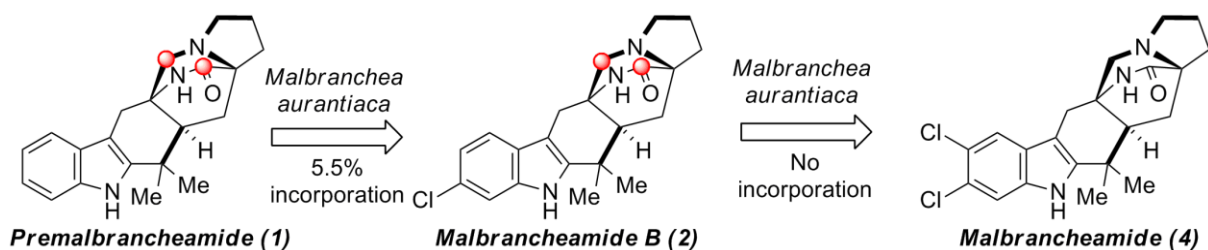


Figure 4-2. Results from incorporation studies using isotopically labeled premalbrancheamide.

malbrancheamide B and isomalbrancheamide B have also been isolated and identified by the Mata group.^{53,143} Previous studies in our lab have shown that isotopically labeled premalbrancheamide fed to the producing organism *Malbranchea aurantiaca* will result in the production of labeled malbrancheamide B, but no production of labeled malbrancheamide (Figure 4-2).⁶² These findings suggested that perhaps the second chlorination event happened much slower than the first, and thus no observation of dichlorinated product was seen. Later, the genome of the producing organism *Malbranchea aurantiaca* was sequenced and mined to identify putative gene clusters containing biosynthetic genes.⁹⁷ These data were used to identify a putative tryptophan halogenase MalA involved in the generation of malbrancheamide via BLAST analysis. We thus hypothesized that MalA would be responsible for the both chlorinations of the indole ring on premalbrancheamide. Further analysis of the protein sequence via BLAST revealed alignment with conserved domains of tryptophan halogenase proteins and possibly also the Lys79 residue (observed at Lys78) known to direct chlorination on tryptophan (Figure 4-14), further supporting our identification of the halogenase in the malbrancheamide biosynthetic pathway.^{140,144}

In this investigation, we sought to biochemically determine the role of MalA as the only identified putative halogenase in the gene clusters of the bicyclo[2.2.2]diazaoctanes. Because no other molecule in the prenylated indole alkaloid family contains halogens, we were particularly interested in elucidating the timing and chemistry of the halogenation event within the malbrancheamide pathway. Additionally, we were curious whether the halogenase would play a part in the IMDA reaction, since its predicted function would occur immediately after or concurrently with the formation of the bicyclo[2.2.2]diazaoctane core. In other words, there was

a possibility that the halogenase could receive the Diels-Alder substrate and mold the molecule into the correct conformation for an IMDA reaction before or while performing its halogenation.

4.2 Results

4.2.1 Determination of MalA as a flavin-dependent halogenase and malbrancheamide synthase

The function of MalA as a putative flavin-dependent halogenase was investigated. The *in vitro* activity of MalA was tested in reactions containing tryptophan, premalbrancheamide, malbrancheamide B, and isomalbrancheamide B. Additionally, flavin reductase HpaC was used to supply reduced flavin to MalA *in vitro*.¹⁴⁵ Malbrancheamide B and isomalbrancheamide B were reacted to form malbrancheamide ([M+H]⁺: 404.10 *m/z*). On the other hand, premalbrancheamide did not react with MalA to form any of the chlorinated compounds (i.e.

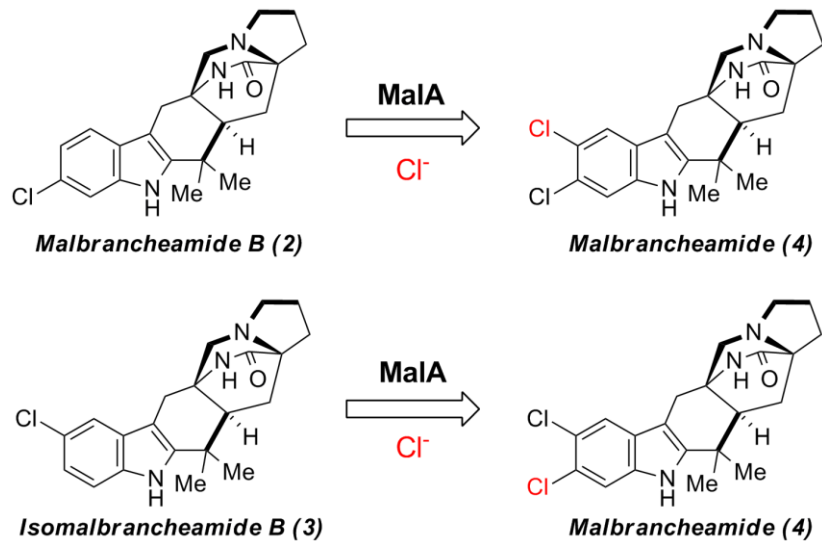


Figure 4-3. Chlorination reactions on malbrancheamide B and isomalbrancheamide B produce malbrancheamide using MalA.

malbrancheamide B, isomalbrancheamide B, or malbrancheamide). This was an unexpected result, as we began this investigation with preliminary evidence supporting the formation of malbrancheamide B from premalbrancheamide.

4.2.2 MalA performs bromination reactions when using bromide as a source ion

Since most halogenases are also able to perform bromination reactions, we decided to investigate MalA's potential in modifying malbrancheamide B and isomalbrancheamide B with bromine atoms. Thus, we performed similar reactions using NaBr instead of NaCl in solution. As expected, we were able to observe a brominated compound for each reaction with an observed [M+H]⁺ peak at 448.00 *m/z*. These reactions should thus be forming two new compounds depending on which substrate was used for the reaction (Figure 4-4). For my dissertation, I have temporarily assigned the names malbrancheamide D and isomalbrancheamide D to these

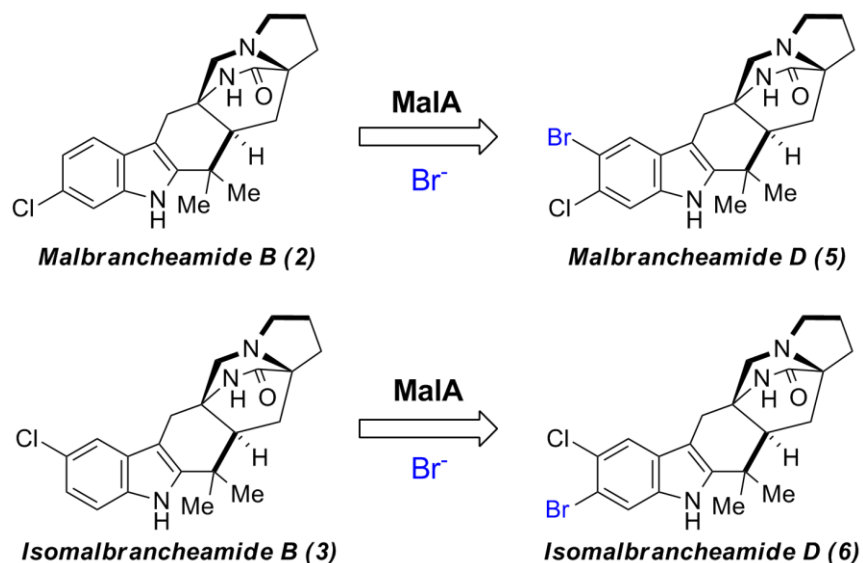


Figure 4-4. Bromination reactions on malbrancheamide B and isomalbrancheamide B produce malbrancheamide D and isomalbrancheamide D using MalA.

compounds, as they do not yet have formal names.

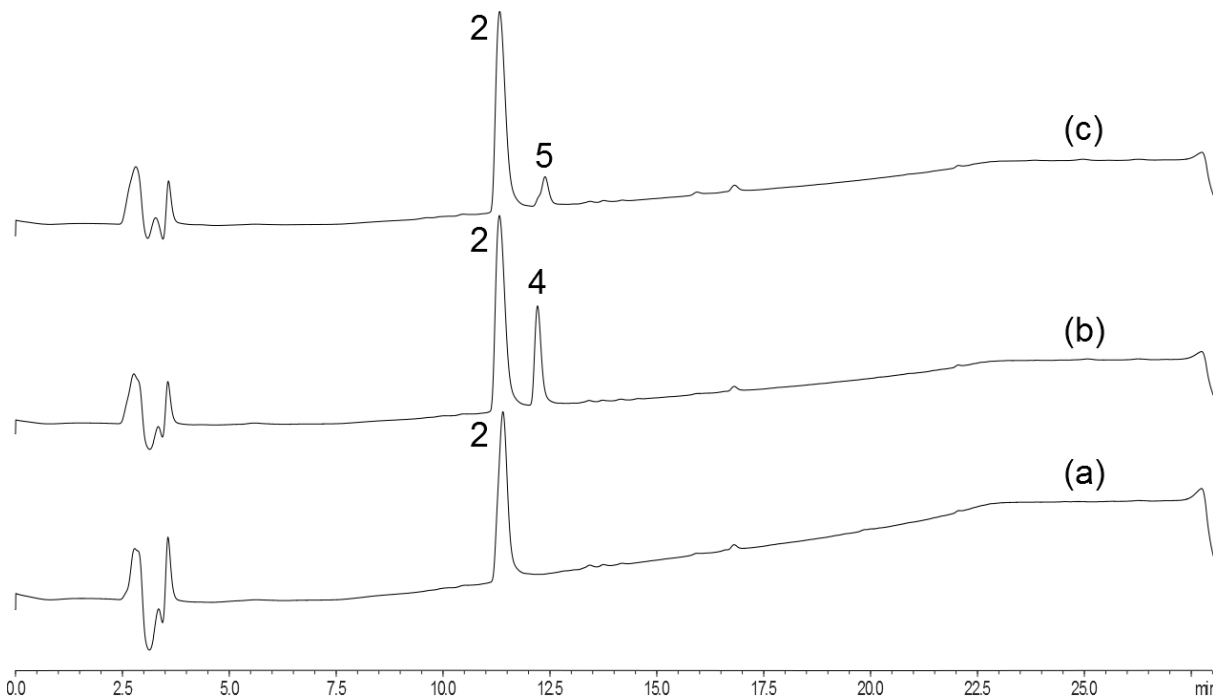


Figure 4-5. HPLC traces of reactions using MalA and malbrancheamide B. HPLC traces depict (a) negative control reaction with no enzyme, (b) reaction + MalA + NaCl, (c) reaction + MalA + NaBr.

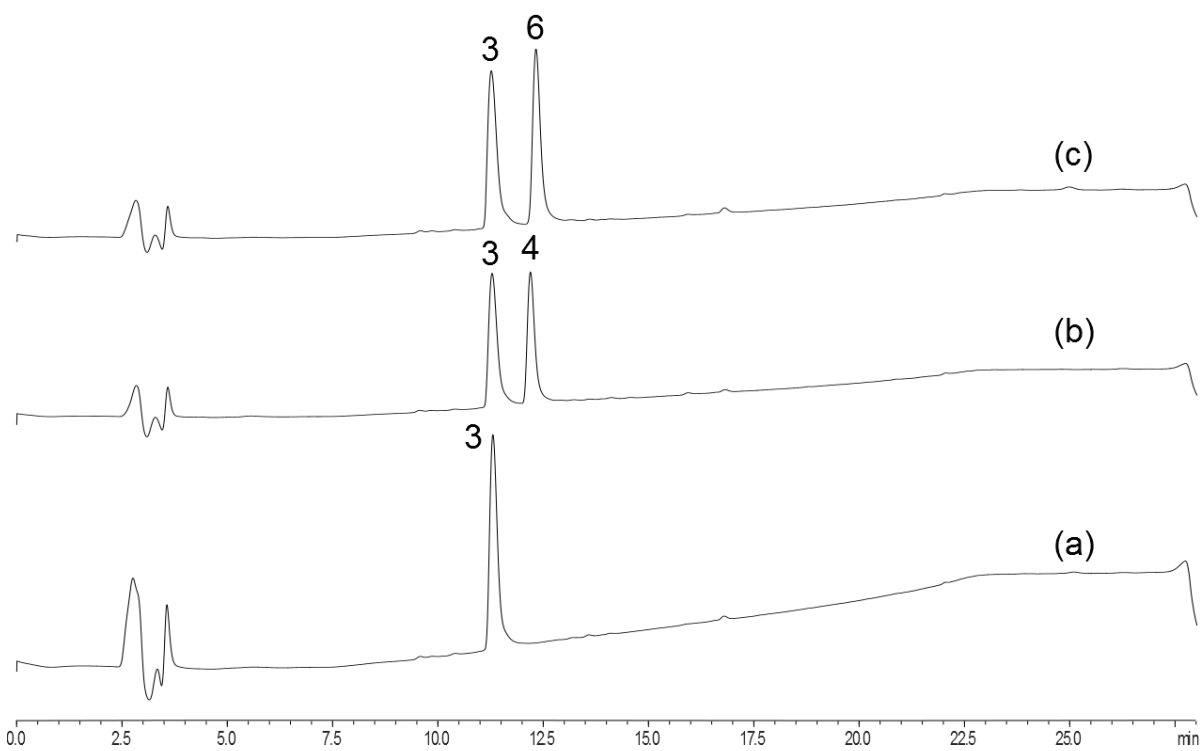
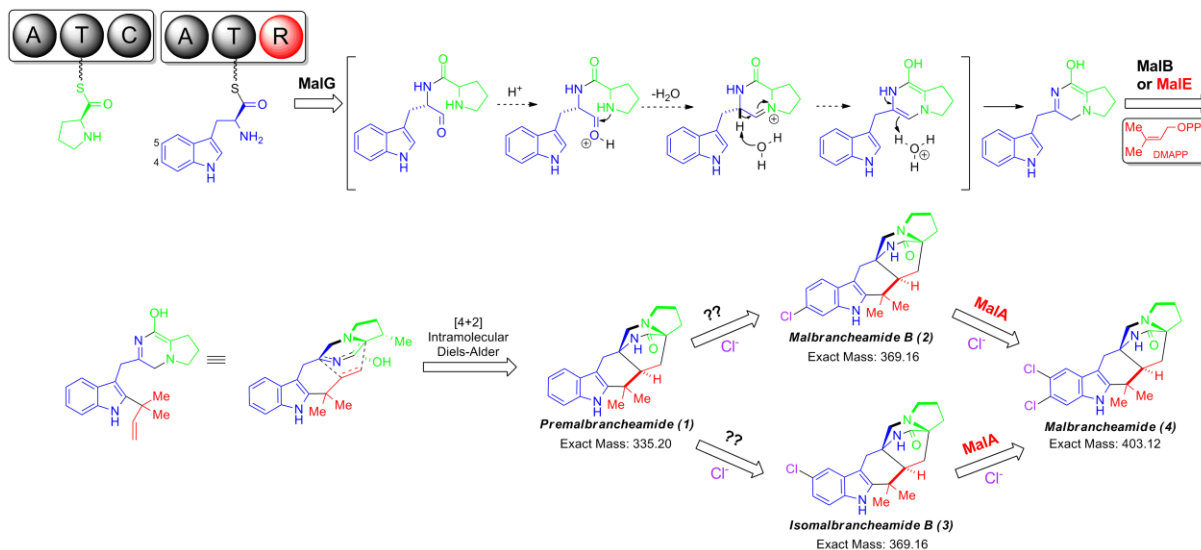


Figure 4-6. Traces of reactions containing MalA and isomalbrancheamide B. HPLC traces depict (a) negative control reaction with no enzyme, (b) reaction + MalA + NaCl, (c) reaction + MalA + NaBr.

4.3 Conclusion

In conclusion, MalA was found to be responsible for the second chlorination event, but it unexpectedly plays no part in the first chlorination event. This finding more or less eliminates MalA from being a candidate for the IMDA reaction, as it would accept a substrate later in the biosynthetic pathway. Strangely, the data also would imply that a second halogenase, likely halogenating premalbrancheamide based on isotopic feeding studies, is involved in the biosynthesis of malbrancheamide, but no second halogenase has been identified in or near the gene cluster. As an alternative option, we did not investigate the potential interaction between the halogenase and the NRPS module due to not having active NRPS, as halogenases are also known to react with substrates tethered to their peptidyl or acyl carrier proteins.¹³⁶



Scheme 4-1. Adjusted malbrancheamide biosynthetic pathway based on MalA investigation results.

We were excited to see that MaIA would be able to perform the bromination reactions, thus resulting in two new malbrancheamide compounds with a hybrid halogen modification on

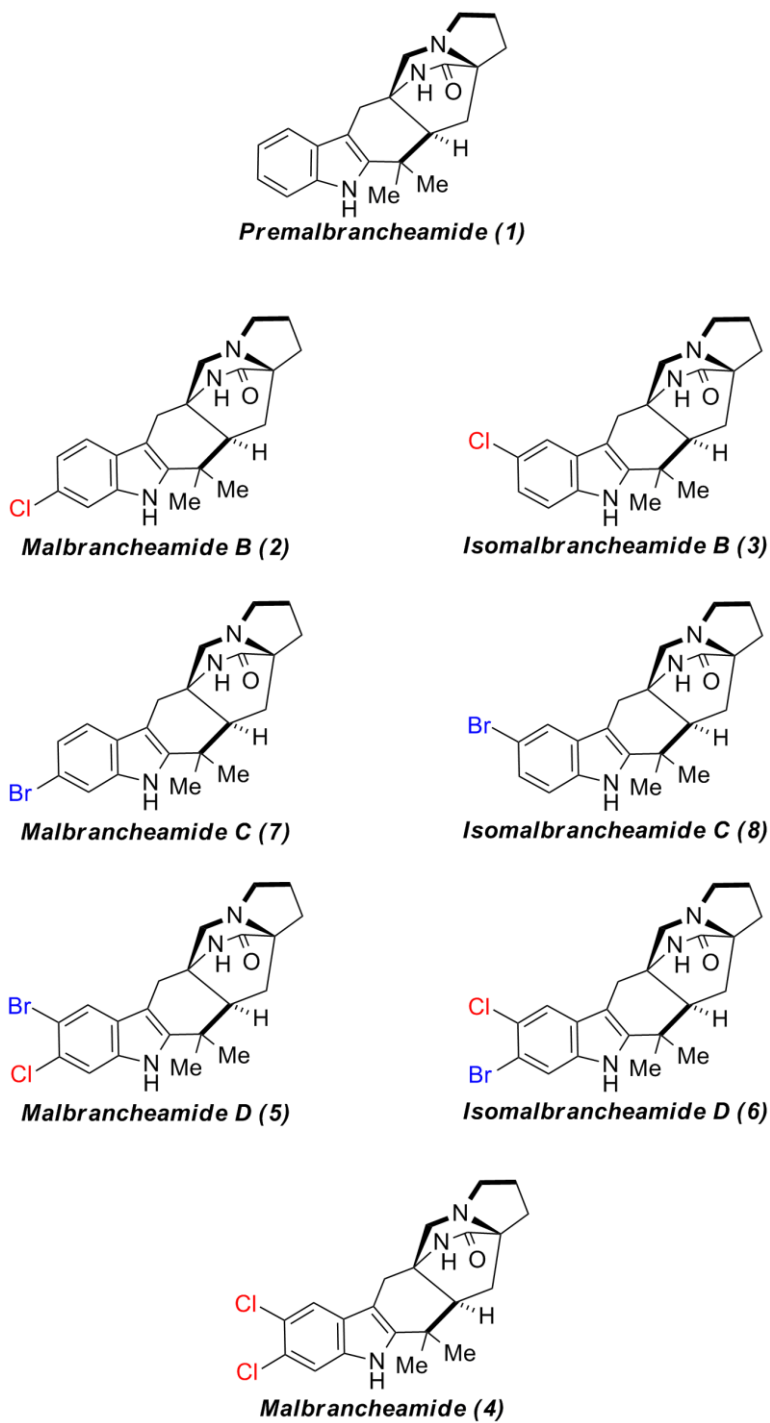


Figure 4-7. Currently discovered malbrancheamides with different halogen modifications.

the indole ring. The result is in agreement with the literature in that flavin halogenases are able to perform bromination reactions in addition to chlorination reactions.¹⁴⁶ Interestingly, only the single brominated compounds, malbrancheamide C (**7**) and isomalbrancheamide C (**8**), have been isolated previously from related fungus *M. graminicola* when grown in medium containing bromide ions (Figure 4-7).⁸⁴ Comparison of the two gene clusters from *M. aurantiaca* and *M. graminicola* show a 99% DNA sequence identity (unpublished data), suggesting that these compounds use identical biosynthetic pathways and that the brominated compounds could also be generated by the *M. aurantiaca* strain using the right growth conditions.

Investigations are currently being pursued to fully characterize the structures of malbrancheamide D and isomalbrancheamide D. Reactions shown here will be scaled up for isolation of purified product, which will then be used in 2D NMR experiments. We expect to find data corresponding to the structures shown here (Figure 4-3, Figure 4-4), as the collected mass spectrometry data support the current structures in mass and observed isotopic distribution patterns (see Appendix). However, while we are fairly confident in the identities of our products, we are unable to say with certainty that the structures of malbrancheamide D and isomalbrancheamide D are correct until we have gathered the necessary NMR data.

We aim to examine the ability of MalA to halogenate related molecules from the bicyclo[2.2.2]diazaoctane fungal alkaloid family of compounds. With our current data, it is impossible to judge the potential of MalA as a tool in biotechnology for performing halogenation reactions. However, related investigations have been performed using RebH from the rebeccamycin pathway, suggesting that the investigation of MalA as a biocatalyst would merit similar intrigue. RebH has thus far been shown to be able to halogenate arenes,¹³⁹ reengineered to halogenate tryptamine instead of tryptophan,⁵⁹ and improved for better stability and catalytic

lifespan.¹⁴⁷ Therefore, we are interested in employing a similar approach to engineer and utilize MalA as a biocatalyst for generating new compounds of interest.

In summary, we have elucidated the activity of MalA, a predicted FAD-dependent halogenase from the malbrancheamide biosynthetic pathway. The enzyme is a welcome addition to the current scarcity of identified eukaryotic halogenases, including the DIF-1 halogenase from *Dictyostelium discoideum*¹⁴⁸ and fungal halogenase Rdc2 from *Pochonia chlamydosporia*.¹⁴⁹ MalA accepts both substrates malbrancheamide B and isomalbrancheamide B for chlorination or bromination reactions. The curiously flexible binding pocket and the necessity of the initial chlorine substituent will be further investigated using crystallography by our collaborators in the Smith group. We are excited to report the new compounds malbrancheamide D and isomalbrancheamide D once we have more thorough data to support our hypothesis. MalA is the first of our malbrancheamide enzymes that we have thoroughly characterized, and this investigation expands upon our understanding of the biosynthesis of malbrancheamide as a member of the bicyclo[2.2.2]diazaoctane family.

4.4 Methods

1. Fungal strains and Culture Conditions

Malbranchea aurantiaca spores were generated on YPD agar plates over the course of 7 days. Spores were harvested into 5 mL sterile water per plate by gently scraping the surface of the culture with a sterile inoculating loop. Spores were stored at -80°C until ready to use. Genomic DNA was harvested using Wizard Genomic DNA Purification Kit from Promega.

2. cDNA preparation and cloning of *malE*

Total RNA was extracted from a sample of fungal mycelia collected on the 15th day of culture grown in liquid medium (Difco Potato Dextrose Broth) with 160 rpm agitation at 28°C, using Invitrogen PureLink RNA Mini Kit by following the plant tissue processing protocol. RNA was treated using DNase I. cDNA was generated using Invitrogen Superscript First Strand Synthesis. PCR was used to amplify *malA* from the cDNA template. The amplified gene was then cloned into a pET28b vector using restriction enzyme digest and ligation for an N-term His₆ construct, and a pET21b vector for a C-term His₆ construct. Plasmids were transformed into *E. coli* DH5α for screening and plasmid maintenance.

3. Overexpression and purification of protein for enzymology

The *Escherichia coli* BL21 pRARE transformant containing pET28b-*malA* and Takara chaperone pGro7 was grown at 37°C overnight in LB media containing 50 µg/mL of kanamycin and 100 µg/mL of spectinomycin. 25 mL of culture was used to inoculate 1 L of TB media containing the aforementioned concentrations of antibiotic and 4% glycerol. Cells were grown at 37°C for roughly 4 hours until A₆₀₀ reached 0.6-1.0, and isopropyl β-D-thiogalactoside (IPTG, 0.2 mM) was added to induce protein overexpression overnight at 18°C.

pET11a-*phaC* expression plasmid was transformed into *E. coli* BL21 pRARE cells for expression of His₄-tagged HpaC reductase enzyme.

All purification steps were conducted at 4°C. Briefly, 2 L of expression culture were spun down at 5,500 xg to yield approximately 20 mL of cell pellet volume. Harvested cell pellets were resuspended in 60 ml of lysis buffer (10 mM imidazole, 50 mM NaH₂PO₄, 300 mM NaCl, 10%

v/v glycerol, pH 8) and lysed by sonication. Insoluble material was removed by centrifugation at 38,000 xg for 30 min, and the supernatant was batch-bound for 1 hour to 4 mL of Ni²⁺-NTA slurry (Novagen) that was equilibrated in lysis buffer. This batch-binding mixture was poured through a 50 ml fritted glass column where the retained resin was washed with 100 mL of lysis buffer, 50 mL of wash buffer (20 mM imidazole, 50 mM NaH₂PO₄, 300 mM NaCl, 10% v/v glycerol, pH 8), and finally 10 ml of elution buffer (250 mM imidazole, 50 mM NaH₂PO₄, 300 mM NaCl, 10% v/v glycerol, pH 8). Protein in the eluate was exchanged into storage buffer (50 mM NaH₂PO₄, 1 mM EDTA, 0.2 mM DTT, 10% v/v glycerol, pH 7.3) using PD-10 columns. Samples were then flash frozen with liquid N₂ and stored at -80°C.

4. Enzyme assays and LC-MS analysis

The standard enzyme assay containing 0.5 mM substrate, 2.5 mM NADH, and 20 μM enzyme in 100 μL reaction buffer (50 mM NaH₂PO₄, 1 mM EDTA, 0.2 mM DTT, 10% v/v glycerol, pH 7.3) was performed at 28°C overnight. Each reaction was extracted 3 times with 200 μL chloroform, and the extract was dried down under N₂ gas. The product was resuspended in 100 μL methanol for LC-MS Q-TOF analysis.

4.5 Appendix

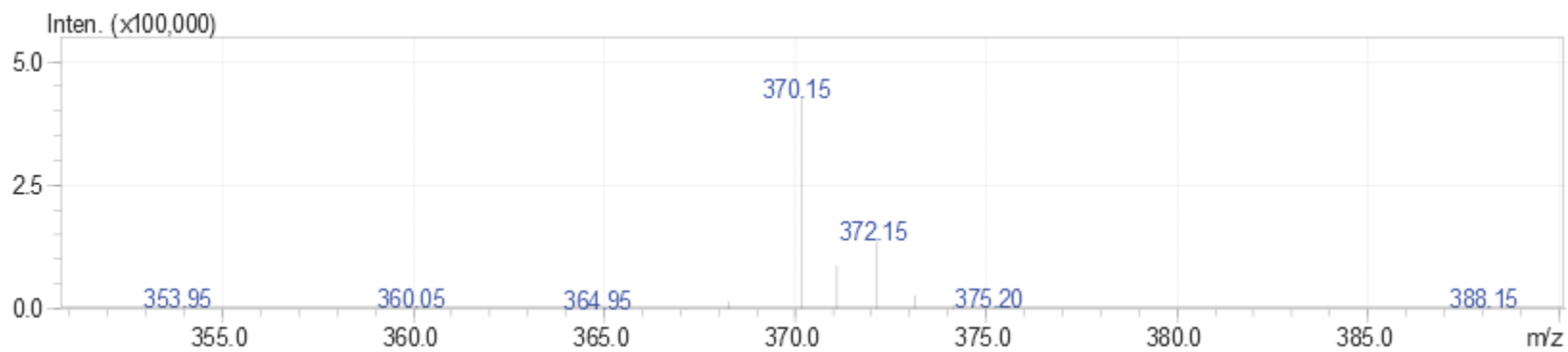


Figure 4-8. Mass spectrum of malbrancheamide B (2) with [M+H] observed at 370.15 m/z.

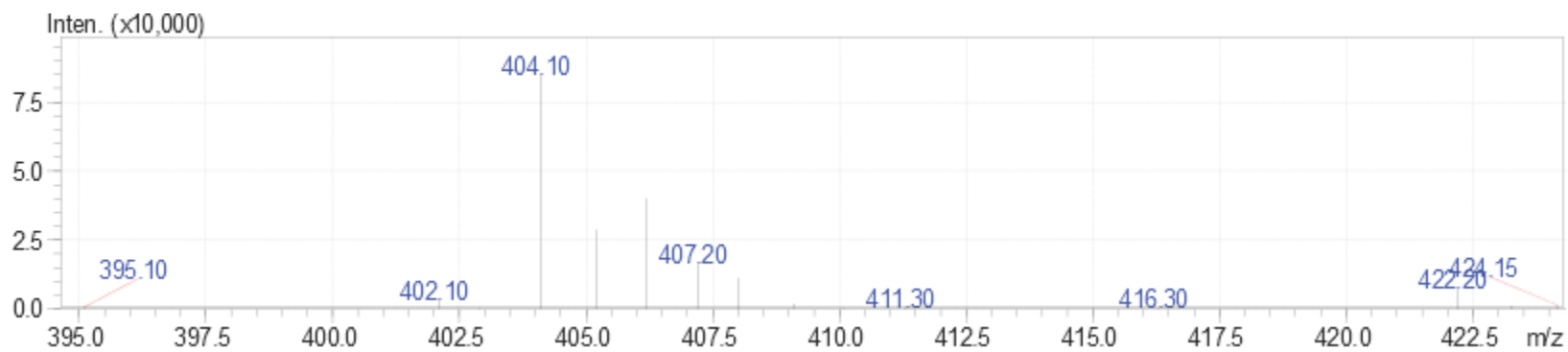


Figure 4-9. Mass spectrum of malbrancheamide product (4) from reaction with malbrancheamide B substrate. [M+H] observed at 404.10 m/z.

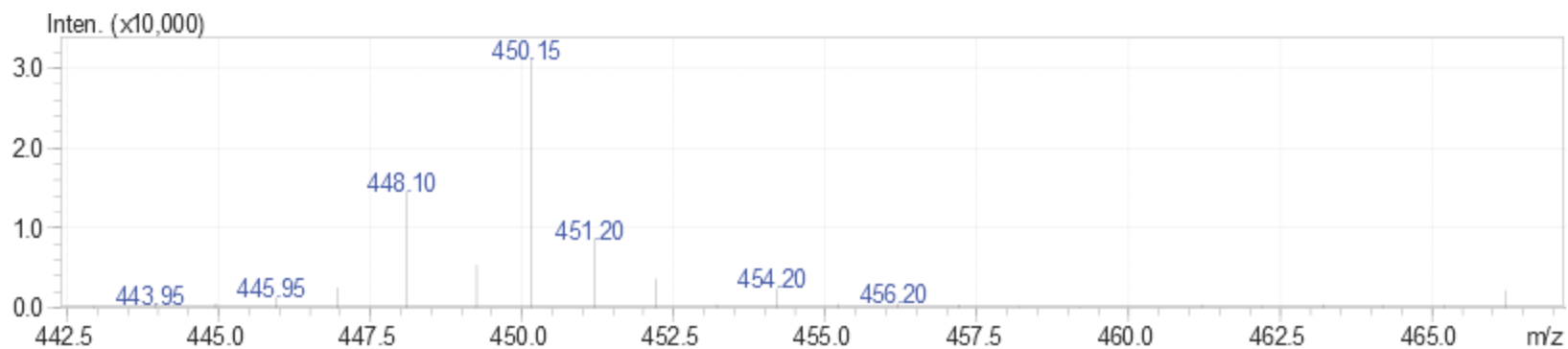


Figure 4-10. Mass spectrum of malbrancheamide D product (5) from reaction with malbrancheamide B substrate. $[M+H]$ observed at 448.10 m/z .

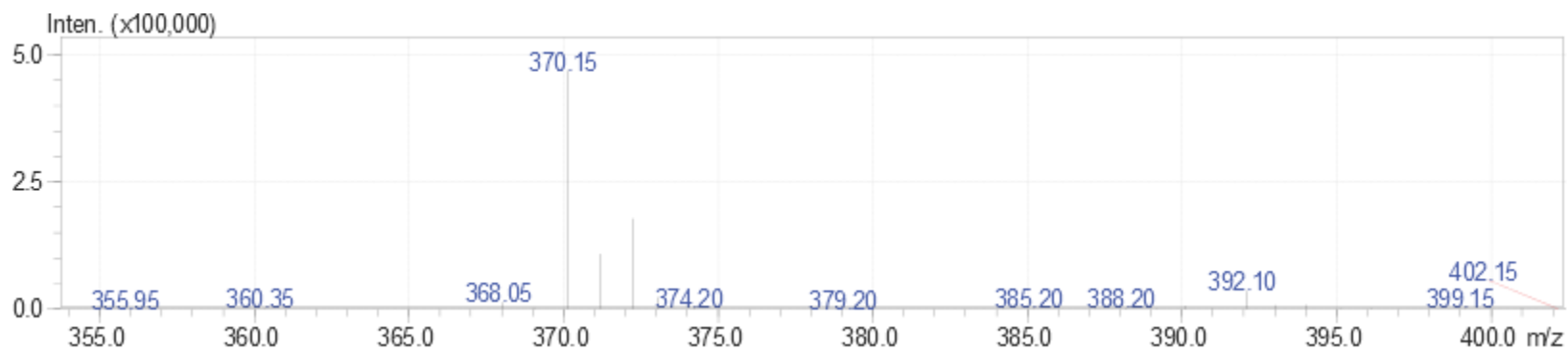


Figure 4-11. Mass spectrum of isomalbrancheamide B (3) with $[M+H]$ observed at 370.15 m/z .

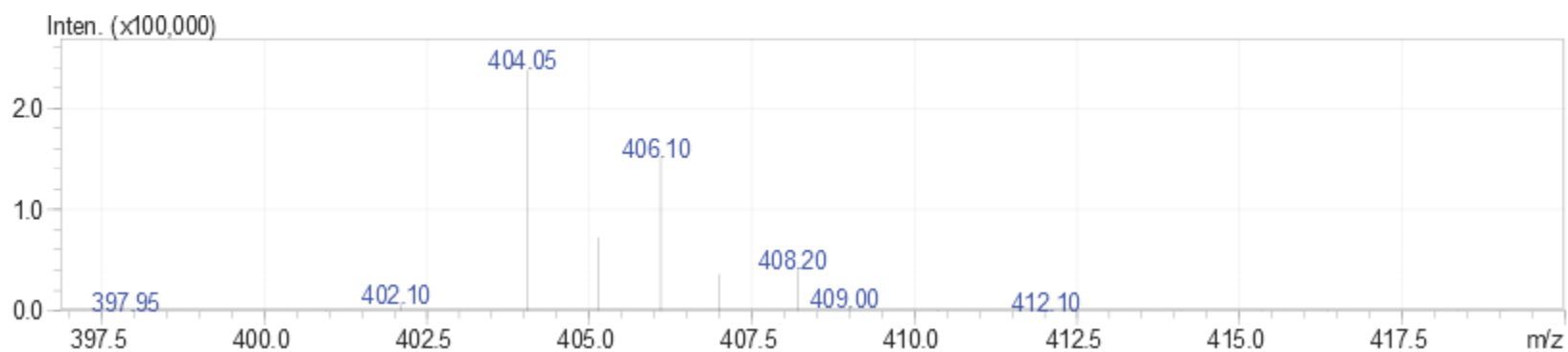


Figure 4-12. Mass spectrum of malbrancheamide product (4) from reaction with isomalbrancheamide B substrate. $[M+H]$ observed at 404.05 m/z .

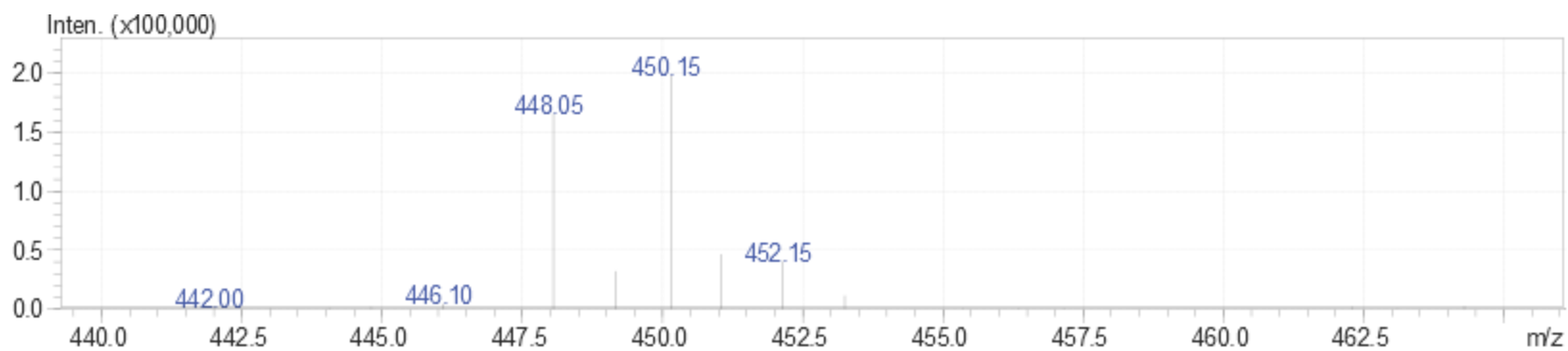


Figure 4-13. Mass spectrum of isomalbrancheamide D product (6) from reaction with isomalbrancheamide B substrate. [M+H] observed at 448.05 m/z.

Author Contributions:

Hong T. Tran and Amy E. Fraley contributed equally to this study. Hong T. Tran, Amy E. Fraley, and David H. Sherman contributed to the experimental design. Hong T. Tran and Amy E. Fraley conducted the experimental work, including enzyme reactions and product analysis. Substrates premalbrancheamide, malbrancheamide B, and isomalbrancheamide B were synthesized and provided by the Williams group (CSU). Hong Tran, Amy Fraley, and David H. Sherman evaluated the data. Ashootosh Tripathi, Andrew Lowell, and Jennifer Schmidt provided helpful discussion. The work contained in this chapter is currently being prepared for a manuscript submission.

Chapter 5

Future Work

In the chapters of my dissertation, I have described my findings regarding three key steps in bicyclo[2.2.2]diazaoctane fungal indole alkaloid biosynthesis. First, we have biochemically characterized three flavin monooxygenases from the notoamide and paraherquamide biosynthetic pathways: NotI, NotI' and PhqK. These flavin monooxygenases were found to be very flexible within their own systems and also were able to be used to diversify the pool of natural products within this class of alkaloids. Second, we investigated the role of the prenyltransferase MalE in the malbrancheamide biosynthetic pathway. We determined that it was an active prenyltransferase with some degree of flexibility for both the mono- and dioxopiperazine substrates. Finally, we tested the role of the MalA halogenase from the malbrancheamide pathway. MalA appears to only react with a malbrancheamide B and isomalbrancheamide B, suggesting that the other chlorine comes from a different source.

Our findings with NotI, NotI', and PhqK indicate that they could be exploited as biocatalysts for the synthesis of new and interesting compounds. In particular, they could be used in a chemoenzymatic approach, combining the strengths of synthetic chemistry and biochemistry, to further expand the diversity of the bicyclo[2.2.2]diazaoctanes, and possibly the diversity of bioactivity and potency of the molecules being created. For this approach, it would be useful to engineer a mutated gene product that would perform as a better catalyst in a similar manner to the PikC mutant used in our laboratory.¹⁵⁰ Perhaps the first step in future directions would be to identify and mutate specific residues to see how the mutations would affect activity.

While we were able to confirm the prenyltransferase activity of MalE, the story led to the development of many new questions regarding the mechanism of the Diels-Alder reaction. We suggested testing various new substrates, particularly molecules that would stabilize the azadiene formation or molecules that would be unable to oxidize to form the aromatic ring. We were unable to determine whether the oxygen atom was being provided by molecular oxygen in the atmosphere or from water based on synthetic investigations. Based on our findings, we believe that there is a possibility of another enzyme being the candidate for the IMDA reaction. Alternatively, there could be some interaction between a pair of proteins, MalE and some other enzyme, that would yield the Diels-Alder product. Our fungal alkaloid collaborative team has discussed this question and decided that investigating the remaining biosynthetic gene products in the malbrancheamide gene cluster would be necessary to answering this question.

The investigation of MalA provided us an insightful story to the halogenation of malbrancheamide. Contrary to what we expected, it only performs the second halogenation event rather than both the first and second. Consequently, it appears as though there may be a second halogenase in the organism that is responsible for the first halogenation event, likely using premalbrancheamide as a substrate based on isotopically enriched precursor incorporation experiments. This study effectively eliminated the possibility of MalA being the Diels-Alderase under the conditions tested, since the enzyme does not accept the IMDA-related substrate. Additionally, we found that MalA was able to brominate malbrancheamide B and isomalbrancheamide B, thus producing new compounds malbrancheamide D and isomalbrancheamide D.

In summary, rather than discovering the existence of a natural Diels-Alderase, I instead characterized three key steps in bicyclo[2.2.2]diazaoctane biosynthesis. A continued

investigation of the relatively small malbrancheamide gene cluster may eventually lead to identification of the IMDA catalyst, assuming the catalyst responsible is an enzyme. The work summarized in this dissertation covers three key gene candidates, leaving four remaining from the malbrancheamide gene cluster to investigate. By process of elimination, we may eventually arrive at the identification of the Diels-Alderase.

Alternatively, a strategy that I had initially proposed but was not included in my thesis work was moving the entire gene cluster to an alternative organism to see if malbrancheamide could be produced. This strategy had been previously employed by the Cox group to transfer the tenellin biosynthetic gene cluster to *A. oryzae*.¹⁵¹ The heterologous reconstruction of a full biosynthetic gene cluster would verify that the seven genes are all that are required for the formation of malbrancheamide, and the approach is feasible because of the relatively small size of the malbrancheamide gene cluster (20 KB). Furthermore, this approach could then be used to generate knockouts of each putative biosynthetic gene for an alternative method to identifying functions of biosynthetic gene products.

Overall, we have made a significant contribution to our understanding of fungal indole alkaloid biosynthesis. There are still many remaining questions to be answered, and further studies can be performed to see if we can use these biocatalysts to produce biologically active pharmaceutical products. The bicyclo[2.2.2]diazaoctanes are an incredibly rich source of interesting chemistry, and the potential for large findings still remains fairly untapped. We look forward to the continued investigation of notoamide, malbrancheamide, and paraherquamide gene products towards the development of novel biocatalysts, understanding of biosynthetic chemistry, and identification of new natural products with improved biological activities. We are also further expanding the breadth of fungal indole alkaloids with the inclusion of the citrinalin

and roquefortine compounds,^{152,153} and look forward to the beginning of our investigations of those gene clusters as well.

References

- (1) Pan, S.-Y.; Litscher, G.; Gao, S.-H.; Zhou, S.-F.; Yu, Z.-L.; Chen, H.-Q.; Zhang, S.-F.; Tang, M.-K.; Sun, J.-N.; Ko, K.-M. *Evid. Based. Complement. Alternat. Med.* **2014**, *2014*, 525340.
- (2) Mahdi, J. G.; Mahdi, A. J.; Bowen, I. D. *Cell Prolif.* **2006**, *39*, 147.
- (3) Nathwani, D.; Wood, M. J. *Drugs* **1993**, *45*, 866.
- (4) Cragg, G. M.; Newman, D. J. *Biochim. Biophys. Acta* **2013**, *1830*, 3670.
- (5) Newman, D. J.; Cragg, G. M. *J. Nat. Prod.* **2007**, *70*, 461.
- (6) Henkel, T.; Brunne, R. M.; Müller, H.; Reichel, F. *Science (80-.)*. **1999**, 643.
- (7) Gullo, V. P. *The Discovery of Natural Products with Therapeutic Potential*; Butterworth-Heinemann: Stoneham, 1994; pp. 49–73.
- (8) Wani, M. C.; Taylor, H. L.; Wall, M. E.; Coggon, P.; McPhail, A. T. *J. Am. Chem. Soc.* **1971**, *93*, 2325.
- (9) Zhou, X.; Zhu, H.; Liu, L.; Lin, J.; Tang, K. *Appl. Microbiol. Biotechnol.* **2010**, *86*, 1707.
- (10) Li, S.-M. *Nat. Prod. Rep.* **2010**, *27*, 57.
- (11) Schardl, C. L.; Panaccione, D. G.; Tudzynski, P. *Alkaloids. Chem. Biol.* **2006**, *63*, 45.
- (12) Williams, R.; Stocking, E.; Sanz-Cervera, J. In *Biosynthesis*; Leeper, F. J.; Vederas, J. C., Eds.; Topics in Current Chemistry; Springer Berlin Heidelberg: Berlin, Heidelberg, 2000; Vol. 209, pp. 97–173.
- (13) Jakubczyk, D.; Cheng, J. Z.; Connor, S. E. O. *Nat. Prod. Rep.* **2014**, *31*, 1328.
- (14) Van Apeldoorn, M. E.; van Egmond, H. P.; Speijers, G. J. A.; Bakker, G. J. I. *Mol. Nutr. Food Res.* **2007**, *51*, 7.
- (15) Raveh, A.; Carmeli, S. *J. Nat. Prod.* **2007**, *70*, 196.
- (16) Carle, J. S.; Christophersen, C. *J. Am. Chem. Soc.* **1979**, *101*, 4012.
- (17) Martínez-Luis, S.; Rodríguez, R.; Acevedo, L.; González, M. C.; Lira-Rocha, A.; Mata, R. *Tetrahedron* **2006**, *62*, 1817.
- (18) Li, S.-M. *J. Antibiot. (Tokyo)*. **2011**, *64*, 45.
- (19) Birch, A. J.; Wright, J. J. *Tetrahedron* **1970**, *26*, 2329.
- (20) Whyte, A.; Gloer, J. B.; Wicklow, D. T.; Dowd, P. F. *J. Nat. Prod.* **1996**, *59*, 1093.
- (21) Tsuda, M.; Kasai, Y.; Komatsu, K.; Sone, T.; Tanaka, M.; Mikami, Y.; Kobayashi, J. *Org. Lett.* **2004**, *6*, 3087.
- (22) Sunderhaus, J. D. J. D.; Sherman, D. H. D. H.; Williams, R. M. R. M. *Isr. J. Chem.* **2011**, *51*, 442.
- (23) Finefield, J. M.; Frisvad, J. C.; Sherman, D. H.; Williams, R. M. *J. Nat. Prod.* **2012**, *75*, 812.
- (24) Sanz-Cervera, J. F.; Stocking, E. M.; Usui, T.; Osada, H.; Williams, R. M. *Bioorg. Med. Chem.* **2000**, *8*, 2407.
- (25) Miller, K. A.; Welch, T. R.; Greshock, T. J.; Ding, Y.; Sherman, D. H.; Williams, R. M. *J. Org. Chem.* **2008**, *73*, 3116.
- (26) Miller, K. A.; Williams, R. M. *Chem. Soc. Rev.* **2009**, *38*, 3160.
- (27) Porter, A. E. A.; Sammes, P. G. *J. Chem. Soc. D Chem. Commun.* **1970**, 1103a.

- (28) Williams, R. M.; Glinka, T.; Kwast, E. *J. Am. Chem. Soc.* **1988**, *110*, 5927.
- (29) Williams, R. M.; Sanz-Cervera, J. F.; Sancenón, F.; Marco, J. A.; Halligan, K. *J. Am. Chem. Soc.* **1998**, *120*, 1090.
- (30) Sunderhaus, J. D.; Sherman, D. H.; Williams, R. M. *Isr. J. Chem.* **2011**, *51*, 442.
- (31) Rateb, M. E.; Ebel, R. *Nat. Prod. Rep.* **2011**, *28*, 290.
- (32) Qian-Cutrone, J.; Huang, S.; Shu, Y.-Z.; Vyas, D.; Fairchild, C.; Menendez, A.; Krampitz, K.; Dalterio, R.; Klohr, S. E.; Gao, Q. Stephacidin A and B: two structurally novel, selective inhibitors of the testosterone-dependent prostate LNCaP cells. *Journal of the American Chemical Society*, 2002, *124*, 14556–14557.
- (33) Emily, M.; Martinez, R. A. a; Louis, A.; Sanz-Cervera, J. F. F.; Williams, R. M. M.; Stocking, E. M.; Silks, L. a. *Studies on the biosynthesis of paraherquamide: concerning the mechanism of the oxidative cyclization of L-isoleucine to beta-methylproline.*; 2001; Vol. 123, pp. 3391–3392.
- (34) Kato, H.; Yoshida, T.; Tokue, T.; Nojiri, Y.; Hirota, H.; Ohta, T.; Williams, R. M.; Tsukamoto, S. *Angew. Chem. Int. Ed. Engl.* **2007**, *46*, 2254.
- (35) Tsukamoto, S.; Yoshida, T.; Hosono, H.; Ohta, T.; Yokosawa, H. *Bioorg. Med. Chem. Lett.* **2006**, *16*, 69.
- (36) Tsukamoto, S.; Hirota, H.; Imachi, M.; Fujimuro, M.; Onuki, H.; Ohta, T.; Yokosawa, H. *Bioorg. Med. Chem. Lett.* **2005**, *15*, 191.
- (37) Tsukamoto, S.; Yamashita, K.; Tane, K.; Kizu, R.; Ohta, T.; Matsunaga, S.; Fusetani, N.; Kawahara, H.; Yokosawa, H. *Biol. Pharm. Bull.* **2004**, *27*, 699.
- (38) Tsukamoto, S.; Tatsuno, M.; van Soest, R. W. M.; Yokosawa, H.; Ohta, T. *J. Nat. Prod.* **2003**, *66*, 1181.
- (39) Tsukamoto, S.; Kato, H.; Samizo, M.; Nojiri, Y.; Onuki, H.; Hirota, H.; Ohta, T. *J. Nat. Prod.* **2008**, *71*, 2064.
- (40) Tsukamoto, S.; Kato, H.; Greshock, T. J.; Hirota, H.; Ohta, T.; Williams, R. M. *J. Am. Chem. Soc.* **2009**, *131*, 3834.
- (41) Tsukamoto, S.; Umaoka, H.; Yoshikawa, K.; Ikeda, T.; Hirota, H. *J. Nat. Prod.* **2010**, *73*, 1438.
- (42) Grubbs, A. W.; Artman, G. D.; Tsukamoto, S.; Williams, R. M.; Greshock, T. J. *Angew. Chem. Int. Ed. Engl.* **2007**, *46*, 2257.
- (43) Finefield, J. M.; Williams, R. M. *J. Org. Chem.* **2010**, *75*, 2785.
- (44) McAfoos, T. J.; Li, S.; Tsukamoto, S.; Sherman, D. H.; Williams, R. M. *Heterocycles.* **2010**, *82*, 461.
- (45) Finefield, J. M.; Kato, H.; Greshock, T. J.; Sherman, D. H.; Tsukamoto, S.; Williams, R. M. *Org. Lett.* **2011**, *13*, 3802.
- (46) Sunderhaus, J. D.; McAfoos, T. J.; Finefield, J. M.; Kato, H.; Li, S.; Tsukamoto, S.; Sherman, D. H.; Williams, R. M. *Org. Lett.* **2013**, *15*, 22.
- (47) Ding, Y.; de Wet, J. R.; Cavalcoli, J.; Li, S.; Greshock, T. J.; Miller, K. A.; Finefield, J. M.; Sunderhaus, J. D.; McAfoos, T. J.; Tsukamoto, S.; Williams, R. M.; Sherman, D. H.; Wet, J. R. De; Thomas, J. *J. Am. Chem. Soc.* **2010**, *132*, 12733.
- (48) Li, S.; Srinivasan, K.; Tran, H.; Yu, F. *Medchemcomm* **2012**, *3*, 987.
- (49) Fischbach, M. A.; Walsh, C. T. *Chem. Rev.* **2006**, *106*, 3468.
- (50) Cox, R. *Nat. Prod. Rep.* **2014**, *00*, 1.
- (51) Miller, K. a; Figueroa, M.; Valente, M. W. N.; Greshock, T. J.; Mata, R.; Williams, R. M. *Bioorg. Med. Chem. Lett.* **2008**, *18*, 6479.

- (52) Martínez-Luis, S.; Pérez-Vásquez, A.; Mata, R. *Phytochemistry* **2007**, *68*, 1882.
- (53) Figueroa, M.; González-Andrade, M.; Sosa-Peinado, A.; Madariaga-Mazón, A.; Del Río-Portilla, F.; González, M. D. C.; Mata, R. *J. Enzyme Inhib. Med. Chem.* **2011**, *26*, 378.
- (54) Harris, C. M.; Kannan, R.; Kopecka, H.; Harris, T. M. *J Am Chem Soc* **1985**, *20*, 6652.
- (55) Gribble, G. W. *Chemosphere* **2003**, *52*, 289.
- (56) Blasiak, L. C.; Drennan, C. L. *Acc. Chem. Res.* **2009**, *42*, 147.
- (57) Neumann, C. S.; Fujimori, D. G.; Walsh, C. T. *Chem. Biol.* **2008**, *15*, 99.
- (58) Flecks, S.; Patallo, E. P.; Zhu, X.; Ernyei, A. J.; Seifert, G.; Schneider, A.; Dong, C.; Naismith, J. H.; van Pée, K.-H. *Angew. Chem. Int. Ed. Engl.* **2008**, *47*, 9533.
- (59) Glenn, W. S.; Nims, E.; O'Connor, S. E. *J. Am. Chem. Soc.* **2011**, *133*, 19346.
- (60) Lang, A.; Polnick, S.; Nicke, T.; William, P.; Patallo, E. P.; Naismith, J. H.; van Pée, K.-H. *Angew. Chem. Int. Ed. Engl.* **2011**, *50*, 2951.
- (61) Dong, C.; Flecks, S.; Unversucht, S.; Haupt, C.; van Pée, K.-H.; Naismith, J. H. *Science* **2005**, *309*, 2216.
- (62) Ding, Y.; Greshock, T. J.; Miller, K. A.; Sherman, D. H.; Williams, R. M. *Org. Lett.* **2008**, *10*, 4863.
- (63) Margrey, K. A.; Chinn, A. J.; Laws, S. W.; Pike, R. D.; Scheerer, J. R. *Org. Lett.* **2012**, *14*, 2458.
- (64) Laws, S. W.; Scheerer, J. R. *J. Org. Chem.* **2013**, *78*, 2422.
- (65) Frebault, F.; Simpkins, N. S.; Fenwick, A. *J. Am. Chem. Soc.* **2009**, *131*, 4214.
- (66) Diels, O.; Alder, K. *Justus Liebig's Ann. der Chemie* **1928**, *460*, 98.
- (67) Stork, G.; Tamelen, E. E. VAN; Friedman, L. J.; Burgstahler, A. W. *J. Am. Chem. Soc.* **1951**, *73*, 4501.
- (68) Oikawa, H.; Tokiwano, T. *Nat. Prod. Rep.* **2004**, *21*, 321.
- (69) Hilvert, D.; Hill, K. W.; Nared, K. D.; Auditor, M. T. M. *J. Am. Chem. Soc.* **1989**, *111*, 9261.
- (70) Tarasow, T. M.; Tarasow, S. L.; Eaton, B. E. *Nature* **1997**, *389*, 54.
- (71) Agresti, J. J.; Kelly, B. T.; Jäschke, A.; Griffiths, A. D. *Proc. Natl. Acad. Sci. U. S. A.* **2005**, *102*, 16170.
- (72) Kelly, W. L. *Org. Biomol. Chem.* **2008**, *6*, 4483.
- (73) Auclair, K.; Sutherland, A.; Kennedy, J.; Witter, D. J.; Van den Heever, J. P.; Hutchinson, C. R.; Vederas, J. C. *J. Am. Chem. Soc.* **2000**, *122*, 11519.
- (74) Oikawa, H.; Watanabe, K.; Yagi, K.; Ohashi, S.; Mie, T.; Ichihara, A.; Honma, M. *Tetrahedron Lett.* **1999**, *40*, 6983.
- (75) Watanabe, K.; Mie, T.; Ichihara, a; Oikawa, H.; Honma, M. *J. Biol. Chem.* **2000**, *275*, 38393.
- (76) Ose, T.; Watanabe, K.; Mie, T.; Honma, M.; Watanabe, H.; Yao, M.; Oikawa, H.; Tanaka, I. *Nature* **2003**, *422*, 185.
- (77) Guimarães, C. R. W.; Udier-Blagović, M.; Jorgensen, W. L. Macrophomate synthase: QM/MM simulations address the Diels-Alder versus Michael-Aldol reaction mechanism. *Journal of the American Chemical Society*, 2005, *127*, 3577–3588.
- (78) Ose, T.; Watanabe, K.; Yao, M.; Honma, M.; Oikawa, H.; Tanaka, I. *Acta Crystallogr. D. Biol. Crystallogr.* **2004**, *60*, 1187.
- (79) Serafimov, J. M.; Gillingham, D.; Kuster, S.; Hilvert, D. *J. Am. Chem. Soc.* **2008**, *130*, 7798.
- (80) Kim, H. J.; Ruszczycky, M. W.; Choi, S.; Liu, Y.; Liu, H. *Nature* **2011**, *473*, 109.

- (81) Hess, B. A.; Smentek, L. *Org. Biomol. Chem.* **2012**, *10*, 7503.
- (82) Li, S.; Finefield, J. M.; Sunderhaus, J. D.; Mcafoos, T. J.; Williams, R. M.; Sherman, D. H. *J. Am. Chem. Soc.* **2012**, *134*, 788.
- (83) Grubbs, A. W.; Artman, G. D.; Tsukamoto, S.; Williams, R. M. *Angew. Chem. Int. Ed. Engl.* **2007**, *46*, 2257.
- (84) Watts, K. R.; Loveridge, S. T.; Tenney, K.; Media, J.; Valeriote, F. a; Crews, P. *J. Org. Chem.* **2011**, *76*, 6201.
- (85) Pistorius, D.; Li, Y.; Sandmann, A.; Müller, R. *Mol. Biosyst.* **2011**, *7*, 3308.
- (86) Xin, M.; Bugg, T. D. H. *ChemBiochem* **2010**, *11*, 272.
- (87) Barton, D. H. R.; Scott, A. I. *J. Chem. Soc.* **1958**, 1767.
- (88) Finkelstein, E.; Amichai, B.; Grunwald, M. H. *Int. J. Antimicrob. Agents* **1996**, *6*, 189.
- (89) Ahmed, S. A.; Scott, F. E.; Stenzel, D. J.; Simpson, T. J.; Moore, R. N.; Trimble, L. A.; Arai, K.; Vederas, J. C. *J. Chem. Soc. Perkin Trans. 1* **1989**, 807.
- (90) Allen, J. D.; van Loevezijn, A.; Lakhai, J. M.; van der Valk, M.; van Tellingen, O.; Reid, G.; Schellens, J. H. M.; Koomen, G.-J.; Schinkel, A. H. *Mol. Cancer Ther.* **2002**, *1*, 417.
- (91) Katsuyama, Y.; Harmrolfs, K.; Pistorius, D.; Li, Y.; Müller, R. *Angew. Chem. Int. Ed. Engl.* **2012**, *51*, 9437.
- (92) Kato, H.; Yoshida, T.; Tokue, T.; Nojiri, Y.; Hirota, H.; Ohta, T.; Williams, R. M.; Tsukamoto, S. *Angew. Chem. Int. Ed. Engl.* **2007**, *46*, 2254.
- (93) Greshock, T. J.; Grubbs, A. W.; Jiao, P.; Wicklow, D. T.; Gloer, J. B.; Williams, R. M. *Angew. Chem. Int. Ed. Engl.* **2008**, *47*, 3573.
- (94) Finefield, J. M.; Sherman, D. H.; Kreitman, M.; Williams, R. M. *Angew. Chem. Int. Ed. Engl.* **2012**, *51*, 4802.
- (95) Artman, G. D.; Grubbs, A. W.; Williams, R. M. *J. Am. Chem. Soc.* **2007**, *129*, 6336.
- (96) Ding, Y.; de Wet, J. R.; Cavalcoli, J.; Li, S.; Greshock, T. J.; Miller, K. A.; Finefield, J. M.; Sunderhaus, J. D.; McAfoos, T. J.; Tsukamoto, S.; Williams, R. M.; Sherman, D. H. *J. Am. Chem. Soc.* **2010**, *132*, 12733.
- (97) Li, S.; Anand, K.; Tran, H.; Yu, F.; Finefield, J. M.; Sunderhaus, J. D.; McAfoos, T. J.; Tsukamoto, S.; Williams, R. M.; Sherman, D. H. *MedChemComm.* **2012**, *3*, 987.
- (98) Sanz-Cervera, J. F.; Glinka, T.; Williams, R. M. *Tetrahedron.* **1993**, *49*, 8471.
- (99) Kato, H.; Nakamura, Y.; Finefield, J. M.; Umaoka, H.; Nakahara, T.; Williams, R. M.; Tsukamoto, S. *Tetrahedron Lett.* **2011**, *52*, 6923.
- (100) Greshock, T. J.; Grubbs, A. W.; Tsukamoto, S.; Williams, R. M. *Angew. Chem. Int. Ed. Engl.* **2007**, *46*, 2262.
- (101) Ding, Y.; Gruschow, S.; Greshock, T. J.; Finefield, J. M.; Sherman, D. H.; Williams, R. M. *J. Nat. Prod.* **2008**, *71*, 1574.
- (102) Cacho, R. A.; Chooi, Y.; Zhou, H.; Tang, Y. *ACS Chem. Biol.* **2013**, *8*, 2322.
- (103) Huang, K. -x.; Fujii, I.; Ebizuka, Y.; Gomi, K.; Sankawa, U. *J. Biol. Chem.* **1995**, *270*, 21495.
- (104) Tsunematsu, Y.; Ishikawa, N.; Wakana, D.; Goda, Y.; Noguchi, H.; Moriya, H.; Hotta, K.; Watanabe, K. *Nat. Chem. Biol.* **2013**, *9*, 818.
- (105) Baran, P. S.; Guerrero, C. A.; Ambhaikar, N. B.; Hafensteiner, B. D. *Angew. Chem. Int. Ed. Engl.* **2005**, *44*, 606.
- (106) Baran, P. S.; Hafensteiner, B. D.; Ambhaikar, N. B.; Guerrero, C. A.; Gallagher, J. D. *J. Am. Chem. Soc.* **2006**, *128*, 8678.

- (107) Finefield, J. M.; Sherman, D. H.; Tsukamoto, S.; Williams, R. M. *J. Org. Chem.* **2011**, *76*, 5954.
- (108) Botta, B.; Vitali, A.; Menendez, P.; Misiti, D.; Delle Monache, G. *Curr. Med. Chem.* **2005**, *12*, 717.
- (109) Botta, B.; Delle Monache, G.; Menendez, P.; Boffi, A. *Trends Pharmacol. Sci.* **2005**, *26*, 606.
- (110) Li, S.-M. *Appl. Microbiol. Biotechnol.* **2009**, *84*, 631.
- (111) Breitmaier, E. *Terpenes: Flavors, Fragrances, Pharmaca, Pheromones*; Wiley-VCH Verlag GmbH & Co. KGaA: Weinheim, Germany, 2006.
- (112) Bochar, D. A.; Freisen, J.; Stauffacher, C. V.; Rodwell, V. W. In *Chemistry, Molecular Sciences and Chemical Engineering*; Elsevier, 1999; pp. 15–44.
- (113) Rohmer, M. *Pure Appl. Chem.* **2007**, *79*.
- (114) Eisenreich, W.; Bacher, a; Arigoni, D.; Rohdich, F. *Cell. Mol. Life Sci.* **2004**, *61*, 1401.
- (115) Chang, W.; Song, H.; Liu, H.; Liu, P. *Curr. Opin. Chem. Biol.* **2013**, *17*, 571.
- (116) Steffan, N.; Grundmann, A.; Yin, W.-B.; Kremer, A.; Li, S.-M. *Curr. Med. Chem.* **2009**, *16*, 218.
- (117) Unsöld, I. a; Li, S.-M. *Microbiology* **2005**, *151*, 1499.
- (118) Saleh, O.; Haagen, Y.; Seeger, K.; Heide, L. *Phytochemistry* **2009**, *70*, 1728.
- (119) Metzger, U.; Schall, C.; Zocher, G.; Unsöld, I.; Stec, E.; Li, S.; Heide, L.; Stehle, T. *Proc. Natl. Acad. Sci. U. S. A.* **2009**, *106*, 14309.
- (120) Unsöld, I. a; Li, S.-M. *Chembiochem* **2006**, *7*, 158.
- (121) Grundmann, A.; Li, S.-M. *Microbiology* **2005**, *151*, 2199.
- (122) Grundmann, A.; Kuznetsova, T.; Afiyatullo, S. S.; Li, S.-M. *Chembiochem* **2008**, *9*, 2059.
- (123) Yin, W.-B.; Grundmann, A.; Cheng, J.; Li, S.-M. *J. Biol. Chem.* **2009**, *284*, 100.
- (124) Schneider, P.; Weber, M.; Hoffmeister, D. *Fungal Genet. Biol.* **2008**, *45*, 302.
- (125) Ding, Y.; Williams, R. M.; Sherman, D. H. *J. Biol. Chem.* **2008**, *283*, 16068.
- (126) Liang, P.-H.; Ko, T.-P.; Wang, A. H.-J. *Eur. J. Biochem.* **2002**, *269*, 3339.
- (127) Preiswerk, N.; Beck, T.; Schulz, J. D.; Milovnik, P.; Mayer, C.; Siegel, J. B.; Baker, D.; Hilvert, D. *Proc. Natl. Acad. Sci. U. S. A.* **2014**, *111*, 8013.
- (128) Siegel, J. B.; Zanghellini, A.; Lovick, H. M.; Kiss, G.; Lambert, A. R.; St Clair, J. L.; Gallaher, J. L.; Hilvert, D.; Gelb, M. H.; Stoddard, B. L.; Houk, K. N.; Michael, F. E.; Baker, D. *Science* **2010**, *329*, 309.
- (129) Blanchflower, S. E.; Banks, R. M.; Everett, J. R.; Manger, B. R.; Reading, C. *J. Antibiot. (Tokyo)*. **1991**, *44*, 492.
- (130) Wageningen, A. van; Kirkpatrick, P. *Chem. Biol.* **1998**, *5*, 155.
- (131) Podzelinska, K.; Latimer, R.; Bhattacharya, A.; Vining, L. C.; Zechel, D. L.; Jia, Z. *J. Mol. Biol.* **2010**, *397*, 316.
- (132) Harris, C. M.; Kannan, R.; Kopecka, H.; Harris, T. M. *J. Am. Chem. Soc.* **1985**, *107*, 6652.
- (133) Gribble, G. W. *Alkaloids. Chem. Biol.* **2012**, *71*, 1.
- (134) Kling, E.; Schmid, C.; Unversucht, S.; Wage, T.; Zehner, S.; van Pée, K. H. *Ernst Schering Res. Found. Workshop* **2005**, 165.
- (135) Doerschuk, A. P.; McCormick, J. R. D.; Goodman, J. J.; Szumski, S. A.; Growich, J. A.; Miller, P. A.; Bitler, B. A.; Jensen, E. R.; Matrishin, M.; Petty, M. A.; Phelps, A. S. *J. Am. Chem. Soc.* **1959**, *81*, 3069.
- (136) Van Pée, K.-H.; Patallo, E. P. *Appl. Microbiol. Biotechnol.* **2006**, *70*, 631.

- (137) Vaillancourt, F. H.; Yeh, E.; Vosburg, D. A.; Garneau-Tsodikova, S.; Walsh, C. T. *Chem. Rev.* **2006**, *106*, 3364.
- (138) Yeh, E.; Garneau, S.; Walsh, C. T. *Proc. Natl. Acad. Sci. U. S. A.* **2005**, *102*, 3960.
- (139) Payne, J. T.; Andorfer, M. C.; Lewis, J. C. *Angew. Chem. Int. Ed. Engl.* **2013**, *52*, 5271.
- (140) Dong, C.; Flecks, S.; Unversucht, S.; Haupt, C.; van Pée, K.-H.; Naismith, J. H. *Science* **2005**, *309*, 2216.
- (141) Dong, C.; Kotzsch, A.; Dorward, M.; van Pée, K. H.; Naismith, J. H. *Acta Crystallogr. D. Biol. Crystallogr.* **2004**, *60*, 1438.
- (142) Zehner, S.; Kotzsch, A.; Bister, B.; Süßmuth, R. D.; Méndez, C.; Salas, J. A.; van Pée, K.-H. *Chem. Biol.* **2005**, *12*, 445.
- (143) Figueroa, M.; Gonzalez, M. D. C.; Mata, R. *Nat. Prod. Res.* **2008**, *22*, 709.
- (144) Yeh, E.; Blasiak, L. C.; Koglin, A.; Drennan, C. L.; Walsh, C. T. *Biochemistry* **2007**, *46*, 1284.
- (145) Chakraborty, S.; Ortiz-Maldonado, M.; Entsch, B.; Ballou, D. P. *Biochemistry* **2010**, *49*, 372.
- (146) Van Pée, K.-H. *Enzymatic chlorination and bromination.*; 1st ed.; Elsevier Inc., 2012; Vol. 516, pp. 237–257.
- (147) Poor, C. B.; Andorfer, M. C.; Lewis, J. C. *Chembiochem* **2014**, *15*, 1286.
- (148) Neumann, C. S.; Walsh, C. T.; Kay, R. R. *Proc. Natl. Acad. Sci. U. S. A.* **2010**, *107*, 5798.
- (149) Zeng, J.; Zhan, J. *Chembiochem* **2010**, *11*, 2119.
- (150) Sherman, D. H.; Li, S.; Yermalitskaya, L. V.; Kim, Y.; Smith, J. a; Waterman, M. R.; Podust, L. M. *J. Biol. Chem.* **2006**, *281*, 26289.
- (151) Heneghan, M. N.; Yakasai, A. a; Halo, L. M.; Song, Z.; Bailey, A. M.; Simpson, T. J.; Cox, R. J.; Lazarus, C. M. *Chembiochem* **2010**, *11*, 1508.
- (152) Pimenta, E. F.; Vita-Marques, A. M.; Tininis, A.; Selegim, M. H. R.; Sette, L. D.; Veloso, K.; Ferreira, A. G.; Williams, D. E.; Patrick, B. O.; Dalisay, D. S.; Andersen, R. J.; Berlinck, R. G. S. *J. Nat. Prod.* **2010**, *73*, 1821.
- (153) Ali, H.; Ries, M. I.; Nijland, J. G.; Lankhorst, P. P.; Hankemeier, T.; Bovenberg, R. a L.; Vreeken, R. J.; Driessen, A. J. M. *PLoS One* **2013**, *8*, e65328.